J Intell Robot Syst (2015) 80:87–138
DOI 10.1007/s10846-014-0143-5

Survey of Unmanned Helicopter Model-Based Navigation and Control Techniques

Jessica Alvarenga · Nikolaos I. Vitzilaios · Kimon P. Valavanis · Matthew J. Rutherford

Received: 31 July 2014 / Accepted: 9 September 2014 / Published online: 3 December 2014

Abstract Unmanned Aircraft Systems (UAS) have seen unprecedented levels of growth during the last two decades. Although many challenges still exist, one of the main UAS focus research areas is in navigation and control. This paper provides a comprehensive overview of helicopter navigation and control, focusing specifically on small-scale traditional main/tail rotor configuration helicopters. Unique to this paper, is the emphasis placed on navigation/control methods, modeling techniques, loop architectures and structures, and implementations. A 'reference template' is presented and used to provide a basis for comparative studies and determine the capabilities and limitations of algorithms for unmanned/autonomous flight, as well as for navigation, and control. A detailed listing of related research is provided, which includes model structure, helicopter platform, control method and loop architecture, flight maneuvers and results for each. The results of this study was driven by and has led to the development of a 'one-fits-all' comprehensive and modular navigation controller and timing architecture applicable to any rotorcraft platform.

This work was supported in part by NSF CNS-1229236.

J. Alvarenga (✉) · N. I. Vitzilaios ·
K. P. Valavanis · M. J. Rutherford
DU Unmanned Systems Research Institute, Daniel Felix Ritchie School of Engineering & Computer Science,
University of Denver, 2390 S. York St., Denver,
CO 80208, USA
e-mail: Jessica.Alvarenga@du.edu

N. I. Vitzilaios
e-mail: Nikolaos.Vitzilaios@du.edu

K. P. Valavanis
e-mail: Kimon.Valavanis@du.edu

M. J. Rutherford
e-mail: Matthew.Rutherford@du.edu
www.du2sri.com

Keywords Helicopter · Rotorcraft · Unmanned Aerial Vehicle (UAV) · Unmanned Aircraft System (UAS) · Navigation · Control · Sensor-based navigation

Mathematics Subject Classification (2000) 19,64,127,93-02

List of Symbols

Acronyms

ACAH	Attitude Command Attitude Hold
AHRS	Attitude Heading Reference System
CG	Center of Gravity
DDP	Differential Dynamic Programming
DGPS	Differential GPS
DOF	Degrees of Freedom
NDI	Nonlinear Dynamic Inversion
EKF	Extended Kalman Filter
EOM	Equations of Motion

FCS	Flight Control System
FLC	Fuzzy Logic Control
GCS	Ground Control Station
GPS	Global Positioning System
KF	Kalman Filter
LQG	Linear Quadratic Gaussian
LQI	LQR with Integral Action
LQIFF	LQI with Feed Forward Control
LQR	Linear Quadratic Regression
LTI	Linear Time Invariant
LTR	Loop Transfer Recovery
MAV	Micro-Aerial Vehicle
MIMO	Multi-Input Multi-Output
MLPID	Multi-Loop PID
MPC	Model Predictive Control
MRAC	Model Referenced Adaptive Control
MTFC	Mamdani-Type Fuzzy Control
NED	North-East-Down
NLMPTC	Nonlinear Model Predictive Tracking Control
NN	Neural Networks
OPFB	Output Feedback
PID	Proportional Integral Derivative
RCAH	Rate Command Attitude Hold
RPA	Remotely Piloted Aircraft
RPAS	Remotely Piloted Aircraft Systems
SISO	Single-Input Single-Output
TPP	Tip-Path Plane
UAS	Unmanned Aircraft System
UAV	Unmanned Aerial Vehicle
UKF	Unscented Kalman Filter

Roman Symbols

a_0	Main rotor collective pitch
a_1	Longitudinal tilt of main rotor blade
b_1	Lateral tilt of main rotor blade
c_b	Blade chord
c_1	Longitudinal tilt of stabilizer blade
d_1	Lateral tilt of stabilizer blade
$d^P(t)$	Distance of particle from body center of mass
$\mathbf{f}$	Force vector $[X, Y, Z]$
g	Gravity
$[l_m,\ y_m,\ h_m]$	Main rotor offset distance from center of mass
$[l_t,\ y_t,\ h_t]$	Tail rotor offset distance from center of mass
m	Mass
p	Pitch rate, $\dot{\theta}$
p^I	Inertial frame position vector
p^B	Body-fixed frame position vector
q	Roll rate, $\dot{\phi}$
q_0	Quaternion constant
q_i	Quaternion parameters
r	Yaw rate, $\dot{\psi}$
$\mathbf{u}_c$	Control input
u_i	Inflow velocity
v^B	Translational velocity vector $[u\ v\ w]^T$
$\mathbf{x}$	State vector
$\mathbf{y}$	Output vector
A_b, B_a	Rotor cross-coupling terms
A_{lon}, B_{lat}	Longitudinal and lateral control derivatives
$C_{l\alpha}$	Main rotor blade lift coefficient
C_D	Main rotor blade drag coefficient
F	Force
$F_{\parallel}$	Force parallel to blade
$F_{\perp}$	Force perpendicular to blade
$\mathcal{F}_B = O_B,\ \mathbf{i}_B,\ \mathbf{j}_B,\ \mathbf{k}_B$	Body-fixed frame
$\mathcal{F}_I = O_I,\ \mathbf{i}_I,\ \mathbf{j}_I,\ \mathbf{k}_I$	Inertial frame
$\mathcal{F}_h = O_h,\ \mathbf{i}_h,\ \mathbf{j}_h,\ \mathbf{k}_h$	Main rotor hub frame
G	Linear momentum
H^{CM}	Angular momentum
$\mathcal{I}$	Inertia tensor
$\mathcal{I}_b$	Rotor blade inertia
J_{xx}	Moment of inertia

J_{xy}	Product of inertia
J	Inertia matrix
K_β	Blade spring stiffness
M^{CM}	Moments about the center of mass
N_{mb}	Number of main rotor blades
N_{tb}	Number of tail rotor blades
P	Particle point mass
$Q = [q_0, q_1, q_2, q_3]$	Quaternion angle representation
Q_{mr}	Main rotor counter-torque
Q_{tr}	Tail rotor counter-torque
R	Rotation matrix
R_b	Main rotor disc radius
T_{mr}	Main rotor thrust
T_{tr}	Tail rotor thrust
U	Total air velocity on blade
U_T	U component $\parallel$ to the hub plane and $\perp$ to the blade
U_P	U component $\perp$ to the hub downward
U_R	U component radially outward from the blade
V	Volume
V_∞	Free stream velocity

Greek Symbols

Θ	Attitude vector $\Theta = [\theta, \phi, \psi]$
ω	Angular rate vector $[p, q, r]$
υ	Velocity
θ	Pitch angle
ϕ	Roll angle
ψ	Yaw angle
ψ_b	Main rotor blade azimuth angle, $\psi_b = \Omega t$
ψ_t	Tail rotor blade azimuth angle, $\psi_t = \Omega_t t$
Ω	Main rotor blade angular velocity
Ω_t	Tail rotor blade angular velocity
τ	Moment vector $[L, M, N]$
τ_f	Rotor time constant
$\lambda_i, i = 1, 2, 3$	Inflow dynamics
λ_β	Flapping frequency ratio
γ	Lock number
δ_{col}	Main rotor collective input
δ_{ped}	Tail rotor collective input
δ_{lat}	Lateral cyclic angle
δ_{lon}	Longitudinal cyclic angle
β	Blade flapping angle
ξ	Blade lead-lag angle
ζ	Blade pitch/feathering
ϕ_b	Inflow angle
α	Blade angle of attack
Θ_p	Blade pitch angle
α_{hb}	Blade α with respect to hub plane
α_b	Blade α with respect to U
ρ	Volumetric mass density m/V
ρ_a	Air density

Sub- and Super-scripts

$\square^{CM}$	Center of mass
$\square^{p}$	Refers to a point
$\square_N$	Inertial navigation reference frame
$\square_B$	Body-fixed frame

Mathematical Operators and Symbols

$S(\cdot)$, $\hat{x}$	Skew symmetric matrix $\hat{x} = \begin{bmatrix} 0 & -x_3 & x_2 \\ x_3 & 0 & -x_1 \\ -x_2 & x_1 & 0 \end{bmatrix}$
$\square^T$	Matrix transpose
$\square^{-1}$	Matrix inverse
$\square^{-T}$	Matrix inverse transpose
$\dot{\square}$	Time derivative
$\perp$	Perpendicular
$\parallel$	Parallel
$\times$	Cross-product
c_θ	$cos\theta$
s_θ	$sin\theta$
t_θ	$tan\theta$

1 Introduction

Unmanned Aircraft Systems[1] (UAS) functioning at different 'levels of autonomy' have seen unprecedented levels of growth during the past two decades. Although military applications have dominated the field, there is increased interest in using UAS in civilian and public domain applications, and as such, government and civilian authorities worldwide are working towards developing and implementing the roadmap for UAS integration into commercial airspace (national airspace system).

Focusing on real, complex missions in outdoors environments, the two most widely used vehicle configurations are fixed-wing UAVs and rotorcraft[2] UAVs (RUAVs) with each type having advantages and disadvantages, and specific challenges when it comes to the Flight Control System (FCS) design. While fixed-wing UAVs are ideal for long flight and high payload applications, rotorcraft has distinct advantages in maneuverability through the use of rotary blades, which allows for rotorcraft to produce the necessary aerodynamic thrust forces without the need of relative velocity, resulting in vertical take-off and landing (VTOL), hovering, and flight at very low altitude. These valid reasons and the fact that rotorcrafts do not require any runway infrastructure contribute to why they are preferred for a wide spectrum of applications (and in terrains unreachable by fixed-wing UAVs) [93].

However, control of rotorcraft has inherent challenges as helicopters are highly nonlinear underactuated systems (fewer control inputs than system states) with significant dynamic coupling that is attributed to the force and torque generation process, and significant parameter and model uncertainty due to the complicated aerodynamic nature of the thrust generation. Therefore, there is major interest in theoretical, applied and application-specific perspectives of helicopter controller designs and their actual testing and implementation to autonomous flight. Although most control designs were initially based on linearized helicopter dynamics using the widely adopted concept of stability derivatives, in recent years there has been considerable research related to helicopter flight control based on nonlinear dynamic representations. There exist a number of general surveys providing a broad overview of rotorcraft navigation, but with little focus placed on control methods and architectures used for rotorcraft navigation and control. These surveys focus on FCS hardware and software, perception techniques, and application-specific implementations, with only a small section dedicated to actual derivation of control methods/techniques, their applicability and implementation challenges.

Furthermore, actual rotorcraft platforms and/or rotorcraft platform models mentioned in the literature that have been used to design FCS and navigation/control algorithms range from full-to small-scale ones, which can be flown with/without pilot commands and, especially in early research, (small-scale ones) may have been mounted on an experimental gimbaled stand to facilitate indoor flight. Advances in both sensing and computing technology have led to increased precision and reliability as well as significantly higher update rates in on-board navigational sensors (i.e., Global Positioning Systems (GPS)/Differential GPS (DGPS), IMUs, altimeters, etc.) and increased processing capabilities for the flight computer. As a result, along with advancements in control theory, a number of control strategies has been implemented for various rotorcraft flight modes and maneuvers, validated using numerical simulations and/or experimental results.

Flight controllers typically fit in one of three main categories, linear, nonlinear, or model-free, depending on the model representation used to describe the rotorcraft dynamics, which are inherently nonlinear, making derivation of a full and accurate model difficult. Nonlinear models are the most difficult to derive and implement due to the complexity and order of polynomial or differential equations necessary to fully describe the system dynamics. Additionally, there is a number of phenomena that exist in nonlinear systems, such as the presence of multiple equilibria and modes of behavior that cannot be described by a linear model. Linear controllers use a number of assumptions to simplify the nonlinear dynamic models. Usually, linearization occurs about some particular condition. Linear controllers are valid within a small subset of

[1]There is on-going debate about the proper terminology for such systems; several terms are being used, like UAVs, Remotely Piloted Aircraft (RPA), and RPA Systems (RPAS). In this paper, the term UAS is chosen to reflect the overall system, while the term UAV is preferred for just the unmanned aerial vehicle itself.

[2]In this paper, rotorcraft or unmanned rotorcraft, helicopter or unmanned helicopter refer to the same type of aerial vehicle.

the entire flight envelope. This limits the capability, maneuvers and flight scenarios of linear controllers. Despite their drawbacks, linear controllers are still the easiest to design and implement. Finally, model-free control designs, as the name suggests, do not require a model of the helicopter dynamics. Instead, model-free control designs utilize learning or human based algorithms. These types of controllers tend to rely heavily on pilot commanded flight testing in order to teach the algorithms that mimic the human pilot behavior and decision making.

This paper deviates from previous studies contributing to providing a comprehensive overview of rotorcraft navigation and control. Unlike other existing surveys, this survey is specific to (the traditional main/tail rotor configuration) helicopters placing in-depth emphasis on existing navigation control methods and modeling techniques, loop architectures and structures, implementations, and a detailed review of research over the past decades. The objective of this study is to determine capabilities and effectiveness of algorithms for autonomous flight, navigation, obstacle avoidance, and performance of acrobatics, therefore, providing a basis for comparison of control techniques and related applications.

The natural outgrowth and another major contribution of this survey, which has been one of its main initial goals and objectives, is the development of a 'one-fits-all' comprehensive,[3] but modular, fault-tolerant and robust sensor-based navigation controller architecture along with the corresponding 'timing architecture', applicable to any rotorcraft platform. The proposed 'one-fits-all' architecture includes a suite of on-board navigational sensors, the navigation controller module, a hierarchical guidance and navigation structure, and human-in/human-on-the-loop capabilities. Under this configuration, the specific (linear, nonlinear, linearized) controller is not but one 'module', while the corresponding sensors may be chosen from the library of available ones. The design facilitates replacement or addition of navigational sensors and the use of any control algorithm without changing the overall structure. The corresponding timing architecture guarantees real-time performance and takes into consideration execution of control laws, sensor feedback, data logging, communication processes, hardware constraints, and task management. For clarification purposes, a specific timing diagram is considered in terms of event sequences and time allocations based on the DU^{2}SRI experimental helicopter platform.

The survey paper is organized as follows: Section 1.1 presents a summary of the already published surveys to justify further the need and importance of this study. Section 2 discusses the 'reference template' for this survey, where each review includes the helicopter platform, model structure, identification method, loop architecture, control technique(s), flight modes, maneuvers, and the type of results obtained. Section 3 is an integral part of the paper as it presents and summarizes helicopter dynamics used to derive specific controllers. Section 4 provides a review of linearization, and a complete linear model structure, while Section 6 details the generalized loop architectures and Section 7 provides a review of control methods. Section 8 discusses a comprehensive listing of research in rotorcraft navigation and control, including model structure, control method, flight maneuvers and results. Section 9 describes the proposed comprehensive navigation control and timing architecture, while Section 10 concludes the paper. The reference list is rather comprehensive and includes model-free approaches, although not surveyed in this paper.

1.1 Summary of Published Surveys

Six surveys, including work conducted by over 25 institutions from around the globe, have already been published on advances in RUAV systems [27, 31, 93, 143, 155, 200], exploring research in the area of guidance, navigation, control, and perception techniques. These surveys include vehicle platforms, control techniques, FCS design, vision systems, visual perception techniques, and a wide range of vehicles. However, very little detail is provided on the control architectures and navigation/control techniques themselves.

Published in 2004, *"Control and Perception Techniques for Aerial Robotics"* [143], was mostly focused on perception techniques, reviewed various methods that have been applied to aerial robotics including different vehicle platforms and flight control hardware. It provided a very brief survey of control architectures and methods. This survey covers a broad range of UAVs and provides only a small number of examples

[3]This architecture has been developed by the authors and other graduate students at the University of Denver Unmanned Systems Research Institute (DU^{2}SRI), www.du2sri.com.

of rotorcraft control techniques. No emphasis is placed on the loop structures, modeling techniques, or simulation results.

Published in 2008, *"A Practical Survey on the Flight Control System of Small Unmanned Helicopter"* [200], reviewed and compared various control methodologies for unmanned helicopters, including linear, nonlinear, and model-free techniques. This survey provided diagrams of the control methodologies, some discussion of flight modes, advantages and disadvantages of each approach. While the examples for each method are discussed in detail, only PID, $\mathcal{H}_\infty$, μ-synthesis, Dynamic Inversion, and Neural Network Adaptive techniques are discussed, with one major example provided for each. The survey does not discuss many of the other control methods that have been used in past research, and lacks discussion of modeling techniques used.

Published in 2010, *"Autopilots for Small Unmanned Aerial Vehicles: A Survey"* [31], presented a survey of autopilot systems intended for use with small or micro UAVs. This survey focuses heavily on the hardware involved in designing autopilots without discussing modeling, loop architectures or providing much detail on control methods used for autopilot design.

Published in 2011, *Linear and Nonlinear Control of Small-Scale Unmanned Helicopters* [155], offered a high-level summary of linear and nonlinear control techniques and presented detailed models of the nonlinear and linear dynamics of a small-scale helicopter. A summary of control methodologies was also presented with details on the states used for modeling, vehicle platforms, and the application of the techniques. Though this survey provides a good summary of control methods, little detail is provided on loop architectures or obtained results.

Published in 2012, *"Survey of Advances in Guidance, Navigation, and Control of Unmanned Rotorcraft Systems"* [93], provided a detailed review of research involving RUAVs over the past 20 years, focusing on Guidance, Navigation and Control (GNC). It presented classifications of RUAVs, from full-scale optionally piloted helicopters down to MAVs. An in depth review was organized by institution, which included the class of vehicle platforms used, most recent research areas and projects, as well as major achievements and milestones. In addition, a characterization of levels of autonomy was presented, providing definitions and categorizations for levels of autonomy in GNC. A summary of advances in modeling and identification techniques was also provided. Flight control systems were classified into three main categories: linear, nonlinear, and learning-based controllers. A review of existing work was outlined, including the specific method (PID, $\mathcal{H}_\infty$, LQR, etc.), operating condition, and type of results, whether simulated or experimental. However, little detail was provided on the exact structure of each approach or the states used and in the model design. Additionally, this work focuses on navigation systems, including hardware, vision techniques and algorithms, sensing technology, and work conducted with quadrotors and MAVs.

Published in 2014, *"A Survey of Small-Scale Unmanned Aerial Vehicles: Recent Advances and Future Development Trends"* [27], provided a detailed overview of advances of small-scale UAVs including platforms and scientific research areas. This study covers multiple UAV types, categorized as fixed-wing, rotorcraft, and flapping wing vehicles. The survey provided an overview of the recent advances in UAV platforms, with a classification based on size and military or civilian applications. Advances in flight control hardware, including processing hardware, sensors, and GCS were presented. Key achievements in UAV research, including platform design, dynamic modeling and control methods were summarized. However, this survey provides only a brief overview of flight control of small-scale rotorcraft UAVs in the form of a table listing a key example for each control technique. This list includes works for all types of rotorcraft and is not limited to helicopters. Little detail is provided about loop structures and architectures.

To the best of the authors' knowledge, the presented comprehensive study in subsequent sections offers the foundations for unmanned rotorcraft navigation and control providing at the same time justifications for the use of specific algorithms based on mission profiles.

2 Reference Template for the Comparative Study

In order to provide an as comprehensive as possible comparison of existing research, a thorough review of model-based control techniques and loop architectures is conducted and discussed along with limitations and advantages of each technique. Each review includes the helicopter platform, model structure, identification method, loop architecture, control technique(s), flight modes, maneuvers, and the type of results obtained. Thus, in order to provide the same 'reference template' for comparison purposes, the following has been considered throughout the survey:

Helicopter Platform: This refers to the helicopter platform that consists of a base helicopter, added flight control hardware, software and sensors, and ground control station (GCS). Because no two helicopters perform the same, the base helicopter platform is identified for comparison purposes; two examples include the Yamaha RMAX and Raptor SE90.

Helicopter model and identification method: The helicopter model structure and parameter identification process plays an important role in navigation control, as it determines the model used for controller design and, subsequently, simulation studies or experimentation. Because of the challenges inherent in control of rotorcraft, there are a number of problems that must be solved to design a successful flight controller. In order to develop a flight controller that can be successfully applied to the majority of small-scale rotorcraft platforms, it is important to select a model structure consisting of parameters that provide the most meaningful physical description of the helicopter dynamics while keeping the order of the model at a minimum. Additionally, this model must be selected in such a way that the predicted responses are identical to the response of the actual helicopter dynamics. The model is categorized as either linear or nonlinear (the linearized model is obtained from the nonlinear model). While linear approaches are generally easier to implement, the linear model is limited to the dynamics around a specific flight condition, most commonly hover or cruise flight. Nonlinear models cover a much wider flight envelope, though are generally far more complex. For derivation purposes, the helicopter assumed is to be a 6 Degrees of Freedom (DOF) rigid body structure under Newton-Euler equations. Next, the values of the parameters in the dynamic model must be extracted. One such method is parameter identification, which requires flight testing to determine the input-output (I/O) dynamics of the system. There exist a number of methods (i.e. time-domain analysis, frequency-domain analysis) and computational tools (i.e. MATLAB, CIFER) for system identification. In addition to determining the general model structure, the order of the parametric dynamic model and specific state vector used in control design must be identified. Figure 1 illustrates an example process of helicopter modelling, control design, parameter identification using CIFER and recursive least squares (RLS) approaches, and validation for both linear and nonlinear controllers using the *X-Plane* flight simulator [155].

Control loop architecture: The control loop architecture depends highly on the type of model used and specific control mode to be performed (hover, cruise, etc.). The flight controller can be designed to provide varying degrees of control, from assisting the pilot in stabilization of the helicopter dynamics, most commonly attitude and altitude, to fully autonomous navigation. A feedback control law $\Phi(y)$ must be designed to track this commanded reference or predefined trajectory $y_r(t)$ and that guarantees the control inputs remain within their operational bounds. The tracking objective is given as $\lim_{t\to\infty} ||y(t) - y_r(t)|| = 0$. The design of this control law is dependent on the loop architecture and helicopter dynamic model. This control design process is shown in Fig. 2 for both linear and nonlinear models. The most common loop architecture in helicopter dynamics consists of a translational outer-loop and attitude inner-loop structure (as described in subsequent sections).

Control technique: The surveyed control techniques may be classified into one of three categories: linear, nonlinear and model-free. After summarizing each controller, and its application, each control approach is categorized accordingly as in the comparative table shown in Fig. 3. The linear methods are divided into single-input single-output (SISO) and multi-input multi-output (MIMO) methods. Proportional-Integral-Derivative (PID) controllers fall under the SISO linear control category. MIMO linear controllers consist of linear feedback controllers, such as linear quadratic regulators (LQR), Linear Quadratic Gaussian (LQG), $\mathcal{H}_\infty$ controllers, and gain scheduling controllers that may utilize synthesis techniques. Nonlinear methods are divided into linearized and fully nonlinear methods. Linearized techniques start with a nonlinear

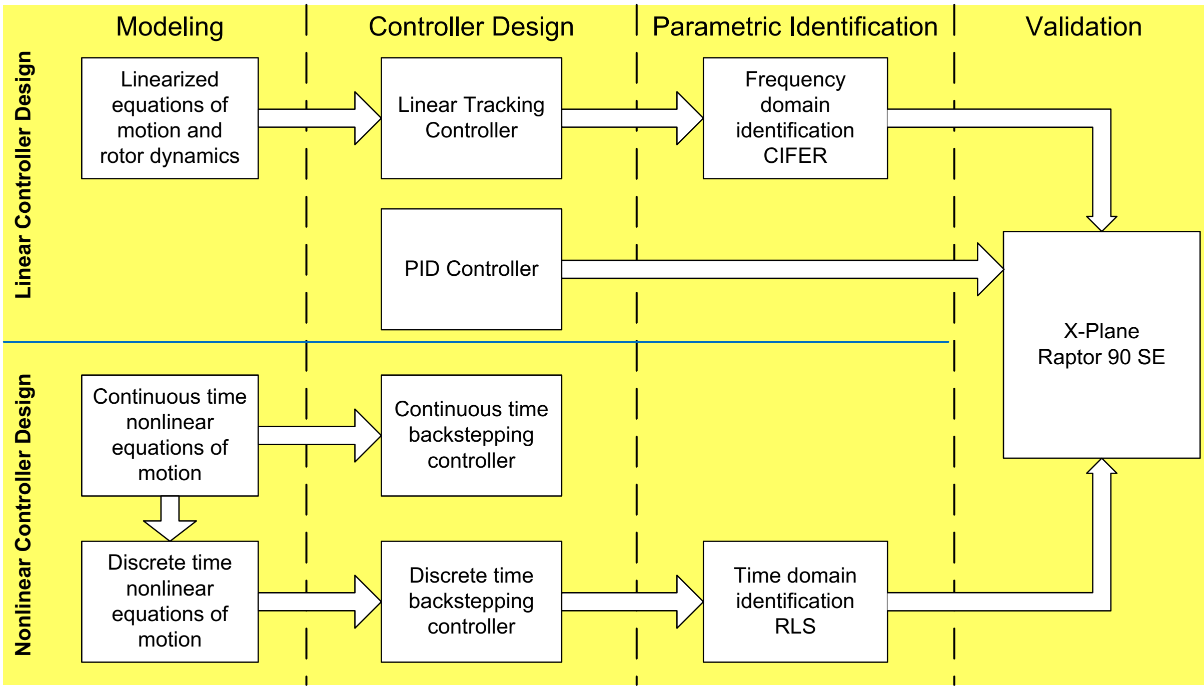

Fig. 1 Model identification and control design [155]

model, and utilize various techniques to linearize the system dynamics, including input/output feedback linearization. Other methods can, then, be applied, including adaptive control, model predictive control (MPC), and nested saturation loops. Backstepping control approaches utilize fully nonlinear models. Lastly, model free and learning-based methods include neural networks (NN), fuzzy logic, and human-based learning techniques. Human-based learning techniques include differential dynamic programming (DDP) and reinforcement learning. Model-free methods are not surveyed in this paper.

Flight mode and maneuvers: The capability of a navigational controller is largely dependent on the specific type of maneuver and flight mode under consideration. Typically, linear methods are restricted to maneuvers that are valid within the flight condition (i.e. hover, cruise) used to derive the model. More complex controllers, such as gain switching or nonlinear methods, allow for more aggressive maneuvers and operation within a wider flight envelope. Helicopter maneuvers include i.)basic (non-aggressive) maneuvers, like hover, level flight, turns, and climbs or descents, and ii.) advanced (aggressive) maneuvers, including pirouettes, Figure-∞, and auto-rotation landings.

Results: Validation of control design may be classified in one of three categories, theoretical, simulation, and experimental. Theoretical validation of control approaches provide proof that a technique is capable of providing a solution to the control problem. However, validation of the controller performance requires both simulated and experimental results. Simulation of navigational controllers can be done using either a model of the helicopter dynamics for example, *Simulink*/MATLAB, or a flight simulator, such *X-plane* or *Flight Gear*. While using a flight simulator eliminates the need to develop a mathematical model, not all platforms are available in the associated libraries. Mathematical model simulation allows for matching the dynamics of a particular platform, but requires the full nonlinear dynamic model to provide the most realistic simulation. An alternative approach is to combine the two; for example, one may use *Simulink*/MATLAB to simulate the dynamics and output the flight data to a flight simulator for visualization purposes. The most common approaches

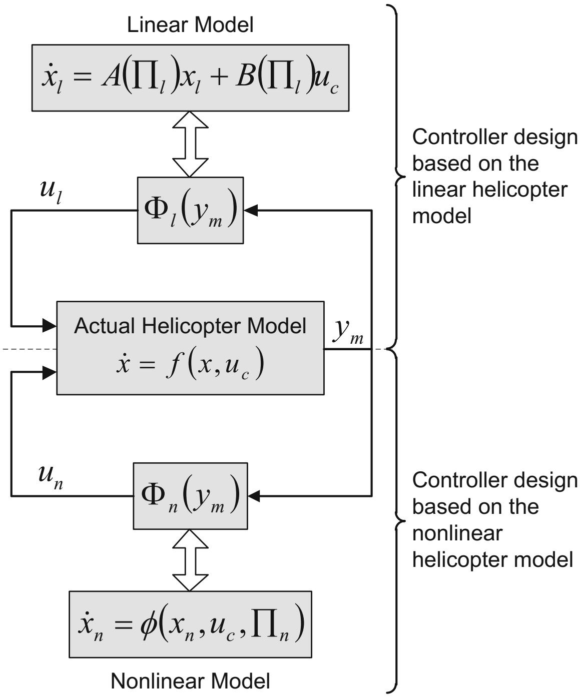

Fig. 2 This diagram illustrates the controller design process. Here, $u_l = \Phi_l(y_m)$ is the linear feedback control law, $u_n = \Phi_n(y_m)$, is the nonlinear feedback control law, Π_l and Π_n are the linear and nonlinear parameter vectors, y_m is the system measurement vector, and x_l and x_n are the linear and nonlinear state vectors. The actual helicopter dynamics is given by $\dot{x} = f(x, u_c)$, the nonlinear model is given by $\dot{x}_n = \phi(x_n, u_c, \Pi_n)$, and the linear model is given by a set of first-order differential equations where A is the state matrix, and B is the output matrix [155]

to simulation-based control validation utilize a non-linear model, even if a linearized model is used for controller design. Although experimental results are the most desirable outcome of validation methods, they are the most difficult to obtain and they are usually limited to a more conservative control technique.

3 Helicopter Dynamics

The commonly used helicopter configuration with one main and tail rotor is governed by the typical dynamics structure shown in Fig. 4. The helicopter is considered as a 6 DOF rigid body with forces and moments affecting vehicle dynamics being generated by the rotors, body, gravity and aerodynamics. In detail, helicopter components that affect dynamics may be lumped into the following subsystems for modeling purposes: main rotor; tail rotor; fuselage body; tail horizontal stabilizer (fin); tail vertical stabilizer (fin); stabilizer or flybar; engine; servo linkages and swash plate; actuators or servos. Forces and moments generated by each subsystem are first determined and, then, combined into generalized forces and moments relative to a body-fixed coordinate system. Forces may be either controlled (rotor thrust) or uncontrolled (drag forces, wind gusts), and they are modeled as functions of the helicopter states, pilot inputs, and environmental factors. These forces, ultimately, drive the helicopter's rigid body dynamics and kinematics equations, which define the helicopter dynamic model.

Aerodynamic forces modeling is complicated and difficult; thus, in order to achieve high-fidelity models of the helicopter aerodynamic properties, in principle, finite-element techniques are used, which are time consuming and computationally complex. However, for controller design purposes, the 'helicopter system' may be divided into lumped-parameter models for each subsystem using simplified aerodynamics. This way, each helicopter subsystem is viewed and modeled separately in order to approximate the dynamics while considering certain assumptions. This approach can significantly reduce the system state-space and the number of parameters describing its behavior.

For navigational purposes, a fixed reference coordinate system is established. This is an Earth-fixed coordinate system defined by the FCS designer, and fully dependent on where the helicopter will be operating. Typically, GPS receivers are used for navigational feedback.

3.1 Helicopter Rigid Body Equations of Motion

The helicopter motion is defined relative to an inertial reference frame in order for Newtonian mechanics to hold true. However, establishing a reference frame fixed to the helicopter body significantly simplifies the analysis of forces acting on the helicopter. The set of equations describing helicopter motion is derived based on two Cartesian reference frames as follows:

– The body-fixed Cartesian frame is defined as $\mathcal{F}_B = \{O_B, \mathbf{i}_B, \mathbf{j}_B, \mathbf{k}_B\}$; the origin is fixed at

Fig. 3 Classification of control techniques

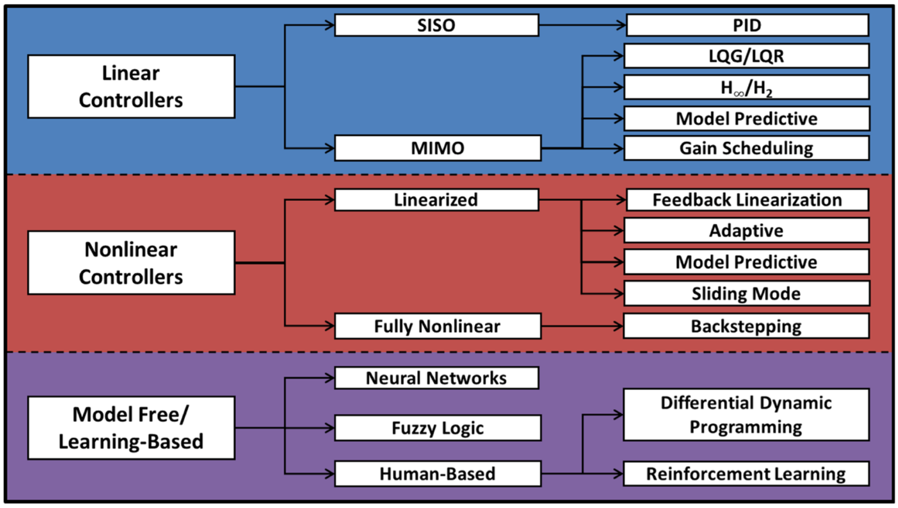

the helicopter center of mass. The unit vector $\mathbf{i}_B$ points from the origin toward the helicopter nose. The unit vector $\mathbf{j}_B$ points from the origin to the right of the fuselage. The unit vector $\mathbf{k}_b$ points downward. The orientation of these vectors in relation to the helicopter body is seen in Fig. 5.

– The inertial Earth-fixed Cartesian frame follows the North-East-Down (NED) directional convention, defined as $\mathcal{F}_I = \{O_I, \mathbf{i}_I, \mathbf{j}_I, \mathbf{k}_I\}$. The unit

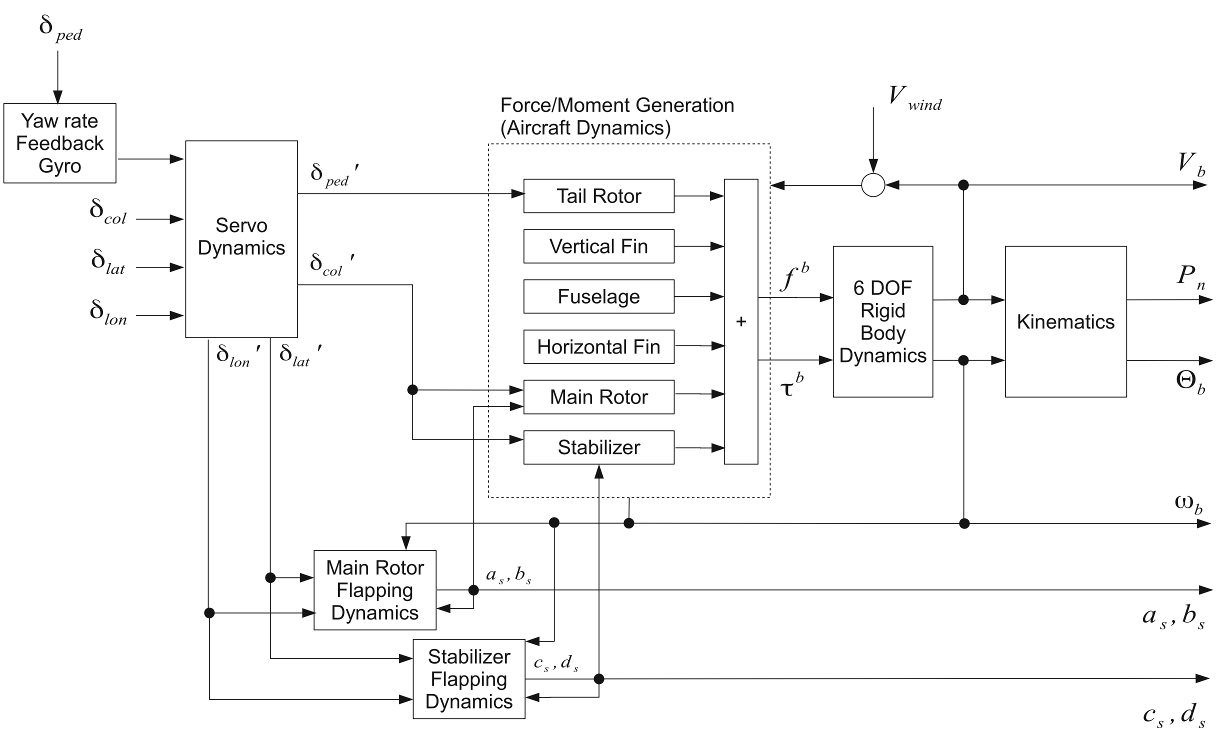

Fig. 4 Helicopter dynamics

vectors $\mathbf{i}_I$, $\mathbf{j}_I$, and $\mathbf{k}_I$, point North, East and Down towards the center of the Earth, respectively, as shown in Fig. 6.

Rigid body dynamics are governed by the following Newton-Euler laws of motion:

$$F_{net} = \frac{d}{dt}G(t) \tag{1}$$

$$M_{net}^{CM} = \frac{d}{dt}H^{CM}(t) \tag{2}$$

These equations provide information on translational and angular velocities as a result of forces acting on the rigid body. The net external forces, F_{net}, are defined as the rate of change of the body's linear momentum, $G(t) = mv(t)$. The net external moments about the body's center of mass, M_{net}^{CM}, are equal to the rate of change of angular momentum about the center of mass, $H^{CM} = \mathcal{I}\omega$. These moments are derived here for a rigid body following the procedures in [13, 14] and [7].

The forces and moments acting on the body with respect to the inertial frame are given as follows:

$$F_I(t) = m\dot{v}_I^{CM}(t) \tag{3}$$

$$M_I^{CM} = \dot{R(t)}J\omega_B(t) + R(t)J\dot{\omega}_B(t) \tag{4}$$

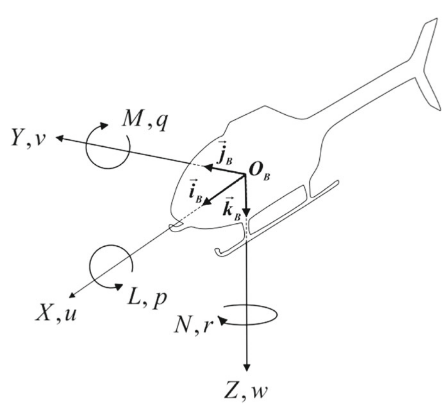

Fig. 5 Body-fixed frame coordinate system, [155]

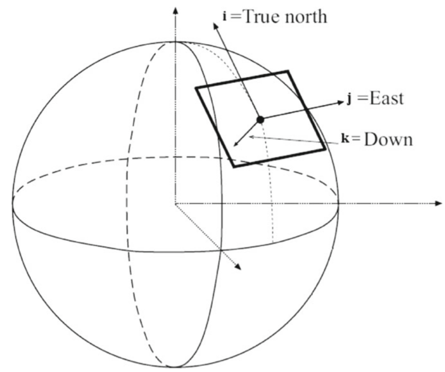

Fig. 6 North-East-Down Earth-fixed reference frame, [46]

The forces and moments may be expressed in the body-fixed frame following the procedure in [13] as:

$$F_B(t) = m\left(\omega_B(t) \times v_B^{CM}(t) + \dot{v}_B^{CM}\right) \tag{5}$$

$$M_B^{CM} = \omega_B \times J\omega_B(t) + J\dot{\omega}_B(t) \tag{6}$$

The helicopter equations of motion described in Eqs. 5 and 6 are known as the Newton-Euler equations of motion for a rigid body, where $f_B = F_B^{CM}$ and $\tau^B = M_B^{CM}$, and are given in matrix-vector as:

$$\begin{bmatrix} mI_3 & 0 \\ 0 & J \end{bmatrix}\begin{bmatrix} \dot{v}_B \\ \dot{\omega}^B \end{bmatrix} + \begin{bmatrix} \omega^B \times mv^B \\ \omega^B \times J\omega^B \end{bmatrix} = \begin{bmatrix} f^B \\ \tau^B \end{bmatrix} \tag{7}$$

The forces, moments, translational velocities, and angular rates may be separated into components corresponding to each of the principal axes of the body-fixed frame as $f^B = [X \ Y \ Z]^T$, $\tau^B = [L \ M \ N]^T$, $v_B^{CM} = [u \ v \ w]^T$, and $\omega_B = [p \ q \ r]$, respectively.

3.2 Position and Orientation Dynamics

For flight navigation, it is necessary to express the position and orientation of the helicopter with respect to an Earth-fixed inertial reference frame. To do so, a relationship between the body-fixed and inertial frames is established to provide a method of describing the orientation of the frames relative to one another. This relationship is accomplished in terms of the *rotation matrix* R that represents a series of rotations from the body-fixed frame to the final orientation of the inertial frame [38, 177]. The rotation matrix is expressed in terms of roll (ϕ), pitch (θ), and yaw (ψ) Euler angles with the rotations occurring in a specific sequence as seen in Figs. 7, 8 and 9. The first rotation moves the helicopter an angle of ψ about the $\hat{k}$ axis. The second rotation moves the helicopter an angle of θ about the new $\hat{j}$ axis. Finally, the last rotation moves the helicopter an angle of ϕ about the new helicopter $\hat{i}$ axis.

The final rotation matrix is obtained by multiplying the individual rotation matrices in Eq. 8 following the properties of transformations [177]:

$$R_\psi = \begin{bmatrix} \cos\psi & \sin\psi & 0 \\ -\sin\psi & \cos\psi & 0 \\ 0 & 0 & 1 \end{bmatrix} \quad R_\theta = \begin{bmatrix} \cos\theta & 0 & -\sin\theta \\ 0 & 1 & 0 \\ \sin\theta & 0 & \cos\theta \end{bmatrix} \quad R_\phi = \begin{bmatrix} 1 & 0 & 0 \\ 0 & \cos\phi & \sin\phi \\ 0 & -\sin\phi & \cos\phi \end{bmatrix} \tag{8}$$

$$R(\Theta) = \begin{bmatrix} \cos\psi\cos\theta & \cos\psi\sin\phi\sin\theta - \cos\phi\sin\psi & \sin\phi\sin\psi + \cos\phi\cos\psi\sin\theta \\ \cos\theta\sin\psi & \cos\phi\cos\psi + \sin\phi\sin\psi\sin\theta & \cos\phi\sin\psi\sin\theta - \cos\psi\sin\phi \\ -\sin\theta & \cos\theta\sin\phi & \cos\phi\cos\theta \end{bmatrix} \tag{9}$$

The rotation matrix time derivative, derived using the proof in [177], is given as:

$$\dot{R} = R\hat{\omega}_B \tag{10}$$

where $\hat{\omega}_B$ is the skew-symmetric matrix representation of the angular rate vector. The orientation dynamics are derived using Eq. 10 [70, 138, 155, 177] as:

$$\dot{\Theta} = \begin{bmatrix} \dot{\phi} \\ \dot{\theta} \\ \dot{\psi} \end{bmatrix} = \Psi(\Theta)\omega^B \tag{11}$$

where $\Psi(\Theta)$ is given as:

$$\Psi(\Theta) = \begin{bmatrix} 1 & \sin\phi\tan\theta & \cos\phi\tan\theta \\ 0 & \cos\phi & -\sin\phi \\ 0 & \sin\phi/\cos\theta & \cos\phi/\cos\theta \end{bmatrix} \tag{12}$$

3.3 Complete Helicopter Dynamics

The position and velocity dynamics together with the orientation dynamics form the complete helicopter equations of motion in terms of the helicopter's body-fixed frame forces and moments, and are given as:

$$\begin{aligned} \dot{p}^I &= v^I \\ \dot{v}^I &= \frac{1}{m} R f^B \\ \dot{R} &= R\hat{\omega}^B \\ I\dot{\omega}^B &= -\omega^B \times (I\omega^B) + \tau^B \end{aligned} \tag{13}$$

with p^I and v^I denoting the position and linear velocity of the helicopter center of gravity (CG) with respect to an earth-fixed reference frame. In addition to the forces acting on the body, the effect of gravity on the body frame is considered by transforming the gravity vector from the inertial frame, $g_I = [0 \;\; 0 \;\; g]^T$, to body-frame, $g_B = R^T(t)g_I$. Expanding the Newton-Euler equations of motion in Eq. 7 and adding the force of gravity, the translational velocity and angular rate equations

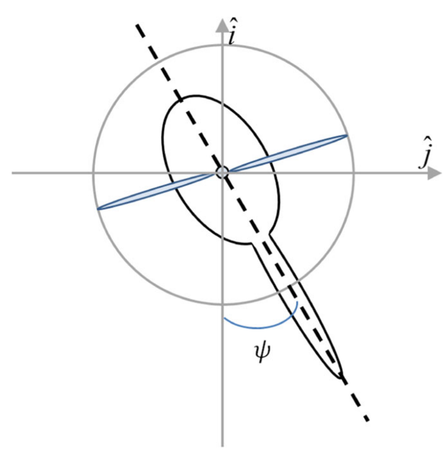

Fig. 7 Helicopter yaw motion

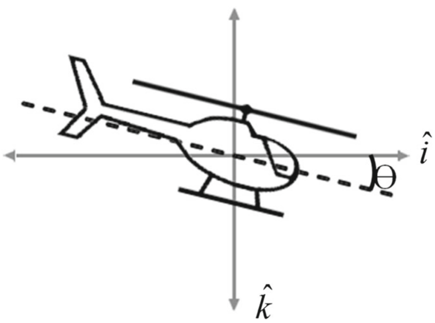

Fig. 8 Helicopter longitudinal motion

of motion with respect to the body-fixed frame are given as:

$$\dot{u} = rv - qw + R_{31}g + X/m \tag{14}$$

$$\dot{v} = pw - ru + R_{32}g + Y/m \tag{15}$$

$$\dot{w} = qu - pv + R_{33}g + Z/m \tag{16}$$

$$\dot{p} = qr(J_{yy} - J_{zz})/J_{xx} + L/J_{xx} \tag{17}$$

$$\dot{q} = pr(J_{zz} - J_{xx})/J_{yy} + M/J_{yy} \tag{18}$$

$$\dot{r} = qp(J_{xx} - J_{yy})/J_{zz} + N/J_{zz} \tag{19}$$

The position and orientation trajectory dynamics may be obtained by integrating the rigid body dynamics in Eqs. 14 – 19 through the kinematic equations in Eq. 13. The inertial position can be found given the body velocities through $\dot{p}^I = v^I = Rv^B$. The Euler rates can be found through the relationship $\dot{\Theta} = \Omega(\Theta)\omega_b$ in Eq. 11.

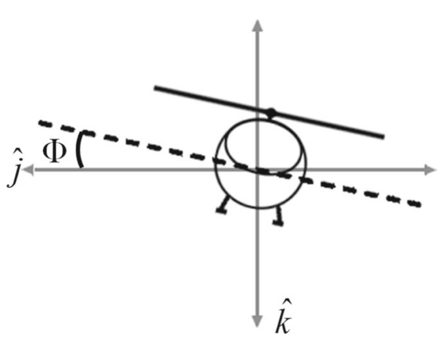

Fig. 9 Helicopter lateral motion

The final position and orientation dynamics are given as:

$$\dot{x}^I = c_\theta c_\psi u + (s_\theta s_\phi c_\psi - c_\phi s_\psi)v + (s_\theta c_\phi c_\psi + s_\phi s_\psi)w \tag{20}$$

$$\dot{y}^I = c_\theta c_\psi u + (c_\phi c_\psi + s_\phi s_\psi s_\theta)v + (c_\theta s_\psi s_\theta - c_\psi s_\phi)w \tag{21}$$

$$\dot{z}^I = -s_\theta u + c_\theta s_\phi v + c_\phi c_\theta x \tag{22}$$

$$\dot{\phi} = p + s_\phi t_\theta q + c_\phi t_\theta r \tag{23}$$

$$\dot{\theta} = c_\phi q - s_\phi r \tag{24}$$

$$\dot{\psi} = \frac{s_\phi}{c_\theta} q + \frac{c_\phi}{c_\theta} r \tag{25}$$

3.4 Forces and Torques

A result of the main and tail rotor rotation is the generation of thrust and torques acting on the helicopter body. Gravity is also acting on the helicopter body, and must be taken into account while determining the total body forces on the helicopter. The forces and torques acting on the helicopter are functions of the main rotor thrust, T_{MR}, tail rotor thrust, T_{TR}, and the main rotor cyclic angles, a_1 and b_1 [70].

The torques acting on the helicopter body are a result of the forces being offset from the center of gravity. The relation below defines the relationship between the force (F), distance (d) and the resultant torque:

$$\tau = Fd \tag{26}$$

The thrust generated by the main rotor results in a translational force on the helicopter. This thrust is perpendicular to the Tip-Path-Plane (TPP) which is the plane formed by the blade tips. This force vector can be decomposed into components along the body-frame x, y, and z axis. The magnitude of the thrust vector is represented as T_{MR}. The components of the main rotor forces as a result of the blade flapping and thrust are given by:

$$F^B_{MR} = \begin{bmatrix} X_{MR} \\ Y_{MR} \\ Z_{MR} \end{bmatrix} = \begin{bmatrix} -T_{MR}\sin a_1 \\ -T_{MR}\sin b_1 \\ -T_{MR}\cos a_1 \cos b_1 \end{bmatrix} \tag{27}$$

Unlike the main rotor, the tail rotor generates a force perpendicular to the rotor hub. The pilot has no control of the flapping angles. As a result, the resulting force component is in the y-direction only. The components of the tail rotor thrust are given by:

$$F_{TR}^{B} = \begin{bmatrix} X_{TR} \\ Y_{TR} \\ Z_{TR} \end{bmatrix} = \begin{bmatrix} 0 \\ T_{TR} \\ 0 \end{bmatrix} \tag{28}$$

The gravitational force on the helicopter is represented in the inertial Earth-fixed frame in the downward direction given as $F_g^I = [0\ 0\ mg]^T$. This force may be expressed as components with respect to the body-fixed frame, given as follows [13, 70, 106]:

$$F_g^B = \begin{bmatrix} X_g \\ Y_g \\ Z_g \end{bmatrix} = R(\Theta)F_g^I = \begin{bmatrix} -\sin\theta mg \\ \sin\phi\cos\theta mg \\ \cos\phi\cos\theta mg \end{bmatrix} \tag{29}$$

For the main rotor torque, the main rotor offset distance from the helicopter center of gravity is defined as $[l_m, y_m, h_m]^T$ [154]. The resulting torque contributed by the main rotor is given as:

$$\begin{bmatrix} L_{MR} \\ M_{MR} \\ N_{MR} \end{bmatrix} = \begin{bmatrix} Y_{MR}h_m - Z_{MR}y_m \\ -X_{MR}h_m - Z_{MR}l_m \\ X_{MR}y_m + Y_{MR}l_m \end{bmatrix} \tag{30}$$

For the tail rotor torque, the distance offset of the tail rotor from the helicopter center of gravity is defined as $[l_t, 0, h_t]^T$. The resulting torque contributed by the main rotor is given by:

$$\begin{bmatrix} L_{TR} \\ M_{TR} \\ N_{TR} \end{bmatrix} = \begin{bmatrix} Y_{TR}h_t \\ 0 \\ -Y_{TR}l_t \end{bmatrix} \tag{31}$$

The main rotor generates an aerodynamic drag as it rotates. This drag results in a torque, Q_{MR} [70, 100], which is perpendicular to the TPP and can be decomposed into components along the body frame by projecting the torque vector on to the hub plane. The resultant components are given as:

$$\begin{bmatrix} L_D \\ M_D \\ N_D \end{bmatrix} = \begin{bmatrix} Q_{MR}\sin a_1 \\ -Q_{MR}\sin b_1 \\ Q_{MR}\cos a_1 \cos b_1 \end{bmatrix} \tag{32}$$

3.5 Main and Tail Rotor

The helicopter receives most of its propulsive force from the main and tail rotors. The aerodynamics of the rotors, especially that of the main rotor, are highly nonlinear and complex. In order to reduce the complexity and simplify the dynamics for modeling and control design purposes, a number of assumptions are considered [13, 32, 33, 154, 155] as follows: rotor blades are rigid in both bending and torsion, small flapping angles, uniform inflow across rotor blade, no inflow dynamics used, effects of coning, due to flapping angles, is constant, forward velocity effect omitted, coupling ratio for pitch-flap is disregarded, and constant rotor speed.

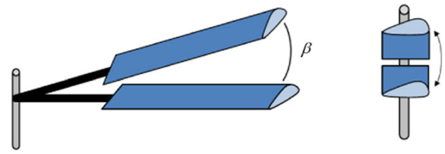

Fig. 10 Helicopter blade flapping motion

The dynamics of the main and tail rotors are controlled by input control commands. However, they are also affected by the motion of the helicopter. These control commands are represented by $\mathbf{u}_c = [\delta_{lon}\ \delta_{lat}\ \delta_{ped}\ \delta_{col}]^T$. The thrust magnitudes of the main and tail rotors are controlled by the collective commands δ_{col} and δ_{ped}, respectively. The main rotor blade flapping dynamics is controlled by the cyclic inputs δ_{lon} and δ_{lat}, which control the tilt of the TPP. Control of the propulsive forces is achieved by controlling the direction and inclination of the TPP. Thrust produced by the rotor blades is perpendicular to the TPP.

The orientation of the TPP is dependent on main rotor blade flapping dynamics. During rotation, the blades exhibit a flapping motion, a lead-lagging motion, and a pitching motion of the blade, as shown in Figs. 10, 11, and 12 respectively. These motions make-up the rotor blade DOF and are denoted by β, ξ, and ζ, respectively.

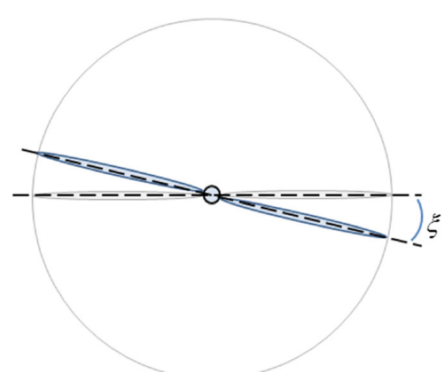

Fig. 11 Helicopter blade lead-lagging motion

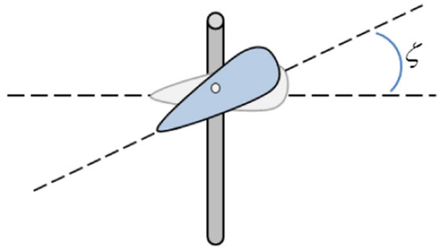

Fig. 12 Helicopter blade pitching motion

The aerodynamic forces on the rotor blade depend on the orientation of the blade at any time. The blade's pitch angle, ζ, affects the lift and drag of the blade elements. The flapping angle of the blade affects the inertial forces on the blade along the direction of the main rotor thrust vector. Determining the lift and drag generated by the main rotor requires consideration of the blade's flapping motion, ζ, helicopter forward velocity with respect to the air, also known as free stream velocity denoted by V_∞, rotation of the blade about the shaft in the form of angular velocity, Ω, and also the inflow velocity of air through the rotor [155]. This total air velocity on the blade, U, can be decomposed into three components. These components are defined in relation to the plane perpendicular to the rotor shaft, known as the hub plane. The plane hub frame is defined as $\mathcal{F}_h = \{O_h, \mathbf{i}_h, \mathbf{j}_h, \mathbf{k}_h\}$ where $\mathbf{i}_h$ points backwards towards the tail, $\mathbf{j}_h$ points to the right of the helicopter, and $\mathbf{k}_h$ points up. Two components are in the hub plane while the third is out of the plane. All three components are normal to the hub plane. The out of plane component is perpendicular to the hub plane pointing downward and is denoted by U_P, as seen in Fig. 13c. The next component, U_T, is parallel to the hub plane and tangential to the blade in the direction of the blade rotational motion as seen in Fig. 13a and d. The last component, U_R, lies on the hub plane and points radially pointing outward in the direction of and parallel to the blade, as seen in Fig. 13a and c. The total air velocity seen by the blade is given as $U = \sqrt{U_T^2 + U_P^2}$.

At any time during flight, the blade experiences a pitch angle, $\zeta = \alpha_b + \phi_b$, related to the angle of attack α_b of the blade with respect to the airstream U, which approaches the blade at an inflow angle ϕ_b, as seen in Fig. 14.

The lift and drag on the blade are determined through blade element analysis. By considering the blade as a two-dimensional airfoil, the lift and drag vectors at each blade element may be determined. The

Fig. 13 Air velocity components relative to the blade element [155]

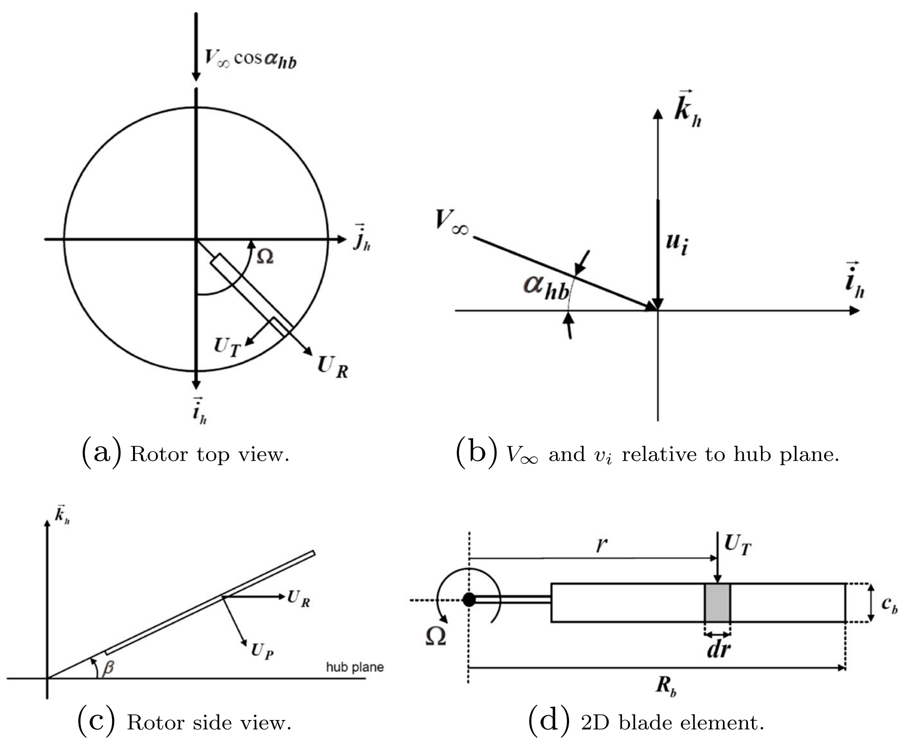

(a) Rotor top view.

(b) V_∞ and v_i relative to hub plane.

(c) Rotor side view.

(d) 2D blade element.

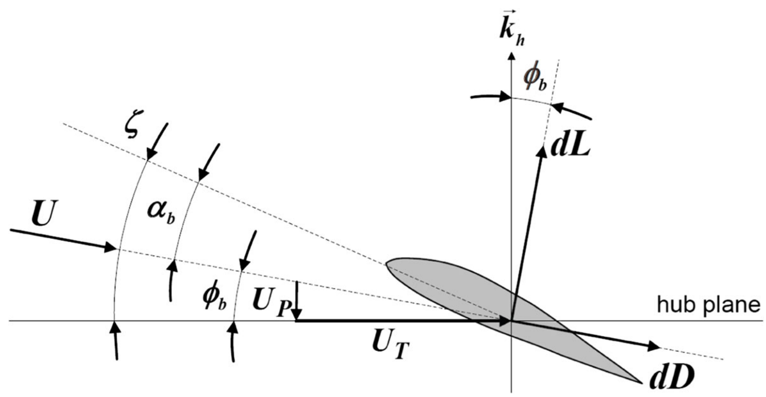

Fig. 14 Helicopter blade cross-section [155]

infinitesimal lift and drag of the blade element dr are given as:

$$dL = 1/2\rho_a U^2 c_b C_{l\alpha}\alpha_b dr \tag{33}$$

$$dD = 1/2\rho_a U^2 c_b C_d dr \tag{34}$$

The forces perpendicular and parallel to the hub plane can be expressed in terms of the lifting and drag forces as follows:

$$dF_{\parallel} = dL \sin\phi_b + dD\cos\phi_b \tag{35}$$

$$dF_{\perp} = dL\cos\phi_b - dD\sin\phi_b \tag{36}$$

Following the procedures from [13, 155], the total force on the blades parallel ($F_{\parallel}$) and perpendicular ($F_{\perp}$) to the hub plane can be expressed in terms of the air stream velocity components as:

$$dF_{\parallel} \approx \frac{1}{2}\rho c_b C_{l\alpha}\left(\zeta U_T U_P - U_P^2\right)dr + \frac{1}{2}\rho c_b C_D U_T^2 dr \tag{37}$$

$$dF_{\perp} \approx \frac{1}{2}\rho c_b C_{l\alpha}(\zeta U_T^2 - U_T U_P)dr \tag{38}$$

The total pitch of the blade is given as $\zeta = \zeta_0 - \zeta_1\cos\psi_b - \zeta_2\sin\psi_b$, where ζ_0 is the collective pitch to control the thrust of the rotor and $\zeta_1 = A_{lon}\delta_{lon}$, $\zeta_2 = B_{lat}\delta_{lat}$ are the linear functions of the pilot's lateral and longitudinal cyclic control stick inputs (δ_{lat}, δ_{lon}) and lateral and longitudinal control derivatives (A_{lon}, B_{lat}).

As seen in Fig. 15, the blade is modeled as a rigid thin plate rotating about the shaft at an angular rate of Ω. The angular position of the blade in the hub plane is denoted as ψ_b measured from the tail axis. The blade flapping hinge is modeled as a torsional spring with stiffness K_β. The moments acting on the blade are due to the lifting force described in Section 3.5, weight of the blade, the inertial forces acting on the blade, and the restoring force of the spring. Equating all the moments acting on the blade results in:

$$\begin{aligned}\ddot{\beta}\cdot(\Omega^2\cdot\frac{K_\beta}{\mathcal{I}_b}\cdot\frac{1}{2\mathcal{I}_b}m_b g R_b^2)\beta \\ = \frac{1}{2\mathcal{I}_b}\rho c_b C_{l\alpha}\int_0^{R_B} r(\zeta U_T^2 - U_T U_P)dr\end{aligned} \tag{39}$$

where the blade's inertia is given by $\mathcal{I}_b = \int_0^{R_b} m_b r^2 dr$.

The flapping dynamics, $\beta(t)$ in Eq. 39, can be expressed as a Fourier series neglecting the higher order terms, only keeping the first order harmonics, as:

$$\beta(t) = a_0 - a_1\cos\psi_b - b_1\sin\psi_b \tag{40}$$

Differentiating Eq. 40 and substituting β, $\dot{\beta}$, and $\ddot{\beta}$ into Eq. 39, the flapping dynamics can then be written as a system of the form $\ddot{x} + D\dot{x} + Kx = F$. Here, the

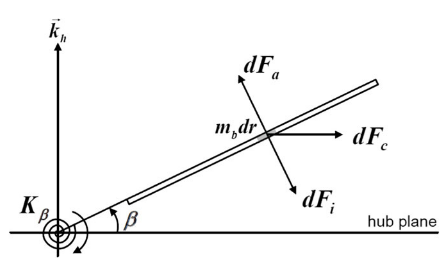

Fig. 15 Blade spring model [155]

state vector $x = [a_0\ a_1\ b_1]^T$, a_0 is the coning, a_1 is the longitudinal tilt, and b_1 is the lateral title angle of the TPP. The state space representation, where $x_1 = x$ and $x_2 = \dot{x}$, is given as:

$$\begin{bmatrix} \dot{x}_1 \\ \dot{x}_2 \end{bmatrix} = \begin{bmatrix} 0 & I \\ -K & -D \end{bmatrix} \begin{bmatrix} x_1 \\ x_2 \end{bmatrix} \tag{41}$$

The TPP dynamics are simplified [13, 155] by assuming a constant coning angle, disregarding the hinge offset, assuming a zero pitch-flap coupling ratio, and disregarding the effects of forward velocity. The simplified dynamics are given in Eq. 42 for the longitudinal dynamics and Eq. 43 for the lateral dynamics as follows:

$$\tau_f \dot{a} = -a - \tau_f q + A_b b + A_{lon} \delta_{lon} \tag{42}$$

$$\tau_f \dot{b} = -b - \tau_f p + B_b a + B_{lat} \delta_{lat} \tag{43}$$

Here, the time rotor constant, $\tau_f = \frac{16}{\gamma \Omega}$, is a function of the angular velocity, Ω, and the Lock number, $\gamma = \frac{16}{\gamma \Omega}$. Additionally, $A_b = -B_a = \frac{8}{\gamma}(\lambda_b^2 - 1)$, are the rotor cross coupling terms, and $\lambda_\beta = \frac{K_\beta}{\Omega^2 \mathcal{I}_b} + 1$ is the flapping frequency ratio.

The total thrust and counter-torque produced by the main rotor is a function of the forces acting on the blades perpendicular and parallel to the hub plane. The expressions are given as:

$$T_{mr} = \frac{N_{mb}}{2\pi} \int_0^{2\pi} \int_0^{R_t} dF_{\perp,t} \cos\beta d\psi_m \tag{44}$$

$$Q_{mr} = \frac{N_{mb}}{2\pi} \int_0^{2\pi} \int_0^{R_t} l dF_{\parallel,t} d\psi_m \tag{45}$$

Unlike the main rotor, the tail rotor only has a collective pitch, ζ_t. The tail rotor blade experiences induced air velocity and has flow components similarly to the main rotor. The perpendicular and parallel force components resemble Eqs. 37 and 38 of the main rotor. The tail rotor thrust and counter-torque can be found using Eqs. 46 and 47 [13] and are given as:

$$T_{tr} = \frac{N_{tb}}{2\pi} \int_0^{2\pi} \int_0^{R_t} dF_{\perp,t} d\psi_t \tag{46}$$

$$Q_{tr} = \frac{N_{tb}}{2\pi} \int_0^{2\pi} \int_0^{R_t} r dF_{\parallel,t} d\psi_t \tag{47}$$

3.6 Complete Set of Helicopter Equations of Motion

The key equations that describe the helicopter motion and are necessary for flight controller design are summarized in Table 1.

4 Linearization

Model linearization is a common practice that greatly reduces the complexity of nonlinear differential equations. Linear models provide a simplified representation of the helicopter model that sufficiently describes of the helicopter dynamics around a set of assumptions and flight conditions. Linear helicopter models are used to derive optimal feedback gains for a number of control techniques, including PID, LQR and $\mathcal{H}_\infty$ methods. These approaches have a greatly reduced number of complex calculations than that required of nonlinear control approaches.

4.1 Trim

Aircraft in steady flight must operate at some conditions where the forces and moments are in equilibrium about the center of gravity, known as trim flight [154]. Trim conditions correspond to certain trim values of the state and input variables, given by x_0 and δ_0, respectively. The first step in determining trim values for the helicopter, is to define the equations of equilibrium and reference flight conditions. These trim values can be found both analytically, as seen in [154], or numerically, as seen in [160].

4.2 Linearization

Linearization is achieved either by Taylor series expansion about some initial condition [70], or by small perturbation theory. Small perturbation theory is widely used to linearize the nonlinear helicopter dynamics about a trim flight condition, usually hover. Examples may be found in [16, 53, 56, 71, 72, 76, 80, 97–99, 103, 127, 171, 184, 191, 192, 194, 195]. In the case of the helicopter dynamics, the total force is made up of the forces and torques contributed by the various helicopter subsystems. These forces, listed in

Table 1 Helicopter equations of motion used for controller design

Newton-Euler equations:

$$\begin{bmatrix} mI_3 & 0 \\ 0 & J \end{bmatrix}\begin{bmatrix} \dot{\upsilon}_B \\ \dot{\omega}^B \end{bmatrix} + \begin{bmatrix} \omega^B \times m\upsilon^B \\ \omega^B \times J\omega^B \end{bmatrix} = \begin{bmatrix} f^B \\ \tau^B \end{bmatrix}$$

Expanded Newton-Euler equations:

$$\dot{u} = rv - qw + R_{31}g + X/m$$
$$\dot{v} = pw - ru + R_{32}g + Y/m$$
$$\dot{w} = qu - pv + R_{33}g + Z/m$$
$$\dot{p} = qr(J_{yy} - J_{zz})/J_{xx} + L/J_{xx}$$
$$\dot{q} = pr(J_{zz} - J_{xx})/J_{yy} + M/J_{yy}$$
$$\dot{r} = qp(J_{xx} - J_{yy})/J_{zz} + N/J_{zz}$$

Equations of motion:

$$\dot{p}^I = v^I$$
$$\dot{v}^I = \frac{1}{m}Rf^B$$
$$\dot{R} = R\hat{\omega}^B$$
$$I\dot{\omega}^B = -\omega^B \times (I\omega^B) + \tau^B$$

Rotation matrix:

$$R(\Theta) = \begin{bmatrix} \cos\psi\cos\theta & \cos\psi\sin\phi\sin\theta - \cos\phi\sin\psi & \sin\phi\sin\psi + \cos\phi\cos\psi\sin\theta \\ \cos\theta\sin\psi & \cos\phi\cos\psi + \sin\phi\sin\psi\sin\theta & \cos\phi\sin\psi\sin\theta - \cos\psi\sin\phi \\ -\sin\theta & \cos\theta\sin\phi & \cos\phi\cos\theta \end{bmatrix}$$

Position and orientation dynamics:

$$\dot{x}^I = c_\theta c_\psi u + (s_\theta s_\phi c_\psi - c_\phi s_\psi)v + (s_\theta c_\phi c_\psi + s_\phi s_\psi)w$$
$$\dot{y}^I = c_\theta c_\psi u + (c_\phi c_\psi + s_\phi s_\psi s_\theta)v + (c_\theta s_\psi s_\theta - c_\psi s_\phi)w$$
$$\dot{z}^I = -s_\theta u + c_\theta s_\phi v + c_\phi c_\theta x$$
$$\dot{\phi} = p + s_\phi t_\theta q + c_\phi t_\theta r$$
$$\dot{\theta} = c_\phi q - s_\phi r$$
$$\dot{\psi} = \frac{s_\phi}{c_\theta}q + \frac{c_\phi}{c_\theta}r$$

Forces acting on the helicopter body:

$$F^B = \begin{bmatrix} X \\ Y \\ Z \end{bmatrix} = \begin{bmatrix} -T_{MR}\sin a_1 - \sin\theta mg \\ -T_{MR}\sin b_1 + T_{TR} + \sin\phi\cos\theta mg \\ -T_{MR}\cos a_1\cos b_1 + \cos\phi\cos\theta mg \end{bmatrix}$$

Moments acting on the helicopter body:

$$\begin{bmatrix} L \\ M \\ N \end{bmatrix} = \begin{bmatrix} Y_{MR}h_m - Z_{MR}y_m + Y_{TR}h_t + Q_{MR}\sin a_1 \\ -X_{MR}h_m - Z_{MR}l_m - Q_{MR}\sin b_1 \\ X_{MR}y_m + Y_{MR}l_m - Y_{TR}l_t + Q_{MR}\cos a_1\cos b_1 \end{bmatrix}$$

Flapping dynamics:

$$\tau_f\dot{a} = -a - \tau_f q + A_b b + A_{lon}\delta_{lon}$$
$$\tau_f\dot{b} = -b - \tau_f p + B_b a + B_{lat}\delta_{lat}$$

Table 2, are either controlled, as a result of the pilot input, or uncontrolled, as a result of the dynamic parameters.

Small perturbation analysis involves applying a small incremental force, Δf, resulting in small perturbations to the dynamics. For a helicopter, the dynamic parameters that make up the state vector are given in Eq. 48, while the control inputs are given in Eq. 49:

$$\mathbf{x} = [u\ v\ w\ p\ q\ r\ \phi\ \theta\ \psi\ a_1\ b_1\ c_1\ d_1\ ]^T \tag{48}$$

$$\mathbf{u}_c = \left[\delta_{col}\ \delta_{ped}\ \delta_{lat}\ \delta_{lon}\right]^T \tag{49}$$

Table 2 Input force categorized as controlled versus uncontrolled

Force Type	Notation	Description
Controlled	$f_{\delta_{col}}$	Collective input
	$f_{\delta_{ped}}$	Tail rotor collective
	$f_{\delta_{lat}}$	Lateral cyclic
	$f_{\delta_{lon}}$	Longitudinal cyclic
	$f_{\delta_{thr}}$	Throttle
Uncontrolled	f_u, f_v, f_w	Translational velocities
	f_p, f_q, f_r	Angular rates
	f_ϕ, f_θ, f_ψ	Orientation angles
	f_{a_1}, f_{b_1}	Main rotor cyclic angles
	f_{c_1}, f_{d_1}	Stabilizer cyclic angles

In most cases, the engine throttle is not controlled by the pilot, but rather remains constant during flight. As a result, the engine throttle is not included in the input vector.

In [44], the forces and moments are defined to be strictly functions of the state and input variables. A linear approximation of the forces can be found using a first-order Taylor approximation about the initial condition $x_i(t_0) = a$, given by:

$$f_{x_i} \approx f(a) + f'(a)(x_i - a) \tag{50}$$

Although it may be desired to retain terms of higher order derivatives or nonlinear terms for the sake of accuracy and completeness, as in [106], many times only the first order terms are considered. For small enough motion, the effects of the nonlinear terms (e.g., $\frac{\partial^2 F}{\partial x^2}$), and derivatives of dynamic parameters, (e.g., $\dot{u}$, $\dot{q}$), are insignificant [144].

The derivative of the forces, in terms of the disturbed variables Δx_i and $\Delta\delta_i$, and the disturbed force $\Delta F_{x_i} = f(x + \Delta x) - f(x)$, is given by:

$$\frac{\partial f}{\partial x} = \frac{\Delta F_{x_i}}{\Delta x} \tag{51}$$

This allows for the perturbed forces and moments to be defined as linear functions of the perturbed variables and the force derivatives ($F_{x_i} = \frac{\partial f}{\partial x_i}$). This combination is given by:

$$\Delta F = \sum_{x_i \in \mathbf{x}} F_{x_i} \cdot \Delta x_i + \sum_{\delta_i \in \mathbf{u}} F_{\delta_i} \cdot \Delta\delta_i \tag{52}$$

The derivatives with respect to the controlled inputs are referred to as the *control derivatives*, while those with respect to the uncontrolled states are known as the *stability derivatives*. The notation is simplified to $\frac{\partial f}{\partial \alpha} = F_\alpha$. The derivatives are listed in Table 3. Further detail on the derivatives are given in [22, 73, 77–79, 133, 144, 154].

Table 3 Control and stability derivatives

Derivative type	Notation	Description
Control derivatives	$F_{\delta_{col}}$	Collective input
	$F_{\delta_{ped}}$	Tail rotor collective
	$F_{\delta_{lat}}$	Lateral cyclic
	$F_{\delta_{lon}}$	Longitudinal cyclic
	$F_{\delta_{thr}}$	Throttle
Stability derivatives	F_u, F_v, F_w	Translational velocities
	F_p, F_q, F_r	Angular rates
	F_ϕ, F_θ, F_ψ	Orientation angles
	F_{a_1}, F_{b_1}	Main rotor cyclic angles
	F_{c_1}, F_{d_1}	Stabilizer cyclic angles

The forces ($F = [X\ Y\ Z]$) and moments ($\tau = [L\ M\ N]$) that drive the rigid body dynamics consist of the X, Y and Z body forces and L, M, and N moments about the body axes acting on the helicopter. A small increment of each of these forces and moments is a sum of the derivatives and perturbations, as in Table 3 and Eq. 52, and are given by:

$$\begin{aligned}
\Delta X &= X_u \Delta u + X_v \Delta v + \cdots + X_{\delta_{col}} \Delta\delta_{col} + \cdots \\
\Delta Y &= Y_u \Delta u + Y_v \Delta v + \cdots + Y_{\delta_{col}} \Delta\delta_{col} + \cdots \\
\Delta Z &= Z_u \Delta u + Z_v \Delta v + \cdots + Z_{\delta_{col}} \Delta\delta_{col} + \cdots \\
\Delta L &= L_u \Delta u + L_v \Delta v + \cdots + L_{\delta_{col}} \Delta\delta_{col} + \cdots \\
\Delta M &= M_u \Delta u + M_v \Delta v + \cdots + M_{\delta_{col}} \Delta\delta_{col} + \cdots \\
\Delta N &= N_u \Delta u + N_v \Delta v + \cdots + N_{\delta_{col}} \Delta\delta_{col} + \cdots
\end{aligned} \tag{53}$$

Next, small perturbations ($\delta = \Delta\delta + \delta_0$) are applied to the rigid body dynamics. Applying the perturbed variables to the forward velocity component of the rigid body dynamics reduces to Eq. 54:

$$\begin{aligned}
\dot{u_0} + \Delta\dot{u} \ = \ & (r_0 + \Delta r)(v_0 + \Delta v) - (q_0 + \Delta q)(w_0 + \Delta w) \\
& - \sin(\theta_0 + \Delta\theta) g + \frac{X_0 + \Delta X}{m}
\end{aligned} \tag{54}$$

It is assumed that the perturbations and any derivative have very small values. As a result, the product of perturbations is subsequently very small and negligible [155]. These assumptions result in the following properties: i) $\Delta x \Delta y = 0$, ii) $cos(\Delta\theta) = 1$, and iii) $sin(\Delta\theta) = \Delta\theta$. Applying these properties to the forward velocity component in Eq. 54 gives:

$$\begin{aligned}\dot{u}_0 + \Delta\dot{u} &= r_0 v_0 + r_0 \Delta v + v_0 \Delta r - q_0 w_0 - q_0 \Delta w \\ &\quad - w_0 \Delta q - \sin\theta_0 g - \Delta\theta \cos\theta_0 g \\ &\quad + \frac{X_0}{m} + \frac{\Delta X}{m}\end{aligned} \tag{55}$$

In hover flight the helicopter is operating in conditions where $u_0 = v_0 = w_0 = p_0 = q_0 = r_0 = \dot{u}_0 = 0$. This reduces the forward velocity equation to:

$$\Delta\dot{u} = -\sin\theta_0 g - \Delta\theta \cos\theta_0 g + \frac{X_0}{m} + \frac{\Delta X}{m} \tag{56}$$

At hover, the helicopter flies at nearly level flight such that the attitude angles are very small. For the forward velocity dynamics, this reduces Eq. 56:

$$\Delta\dot{u} = -\theta_0 g - \Delta\theta g + \frac{X_0}{m} + \frac{\Delta X}{m} \tag{57}$$

Finally, in trim flight it is assumed that there are no disturbances so that $\Delta\dot{u} = \Delta\theta = \Delta X = 0$. Given these assumptions, the forward velocity dynamics in Eq. 54 becomes Eq. 58. This equilibrium condition is combined with the forward velocity dynamics at hover given in Eq. 57 to form the trimmed linear forward velocity dynamics at hover. The complete set of equilibrium equations at hover are derived and given as:

$$X_0 = mg \sin\theta_0 \tag{58}$$

$$Y_0 = -mg \sin\phi_0 \cos\theta_0 \tag{59}$$

$$Z_0 = -mg \cos\theta_0 \cos\phi_0 \tag{60}$$

$$L_0 = M_0 = N_0 = 0 \tag{61}$$

$$\dot{x}^I = 0\dot{y}^I = \dot{z}^I = 0 \tag{62}$$

At level cruise, the trim conditions mimic those of hover except that the initial condition for translational velocity, usually forward, is set to a non-zero value. In the case of level forward flight, $u_0 \neq 0$. In [140], the trim condition for a level banked turn is given using a constant forward velocity, constant yaw angle, and no sideslip.

4.3 Comprehensive Linear State Space Model

Following this same procedure with the entire set of dynamic (14)–(19), position and orientation dynamics (20)–(25), and flapping dynamics (42)–(43), a complete set of linear dynamic equations is derived and is given in state space form as:

$$\dot{\mathbf{x}} = A\mathbf{x} + B\mathbf{u} \tag{63}$$

while the state and input vectors, the A and B matrices are explicitly given in Eqs. 64–67.

The state matrix A contains the stability derivatives, the input matrix B contains the control derivatives, $\mathbf{x}$ contains the state variables, and $\mathbf{u}$ contains the input variables. Following procedures from [44, 129, 144, 154, 155], this comprehensive linear model given in Eqs. 64–67 has been derived. What makes this model unique is that it considers the linear dynamics before assuming a specific flight condition. It is from this generalized structure that the helicopter model may be further simplified according to the assumed flight condition (i.e., hover, cruise, turn, etc.). For example, at hover, all of the terms containing initial translational and angular velocity parameters ($u_0, v_0, \cdots$, etc.) are eliminated, and terms with initial condition attitude angles reduce due to trigonometric identities. A structure of this nature can be found in [129]. The remaining derivative terms must be identified by linearization of the forces under the identified trim condition. However, in straight-level cruise or a banked turn, the initial velocities and angular rates must be taken into consideration and included in the model structure. Using the proposed linear model structure, a bank of linear models may be developed by considering various flight conditions. In [87] the linear model derivatives are determined at hover in addition to various forward speeds in straight, level flight.

$$x = \left[\, u \;\; v \;\; w \,\middle|\, p \;\; q \;\; r \,\middle|\, \phi \;\; \theta \;\; \psi \,\middle|\, a_1 \;\; b_1 \,\middle|\, c_1 \;\; d_1 \,\middle|\, r_{fb} \,\right]^T \tag{64}$$

$$u = [\, \delta_{lat} \quad \delta_{lon} \quad \delta_{col} \quad \delta_{ped} \,]^T \tag{65}$$

$$B = \left[\begin{array}{ccc|ccc|ccc|cc|cc|c} X_{\delta_{lat}} & Y_{\delta_{lat}} & Z_{\delta_{lat}} & L_{\delta_{lat}} & M_{\delta_{lat}} & N_{\delta_{lat}} & 0 & 0 & 0 & A_{lat} & B_{lat} & 0 & D_{lat} & 0 \\ X_{\delta_{lon}} & Y_{\delta_{lon}} & Z_{\delta_{lon}} & L_{\delta_{lon}} & M_{\delta_{lon}} & N_{\delta_{lon}} & 0 & 0 & 0 & A_{lon} & B_{lon} & C_{lon} & 0 & 0 \\ X_{\delta_{ped}} & Y_{\delta_{ped}} & Z_{\delta_{ped}} & L_{\delta_{ped}} & M_{\delta_{ped}} & N_{\delta_{ped}} & 0 & 0 & 0 & 0 & 0 & 0 & 0 & 0 \\ X_{\delta_{col}} & Y_{\delta_{col}} & Z_{\delta_{col}} & L_{\delta_{col}} & M_{\delta_{col}} & N_{\delta_{col}} & 0 & 0 & 0 & 0 & 0 & 0 & 0 & 0 \end{array}\right]^T \tag{66}$$

$$A = \left[\begin{array}{ccc|ccc|ccc|cc|cc|c}
X_u & X_v + r_0 & X_w - q_0 & X_p & X_q - w_0 & X_r + v_0 & 0 & -gc_{\theta_0} & 0 & X_{a_1} & 0 & 0 & 0 & 0 \\
Y_u - r_0 & Y_v & Y_w + p_0 & Y_p + w_0 & Y_q & Y_r - u_0 & gc_{\phi_0}c_{\theta_0} & -gs_{\phi_0}s_{\theta_0} & 0 & 0 & Y_{b_1} & 0 & 0 & 0 \\
Z_u + q_0 & Z_v - p_0 & Z_w & Z_p - v_0 & Z_q + u_0 & Z_r & -gs_{\phi_0}c_{\theta_0} & -gc_{\phi_0}s_{\theta_0} & 0 & Z_{a_1} & Z_{b_1} & 0 & 0 & 0 \\
L_u & L_v & L_w & L_p & L_q + J_p r_0 & L_r + J_p q_0 & 0 & 0 & 0 & 0 & L_{b_1} & 0 & 0 & 0 \\
M_u & M_v & M_w & M_p + J_q r_0 & M_q & M_r + J_q p_0 & 0 & 0 & 0 & M_{a_1} & 0 & 0 & 0 & 0 \\
N_u & N_v & N_w & N_p + J_r q_0 & N_q + J_r p_0 & N_r & 0 & 0 & 0 & 0 & 0 & 0 & 0 & N_{r_{fb}} \\
0 & 0 & 0 & 1 & s_{\phi_0}t_{\theta_0} & c_{\phi_0}t_{\theta_0} & 0 & \Omega/c_{\theta_0} & 0 & 0 & 0 & 0 & 0 & 0 \\
0 & 0 & 0 & 0 & c_{\theta_0} & -s_{\theta_0} & -\Omega c_{\theta_0} & 0 & 0 & 0 & 0 & 0 & 0 & 0 \\
0 & 0 & 0 & 0 & \frac{s_{\phi_0}}{c_{\theta_0}} & \frac{c_{\phi_0}}{c_{\theta_0}} & \frac{(q_0 s_{\phi_0} - r_0 c_{\phi_0})t_{\theta_0}}{c_{\theta_0}} & \frac{(q_0 c_{\phi_0} - r_0 s_{\phi_0})}{c_{\theta_0}} & 0 & 0 & 0 & 0 & 0 & 0 \\
0 & 0 & 0 & 0 & -1 & 0 & 0 & 0 & 0 & \frac{-1}{\tau_f} & A_b & A_c & 0 & 0 \\
0 & 0 & 0 & -1 & 0 & 0 & 0 & 0 & 0 & B_a & \frac{-1}{\tau_f} & 0 & B_d & 0 \\
0 & 0 & 0 & 0 & -1 & 0 & 0 & 0 & 0 & 0 & 0 & \frac{-1}{\tau_s} & 0 & 0 \\
0 & 0 & 0 & -1 & 0 & 0 & 0 & 0 & 0 & 0 & 0 & 0 & \frac{-1}{\tau_s} & 0 \\
0 & 0 & 0 & 0 & 0 & K_r & 0 & 0 & 0 & 0 & 0 & 0 & 0 & K_{r_{fb}}
\end{array}\right] \quad (67)$$

5 Guidance and Navigation

Guidance and navigation and control are the key components in UAV flight control systems (FCS). Combined with flight controllers, as seen in Fig. 16, guidance and navigation systems facilitate autonomous flight. The navigation module provides the UAV state vector and environmental data necessary for guidance and control tasks. The UAV state vector includes positions, velocities, attitude and angular rates. The guidance module is either preloaded with mission tasks, or receives tasks in real-time from another source like a ground control station, or, in the case of coordinated flight, from other UAV within the formation. The guidance system then uses navigational data to determine the optimal state trajectory the UAV will follow. This optimal state trajectory describes the three-dimensional position, velocity, or attitude that is used as the reference to drive the flight controller. The flight controller then determines the necessary inputs to the UAV's actuators to track the reference trajectory.

In RUAS, navigation systems are responsible for sensing and determination of a UAV's state vector and its environment. This can be done onboard the UAV, on the ground, or even on another UAV. Typical navigation systems consist of data acquisition hardware, data analysis modules, and state estimation algorithms. Navigation sensors directly measure the UAV's state vector. These sensors can be radio systems that communicate with some transmitter either on the ground, on a satellite, or even on another UAV [92]. These types of sensors are most commonly GPS, radar, or motion capture systems, depending on the type of UAV and environment. A second method of determining the UAV state vector is known as Dead Reckoning, where the UAV's position and velocity are determined relative to the UAV's initial position from a history of continuous measurements. This type of derivation requires specialized sensors that provide information on the UAVs heading, acceleration, speed and orientation. These include gyros to provide angular rates, accelerometers to provide linear accelerations and a magnetic compass to provide heading information. This information is used to derive, on board, the change in the UAV's position and velocities based on previous calculations and the sensor measurements. Other sensors that provide useful information include pressure sensors, cameras, and light detection and ranging (LIDAR) sensors. Modern UAS navigation systems, such as Attitude-Heading

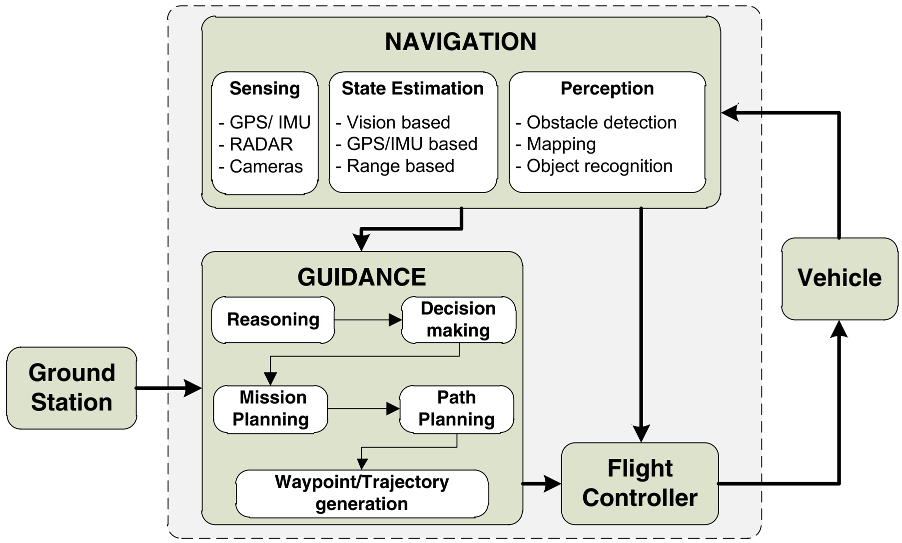

Fig. 16 Flight control system with guidance and navigation modules

and Reference (AHRS) systems, combine various sensors and include state estimation algorithms, such as Kalman filtering, in order to improve the accuracy and increase data rates. Navigation systems may also include high-level functions to facilitate perception and situational awareness, which includes detection of targets or obstacles, object recognition, and mapping functions, as well as classification of situations to predict future behavior of objects in the UAV's environment. Vision-based navigation methods have become widely popular, especially in UAV applications where inertial navigation or GPS cannot be relied upon.

Guidance systems are responsible for handling or steering of the UAV in order to achieve a predefined mission. Guidance system functions typically include trajectory generation, path planning, mission planning, and high-level decision making according to the mission or task to be accomplished. Trajectory generation involves determination of reference motions that are within both the UAV's dynamic constraints and the environmental physical constraints. These trajectories are used to drive the flight controller. Path planning involves the steering of the UAV towards some destination in the safest, most optimal manner possible. Mission planning involves the generation of tasks, coordination of commands and timing, decision making, and switching of control structure and/or gains.

There are a number of methods and algorithms in guidance and navigation. [93] provides a detailed review of research in these areas, outlined in Table 4. A detailed overview of perception techniques in UAVs is presented in [143].

Table 4 Methods of guidance and navigation

Navigation	Sensing	IMU GNSS Altimeters Integrated IMU/GPS
	State estimation	IMU/GPS systems Vision-based Range sensing
	Perception/ Situational awareness	Vision-based Range sensing-based
Guidance	Path planning	Road mapping Potential fields Search algorithms Optimization methods
	Mission planning	Mission planning systems
	Cooperate flight	Coordinated flights Cooperative perception Cooperative mission planning/decision making

6 Control Loop Architectures

Because of their highly complex nature, helicopter dynamics are often simplified and decoupled to facilitate flight control design corresponding to various modes and use of various control methods. In this study, an extensive review of control loop architectures and methods is presented and summarized. First, the loop architectures are categorized according to loop structure and reference command or trajectory to be tracked, with details on the advantages, capabilities, design considerations and required sensor measurements. A generalized diagram is provided for each loop structure. Next, a comprehensive overview of model-based control methods, separated into linear and nonlinear methods, for rotorcraft navigation is presented, including an overview of the theory, advantages, and descriptions of key examples. Finally, a comprehensive survey of research in rotorcraft control is provided following the proposed 'reference template' of Section 2.

Regardless of the type of flight controller used, control architectures consist of a number of interconnected loops in order to facilitate navigation control, translational dynamics and attitude dynamics of the helicopter. For rotorcraft, the attitude dynamics are much faster compared to the translational dynamics. Typically, flight controllers are designed with at least two loops. The inner loop controls the attitude dynamics. The outer loop deals with translational dynamics. An additional outer-most loop may be used for navigational guidance, such as trajectory generation or tracking. A second approach to the control architecture is to separate the lateral-longitudinal dynamics from the heave-yaw dynamics. Both approaches associate the system inputs with a rigid-body dynamic state to be controlled. These states include translational positions and velocities, angular rates, and attitude angles. However, since rotorcraft are underactuated systems many of the helicopter states may be used as intermediate or virtual inputs to subsequent cascaded loops. Generally, the rotorcraft main rotor collective and throttle are associated with heave, or altitude. The tail rotor collective is associated with the yaw motion. Lastly, the main rotor lateral and longitudinal collectives are associated with the roll and pitch of the helicopter, which subsequently results in lateral and longitudinal translation. A third, less frequently used, approach uses classical control analysis in order to manipulate system poles and gain or phase margins to stabilize the helicopter. However, even this structure utilizes multiple loops.

The design of the control loop architecture varies depending on the type of trajectory to be tracked, model structure chosen for controller design, and flight maneuver desired to achieve. This is due to the assumptions or simplifications made and the type of reference input to follow. The most common types of flight controllers can be separated into the following categories: yaw or heading control, attitude or orientation control, altitude control, velocity control, position control. Each of the control structures can be designed using simplified dynamic models specific to the navigational dynamic states and particular flight mode to be controlled. These same controllers may be combined in order to achieve more advanced maneuvers, such as hover control and trajectory tracking.

6.1 Hover Control

Hover control is the most basic maneuver. Most linearizations of dynamic models are done assuming hover conditions. At hover, the goal is to keep the helicopter at a desired position/altitude, sometimes while maintaining a certain heading or yaw rate.

6.2 Yaw or Heading Control

The rotorcraft yaw rate or heading can be controlled using the tail rotor collective input. One important consideration for yaw control is the possible presence of a yaw-rate gyro (in RC helicopters). These gyros are used to provide stabilization in the yaw channel during piloted flight and have their own dynamics that are not described by the dynamic equations of the helicopter. It is possible to create a model of the gyro dynamics through comparison of flight tests with and without the gyro as in [129, 146]. The yaw dynamics are most easily decoupled for a helicopter in hover, while in translational flight a change in heading affects the lateral-longitudinal dynamics. However, for very small changes in heading or at low enough velocities, the controller can be successful. A basic structure of a yaw controller, shown in Fig. 17, may take in as a reference command a constant yaw angle or a yaw rate depending on the maneuver to be performed. The control block represents any type of control that might be used, typically a PID controller.

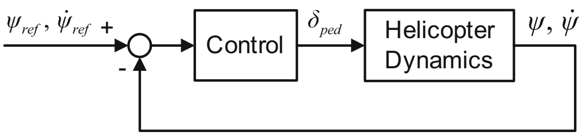

Fig. 17 Yaw control block diagram

6.3 Attitude or Orientation Control

Attitude control is used to stabilize the orientation of the rotorcraft. A typical attitude control architecture is shown in Fig. 18. This control structure uses the rotorcraft cyclic inputs for pitch and roll and tail rotor collective for yaw stabilization. Attitude control is placed as an inner loop. Typically, an attitude controller will either regulate the pitch and roll only, the yaw only, or all three. This depends on how the controller is used in the FCS, whether as part of a larger control structure, such as one for hover or trajectory tracking. The inclusion of a helicopter tail feedback gyro in the control loop may also affect the controller design. For a SISO control architecture, a single controller is used for each channel. However, with MIMO approaches, such as LQR and $\mathcal{H}_\infty$, a single controller may be responsible for two or more channels at once. The method of decoupling the dynamics will determine how these channels can be lumped. Regardless, most approaches keep the pitch and roll angles together.

6.4 Velocity Control

Velocity control is used to ensure that a particular velocity trajectory is achieved. This is mostly used for cruise flight in parallel with a heading and attitude controller or in a trajectory tracking scheme to generate virtual attitude commands for the inner loop of the FCS, given desired positions or velocities. A typical architecture for velocity control is given in Fig. 19. For SISO schemes, the control blocks represent individual controllers for each channel. However, a MIMO control approach can also be used. In most cases, the lateral and longitudinal translational velocities u and v are controlled together. The velocity control block will generate desired roll and pitch orientation angles or rates in order to achieve the desired velocity and feed that *virtual command* to the inner loop attitude controller.

6.5 Altitude Control

Altitude control is used to ensure that the helicopter maintains a desired height during flight. The main rotor collective and, if controllable, the engine throttle inputs are regulated in order to maintain the desired altitude. Sometimes, altitude control is coupled with the inner loop attitude control and decoupled from the lateral-longitudinal dynamics. This is known as lateral-longitudinal outer-loop and heave-yaw inner-loop control. In this type of structure, the outer-loop controller produces the reference roll and pitch trajectories for the inner-loop controller. One such example

Fig. 18 Attitude/orientation control block diagram

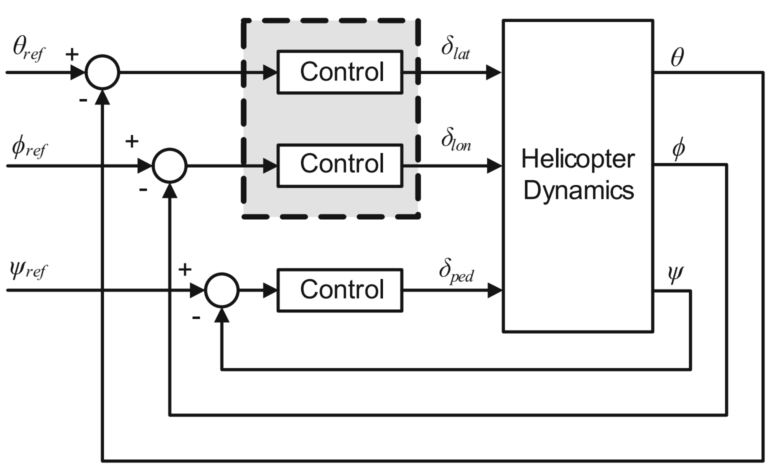

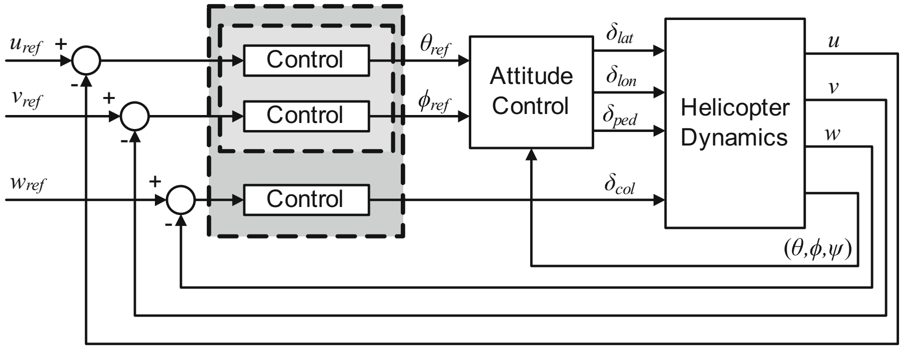

Fig. 19 Velocity control block diagram

is given in Fig. 20. Another approach uses two individual controllers to handle decoupled longitudinal-vertical and lateral-directional dynamics. This type of structure is shown in Fig. 21.

6.6 Position Control and Trajectory Tracking

Position control and trajectory tracking is achieved by providing a desired trajectory reference to the FCS. In order to achieve this, a combination of velocity, altitude, and orientation control must be used, as shown in Fig. 22. For position control, it may be desired to maintain the helicopter at a particular position. This can be achieved by a two loop structure. The outermost loop takes the desired position and determines the necessary helicopter orientation in order to maintain that position. The innermost loop will then determine necessary helicopter control inputs. A three loop structure may also be used. Here the outer-most loop uses the desired trajectory in order to determine desired translational velocities. These velocities act as virtual inputs to the middle loop, which determines ideal attitude trajectories as inputs to the inner-most loop. This inner-most loop determines the necessary helicopter control inputs. Trajectory tracking may have the additional requirement of maintaining a desired heading trajectory.

7 Control Techniques

This Section presents an overview of model-based control methods used for rotorcraft navigation and control. Model-based control methods consist of two types of control approaches, linear and nonlinear techniques. Linear control methods, designed based on a linear MIMO helicopter model, include PID, LQR/LQG, $\mathcal{H}_\infty$, and gain scheduling techniques. Nonlinear control methods, based on rigid body nonlinear equations of motion and force and torque generation, include backstepping, adaptive, model predictive, linearization, and nested saturation techniques. This review includes details on the corresponding theory for each method, design considerations, key

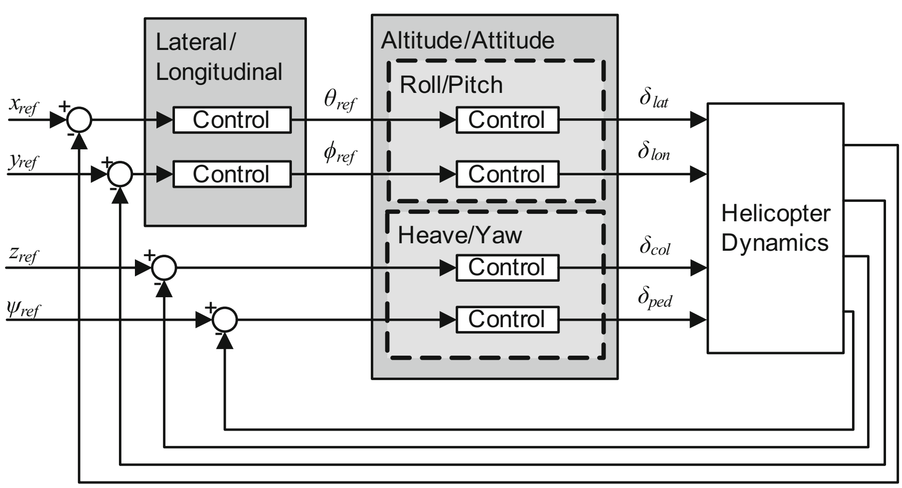

Fig. 20 Lateral-longitudinal and heave-yaw control structure

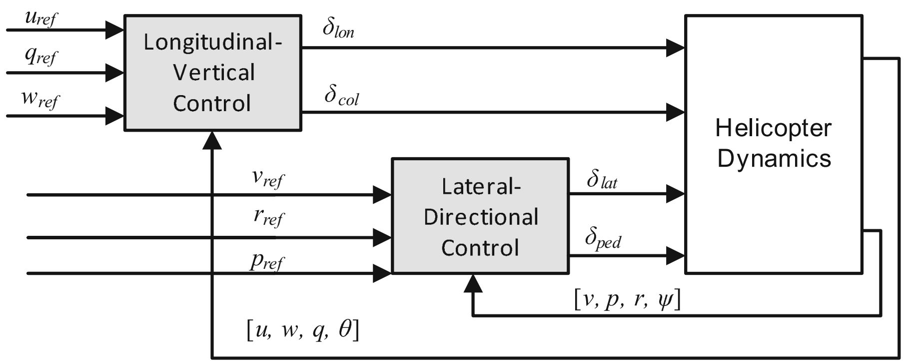

Fig. 21 Longitudinal-vertical and lateral-directional control structure

examples of their use in overall control architectures, advantages of each approach and typical maneuvers that have been achieved through application of each technique, whether in simulation or real flight. Following this review, comprehensive overview of the reviewed control approaches is given in Table 5.

7.1 Linear PID Controllers

PID controllers are a type of single-input/single-output (SISO) control structure in which one controlled input is associated with a single output. The PID algorithm consists of three gains: a proportional, integral, and derivative gain. A great advantage of the PID approach is the ease of implementation. PID controllers can be implemented without any sort of model. This method requires multiple flight tests in order to manually tune each of the gains until a desired response is obtained. While the lack of need for a model may make this approach appealing, it may become tedious and difficult to obtain desired gains, not to mention the added risk of failure or crash if improper gains are chosen.

A second approach to the PID structure is to determine a transfer function, which describes the relationship between the chosen input/output pair to be controlled. Once a satisfactory function is identified and validated, classical methods may be used to determine ideal gains for the PID controller. This can include looking at overshoot, settling or rise times, and even gain and phase margins. Once identified, these ideal gains can be tested during flight, where they may be manually fine tuned according to the observed response. These approaches, however, do not directly deal with the time scaling between the inner loop and outer loop dynamics.

Another structure using PID control requires the use of multiple loops in order to separately address the inner loop and outer loop dynamics. For this type of control structure it is necessary to create virtual inputs from outer loops to the inner control loops. Rather than pairing one of the rotorcraft outputs to

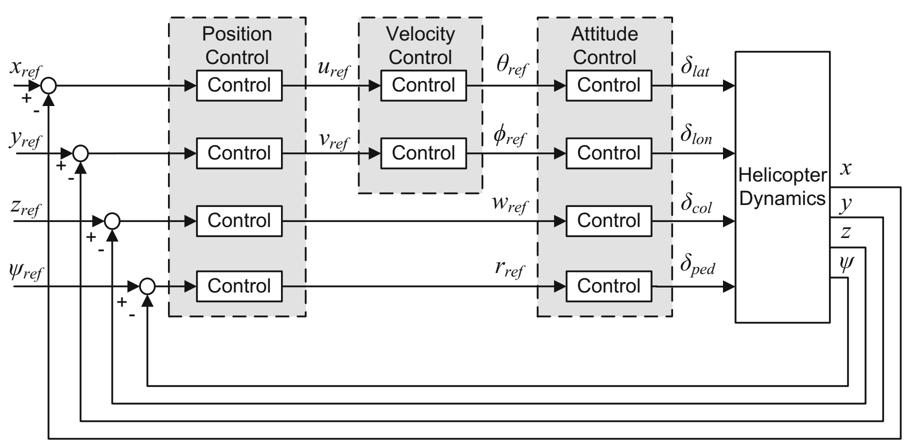

Fig. 22 Block diagram for trajectory tracking

Table 5 Comparison of control techniques, including: Proportional-Integral-Derivative (PID), Linear Quadratic Gaussian/Regression (LQG/LQR), $\mathcal{H}_\infty$, Gain Scheduling (GS), Backstepping (BS), Feedback Linearization (FL), Adaptive Control (AC), and Model Predictive Control (MPC) approaches

Technique		Advantages	Disadvantages	Maneuvers
LINEAR	PID	Easily implemented; Assumes simplified decoupled dynamics; Gains can be tuned in flight	Lacks robustness; Ignores coupling of dynamics	Mostly hovered flight; Attitude/Altitude control; Lateral/ Longitudinal control
	LQG/ LQR	Multivariable capabilities; Used to stabilize both inner and outer loops	Limited to certain flight conditions; Gain calculation is an iterative process	Hovering; Trajectory tracking
	$\mathcal{H}_\infty$	Deals with parametric uncertainty; Can handle unmodeled dynamics; Can be used for loop-shaping	High level of math understanding and computation; Need a reasonably good system model	Hovering; Trajectory tracking
	GS	Larger range of flight envelope and operating conditions; Can use a bank of simple controllers	Requires ability to store a number of gains and control approaches; Transition between switches might be unsteady	Hovering; Trajectory tracking
NONLINEAR	BS	Good technique for underactuated systems	Need a nonlinear model	Trajectory tracking
	FL	Can deal with nonlinearities while allowing for application of linear techniques	Higher computational complexity; Transformed variables and actual output may vary greatly	Auto take-off and landing; Hovering and aggressive maneuvers
	AC	Robust technique; Can adapt to unmodeled dynamics and parametric uncertainty	Complex analysis; Need good knowledge of the system	Formation flight; Vision based navigation
	MPC	Can predict future behavior, to some extent; Can place constraints on the input; Tracking errors can be minimized	Prediction model must be formulated correctly	Target tracking

a controlled input directly, the outer loops create virtual inputs to the inner loops in the form of a desired trajectory needed in order to achieve stability in the outer loop. The inner loops are then tasked to achieve the trajectory determined by the outer loop. An example is a multi-loop PID (MLPID) controller that separates the attitude and translational dynamics. In this type of structure, see Fig. 19, the outer loop is tasked with achieving the desired velocity in 3-axis. Because the cyclic inputs of the helicopter affect the lateral-longitudinal motion of the helicopter most, the lateral-longitudinal velocity controllers output desired pitch and roll in order to achieve the referenced velocities. From there, the inner attitude controller will use these as virtual inputs in order to determine the necessary controlled inputs to the rotorcraft.

In [19], a cascaded control architecture is used for a 13 state linear model of an R-MAX helicopter. The proposed controller is based on a cascaded architecture with an inner and outer loop. However, rather than simply controlling the attitude (inner loop) and tracking (outer loop), this architecture looks at the poles of the dynamic model in order to stabilize the system. The helicopter model is derived from [35]. This linear dynamic model, derived at hover, consists of 14 states that include the linear velocities, angular rates, main rotor and stabilizer flapping dynamics, yaw rate feedback, main blade coning dynamics and first derivative, and the inflow. This model is augmented and then reduced to 13 states. For trajectory tracking, the body frame positions are added, rather than inertia frame which causes nonlinearities. Attitude angles are approximated by time integrals to remove nonlinearities, valid for small roll and pitch angles. Next, the states that are not directly measured are removed, except for the yaw rate feedback. The final state vector includes the body frame positions, linear velocities, attitude, angular rates and yaw-rate feedback. This model is used for the purpose of control synthesis. The control architecture consists of three loops. The innermost loop uses a linear quadratic regulator (LQR) controller to stabilize right hand plane poles. A feedback linearization middle loop controller is used to decouple the input/output pairs. Then a PD controller is used for trajectory tracking. The final cascaded controller's matrices are able to be computed off-line, allowing for relatively simple implementation in real time. A simplified state estimator is used for real time implementation to track the yaw-rate feedback parameter. Lastly, guidance waypoints are transformed to the body frame by a direct cosine matrix. Simulated and experimental results are presented for a figure 8 trajectory with constant altitude.

In [88, 89], an adaptive controller is designed on a 13 state linear model of the Yamaha R-Max with decoupled translational and attitude dynamics. A PD compensator is added to each of the loops.

In [95, 96], a tracking controller using a Multi-Loop PID (MLPID) is designed for a 12 state LTI model of the Berkeley Yamaha R-Max. This 3-loop architecture is similar to that in Fig. 22, consisting of an inner loop for attitude control, middle loop for linear velocity control and the outermost loop for position control. A spiral ascent trajectory is used to compare the performance of the MLPID to that of a Nonlinear Model Predictive Tracking Controller (NMPTC). The results of the simulations show that although the MLPID is still able to track complex trajectory, it does so with a significant increase in error compared to the NMPTC. The simulations show the limitations of PID controllers for maneuvers and flights conditions that deviate from those used in development of the linear model.

In [167, 168], a MLPID controller is designed for an 11 state linear model using a 3-loop architecture shown in Fig. 22. The three loops consist of inner attitude, mid velocity and outer position loop control. Loop gains are acquired using root locus methods for response speed and damping ratio. In this control scheme, loops may be disabled according to the flight maneuver. In cruise mode, only velocity and attitude loops are necessary, whereas in hover mode all loops are needed. Experimental results show adequate performance in hover for nearly 3 minutes with slight yet acceptable oscillatory motion. A pilot uses velocity control to take-off and put the helicopter at a necessary altitude, then engages the hover control.

Lastly, in [163], a mixed controller architecture is used for a 2-loop architecture, lateral/longitudinal and attitude/altitude control, capable of hover, positioning and forward flight at low velocities. Here, PID control is used for the innermost attitude/altitude control.

7.2 Linear LQG/LQR Controllers

Linear Quadratic Gaussian (LQG) and Linear Quadratic Regulator (LQR) controllers are types of optimal feedback controllers that utilize quadratic cost functions. They can be used in SISO or MIMO structures. Linear quadratic controllers use full state feedback in order to obtain an optimal input for the system. LQG controllers consist of a LQR controller and a Kalman filter being based on separation of control (LQR) and estimation (Kalman). LQG controllers are meant to operate in the presence of white noise. LQR controllers seek to find an optimal input that will drive the state to a desired final state by minimizing a quadratic cost, which is a function of the state vector, the input vector, and two gain matrices.

Linear quadratic controllers have their drawbacks. First, if it is not possible to reach the final state from the initial state, then it becomes impossible to determine any input vector. Additionally, in the case that not all the states are observable, it becomes necessary to implement a state observer to feedback the missing measurements for full state feedback. Additionally the output limitations are not considered in the controller design, which may lead to optimal input vectors beyond the operating conditions of the system.

Despite drawbacks, LQG and LQR controllers have been implemented in a number of UAV applications, including rotorcraft. in [17], the LQG controller is used in hover control of a gimbaled model helicopter with a 6 state linear time-invariant (LTI) model. Simulated results are presented for both a 3 DOF and 6 DOF model for hover with pilot commanded attitude. In [136], an LQG controller with setpoint tracking is developed using this same linear model for hover and a low velocity regime. Experimental results are presented for hover stabilization using the 3 DOF stand.

In [19], an LQG controller is used on a 13-state linear model of the Yamaha RMAX for right hand plane stabilization and placed as an innermost loop.

In [58, 130], a LQR controller is used in a two loop architecture where the dynamics are separated into outer longitudinal-vertical and inner lateral-directional dynamics. The outer loop structure and control design is given in detail in [58], where integrators are added to the LQR controller in order to drive the forward speed and altitude rate tracking steady-state error to zero. Because of the limitations of the controller to the operating points assumed for the purpose of linearization of the dynamics, different gains are designed for a set of forward speeds. The inner loop structure is given in detail in [130]. Here the structure follows a similar approach to the outer loop, only integrators are added to the sideways velocity and yaw rate. In both, the LQR control is augmented with feed-forward schemes and notch filters for shaping of closed-loop responses and to compensate for the slight damping of the stabilizer bar, respectively.

In [86], a Linear Quadratic Regulator (LQR) based controller of a linearized model at hover is enhanced with an Unscented Kalman Filter (UKF) for online active model error approximation between the simplified and full dynamic models. The UKF is used because of its ability to handle nonlinear systems with fast dynamics in online applications. UKFs use nonlinear models without the need of some heavy computations that are required of Extended Kalman Filters (EKF). The linearized model consists of 12 states, (linear velocities, angular rates, attitude and position), and 4 inputs, $\mathbf{u}_c = \left[\delta_{col}\ \delta_{ped}\ \delta_{lat}\ \delta_{lon}\right]^T$. Results are presented for simulations comparing the UKF estimation and true model difference that show the UKF's ability to track the true model difference. Secondly, simulation results are presented that show the ability of the enhanced LQR controller to track a desired trajectory.

In [112], a hovering attitude controller is developed from an 8 state linearized model using a Loop Transfer Recovery (LTR) approach, LQG/LTR.

In [202], a Linear Quadratic Gaussian/ Loop Transfer Recovery (LQG/LTR) approach is used on an RC model helicopter on a mechanical stand that allows 6 DOF flight in a 2 meter cube area. The helicopter is modeled as an 18 state linear time-invariant model which includes positions, linear velocities, attitude angles, angular rates, main rotor flapping angles, main rotor time constant, induced main and tail rotor velocities, and motor state (PI for constant speed). Output measurements of position and attitude. The helicopter model is then split into two separate dynamics: i) the heave/yaw motion and ii) the lateral/longitudinal motion. The former consists of vertical position and speed, yaw angle and rate, induced velocities, motor state, and rotor speed. The latter consist of side and forward positions and velocities, roll and pitch angles and rates, main rotor flapping angles. Additionally, a second order Padè approximation (transfer function) is used before each input to model the delay of transmitting the controller commands through the multiplexing radio. This adds 4 states to each subsystem. The controller design goals are to reject disturbances in the low-frequencies while maintaining a good robustness margin. A cascaded PD controller is used for flight in order to determine necessary model parameters. A PD controller is added to each input of the system, with a cascade on the forward/pitch and sideways/roll inputs. Next, a LQG/LTR controller is used, one for each subsystem. The results for the LQG/LTR show unsatisfactory input-output behavior despite good closed-loop behavior. This is is somewhat remedied by leading the reference signal statically to the controller output.

In [163], a mixed 2-loop controller is designed for a 6 state LTI model of an EC Concept electric RC model helicopter. Here, the outer loop handles lateral-longitudinal control while the inner loop handles altitude-attitude control. A LQR is used on the inner loop for heave and yaw control. Simulated results are presented for hover and position control and in a low velocity regime.

7.3 Linear $\mathcal{H}_\infty$ Controllers

$\mathcal{H}_\infty$ control is a type of multi-variable robust model-based control. One major advantage of $\mathcal{H}_\infty$ control is its robustness in the presence of model uncertainties and disturbances. This quality becomes very useful for highly complex systems, since complete modeling of the rotorcraft dynamics is very difficult and a number of assumptions and simplifications are made in order to obtain a workable dynamic model.

In several designs $\mathcal{H}_\infty$ controllers have been applied for both loop shaping, which uses classical control approaches, and synthesis, where a feedback gain is determined.

In [17], an $\mathcal{H}_\infty$ controller for a 6 state linear model of a helicopter on a 3 DOF stand is designed for hover with piloted attitude commands. In this design, the weighting functions are specified for continuous time, and are chosen so that the yaw dynamics are faster than the pitch and roll. The controller is discretized using a bi-linear transformation. It is shown via simulation results that the $\mathcal{H}_\infty$ controller is able to decouple the modes while maintaining fast dynamics. Experimental results are done with a pilot assistance to place the helicopter in hover, then engaging the controller and finally providing attitude commands. Overall, the $\mathcal{H}_\infty$ controller responded quickly on the pitch and roll access with higher damping in the yaw access, allowing for greater and faster disturbance rejection and reduce cross coupling.

In [107], an $\mathcal{H}_\infty$ controller is derived for a 30 state linear model of the CMU Yamaha R-50 helicopter designed for hover operation. This model includes the 9 rigid body states, 6 main rotor states, 4 stabilizer bar states, 3 states for Pitt-Peters inflow dynamics, and 2 states for each of the 4 actuators. This controller uses a 3-loop architecture, as seen in Fig. 22, to perform heading and tracking control. The inner-most loop handles attitude and altitude control. The mid loop handles lateral-longitudinal velocity control. And finally, the outer-most loop handles position control in the form of a reference trajectory. The controller is implemented using four maneuvers: a forward coordinated turn, a backward coordinated turn, a nose-out pirouette, and a nose-in pirouette. In the case of the two turns the helicopter starts at hover, then the pilot commands forward velocity. Afterwards, the pilot commands the turn giving a forward velocity, v_x, and yaw rate command, $\dot{\psi}$, while maintaining zero side-ways velocity, V_y. Since the command is on v_x, the x-position loop is disengaged, however the y-position loop is engaged to drive the tracking error to zero. In the case of the pirouettes the helicopter starts at hover, then the pilot commands a side-ways velocity, v_y, until the turn is commanded. For this, the controller is given a constant v_y and $\dot{\psi}$, while maintaining zero v_x. Similar to the turns, the y-position loop is disengaged, but the x-position loop is engaged to drive the error to zero.

In [201], a robust controller that uses $\mathcal{H}_2$ and $\mathcal{H}_\infty$ methods is designed for position control at hover. The helicopter testbed and model are identical to that in [202]. This control scheme takes advantage of the fact that the interaction between vertical/yaw motion and lateral/longitudinal motion of the helicopter is weak at hover in order to design control of the two systems separately. In the $\mathcal{H}_2$ design, an augmented scheme is used and weighting matrices are presented. In the $\mathcal{H}_\infty$ design, a 2 DOF design is used for the vertical/yaw dynamics in order to deal with resonance and reference tracking. For the lateral/longitudinal dynamics, a weighting scheme is used to shape the sensitivity matrices since the number of measurements is larger than the number of control signals. Results for each controller are compared using the static gain and bandwidths. It is shown that the $\mathcal{H}_\infty$ design shows higher performance, but with the need of additional knowledge than the $\mathcal{H}_2$ design.

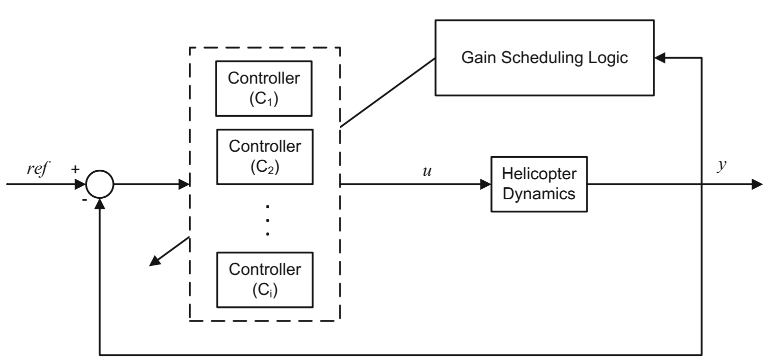

Fig. 23 Gain scheduling control block diagram

7.4 Linear Gain Scheduling Controllers

Gain scheduling is a term that describes approaches seeking to switch between various controllers designed for specific operating conditions. Since linear controllers are designed through linearization about some operating conditions, it may be necessary to determine multiple linear models, controller gains, or even control methods in order to be able to operate the helicopter in a larger flight envelope, as shown in Fig. 23. Some of the considerations with gain scheduling is choosing which parameters and operating points will be used to determine the switching requirements as well as how the switching will occur.

In [181], a switching controller using piece-wise quadratic Lyapunov-like functions is presented, based on Mettler's 13 state linear model of the Yamaha R-50 model parameters identified for hover and cruise [131]. Simulations are chosen with a simple flight scenario, allowing focus on the switching phenomena for smoothing the transition between hover and cruise.

In [58], an adaptive control scheme using neural networks, linear quadratic regulators, and notch filters, is designed for various sets of gains. Each set of gains is determined for 6 forward speed values. Switching occurs between the gains once the helicopter enters a new flight regime.

7.5 Nonlinear Controllers

While linear techniques have proven capable of performing maneuvers in hover or low velocity regimes, there are still a number of limitations associated with linearization and simplification of the dynamics models for the purpose of control law design. By using a nonlinear dynamic model of the helicopter, new control laws can be designed with greater capabilities to perform more complex maneuvers at higher velocities. Much of the work involving nonlinear models includes backstepping, adaptive control, feedback linearization or dynamic inversion, model predictive control, and nested saturation loops.

7.6 Nonlinear Backstepping Controllers

Backstepping is a recursive control method used to find a control Lyapunov function for stabilizing nonlinear systems of a lower triangle form, known as pure-feedback form, [104]. Design of backstepping controllers starts with looking at creating a feedback control law and a Lyapunov function to a general rigid body model of Newton Euler form with force and moments as system inputs, [61]. In order to ensure this cascaded structure, it is common practice to neglect the small parasitic, or small body forces [30, 158]. In [30], a controller is presented based on backstepping techniques for an Euler-Lagrange dynamic model in addition to the traditional Newton-Euler helicopter dynamic model used more commonly.

A theoretical analysis for guaranteed tracking using a Lyapunov based backstepping controller is presented in [122]. The work is continued in [121] on a nonlinear model of the Vario 23cc helicopter. Simulations show the ability of the controller to perform trajectory tracking for position adjustments while in hover and following an ascending helical trajectory.

In [47], a backstepping controller is presented with the purpose of avoiding artificial singularities that are caused by representation of the attitude angles using Euler coordinates. The controller uses an approximate model of the helicopter based on [101]. The helicopter dynamics are represented by a state vector consisting of two elements. The first element is a matrix consisting of the helicopter orientation matrix and translation vector. The second element is a matrix consisting of the angular rate skew-matrix and translational velocity vector in the body axes. The control law is designed with the objective of tracking a smooth, feasible reference trajectory. The translational dynamics are controlled with the use of a quadratic Lyapunov function and PD control law in order to determine desired attitude trajectories. The attitude dynamics are controlled using backstepping techniques in order to track the reference attitude trajectories and stabilize the system. Simulated results are presented for the following four maneuvers: i) point stabilization, ii) point stabilization during inverted flight, iii) trim trajectory tracking of a climbing turn, and iv) transition to inverted flight. The first two maneuvers show similar responses. The third maneuver showed good results, though tracking of a time-parameterized trajectory resulted in aggressive flying and excessive control effort. The final maneuver shows the effect of going through the singularity, causing larger deviations in the second half of the maneuver. However, the results show ability to perform the maneuver.

In [151], a velocity control law based on backstepping techniques is developed for a nonlinear Newton-Euler dynamic model of a Yamaha R-MAX as part of an overall scheme to land the helicopter on a moving platform by tracking its velocity. The model includes forces and torques generated by the main and tail rotors, as well as the flapping and thrust dynamics. Simulations show the ability of the controller to track a desired velocity.

In [4], a position controller using backstepping is designed for a nonlinear model of an Eagle UAV, with tunable parameters for position and velocity control. Again, the model is derived from Newton-Euler equations of motion and includes models of induced velocity, thrust, forces and moments, and flapping dynamics of the rotors and flybar. Simulation shows the ability of the controller to perform position and velocity control.

In [5], backstepping control is used for autonomous landing control using a tether and correction to the flapping and servo dynamics. In [36], backstepping is used to stabilize the translational and attitude dynamics for hover and trajectory tracking. Backstepping is also used to perform trajectory generation for target tracking using a discretized nonlinear controller in [165]. In [182], backstepping is used in attitude control using a nonlinear model-based on quaternion feedback. Other works involving backstepping include [159, 186, 190, 193, 206, 207].

In [155, 157], a backstepping controller is derived for tracking of predefined position and yaw trajectories. The design makes use of the thrust vector to stabilize the position error dynamics, and the rotation matrix for the attitude dynamics while guaranteeing the helicopter will not overturn when trying to track the position trajectory. Simulation results are performed using the parameters for an X-Cell 60 helicopter and show the controller's ability to track the reference trajectory for an ascending ramp trajectory as well as a take-off/figure-8 trajectory. The performance is compared with that of a basic PID controller design proposed in [130]. The results show the superior ability and robustness of the backstepping design compared to the PID controller.

7.7 Nonlinear Adaptive Control

Adaptive control seeks to address issues of parameter uncertainties. This can include parametric, structural

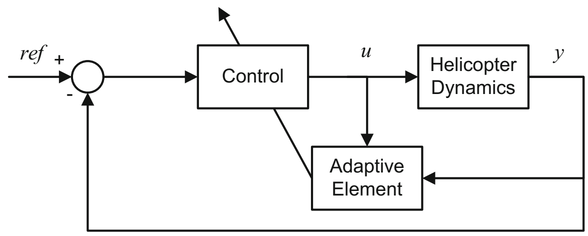

Fig. 24 Adaptive control block diagram

and environmental uncertainties as well as unmodeled or changes in dynamics [82, 187]. The goal of an adaptive controller is to adapt itself to changes in these uncertainties based on desired performance criteria. Adaptive controllers typically include some class of parameter estimator, or adaptive element, and a control law that adapts according to the estimation. The various classes of adaptive controllers result from the choice of estimator and control law [81]. This type of control has great potential for applicability in a much larger flight envelope than other traditional control approaches. The adaptive element or parameter estimator uses the input to the plant as well as the output in order to determine the changes to the control law gains or parameters. This type of structure is shown in Fig. 24. Another type of popular controller utilizes an ideal reference model in addition to the adaptive element, or parameter estimator. This class of adaptive control is known as Model Reference Adaptive Control (MRAC). The desired system behavior is given by the reference model and is governed by the reference input. This type of architecture is shown in Fig. 25.

In [37, 153], an adaptive nonlinear controller design, presented in [29], is implemented on a Yamaha R-50 helicopter which utilized approximate inversion linearization. The controller can be configured for each rotational access as an attitude command attitude hold (ACAH) scheme or rate command controller. The adaptive element is achieved through the use of

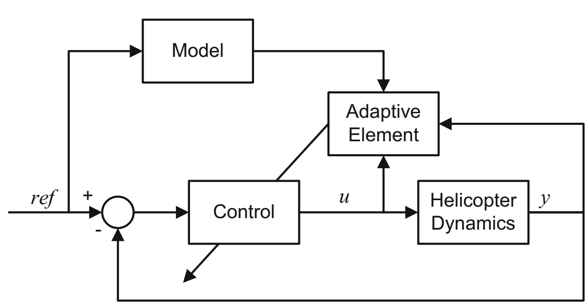

Fig. 25 Model referenced adaptive control block diagram

neural networks for online adaptation and to cancel the effects of inversion errors. Real-time Hardware-in-the-Loop (HIL) testing is performed using piloted commands and visualization software. The simulations show the controller's ability for online learning and tolerance of unmodeled dynamics, noise and delays.

In [69], a high bandwidth inner loop controller for attitude and velocity stabilization is designed for a Vario X-treme helicopter using $\mathcal{L}_1$ adaptive control theory to test the controllers robustness against uncertainties and disturbances. Von Karman wind models and gusts were implemented in simulation. The simulation trajectory included three stages: i) sideways translation, ii) helical motion with nose pointed inward, and iii) hover. The model is based on [39].

7.8 Feedback Linearization Controllers

Feedback linearization, also known as Nonlinear Dynamic Inversion (NDI), is a technique used to find a feedback control law by transforming the nonlinear system dynamics into an equivalent fully or partial linear form through some algebraic transformation. There exist various levels of feedback linearization, from full state feedback linearization, which yields a full linearization, to input-output linearization, where the mapping between inputs and particular outputs of interest are linearized but the state equations are only partially linearized [94]. This method allows for the application of linear control techniques to the system.

In [11], a 3 DOF reduced-order nonlinear model of a scale model helicopter mounted on an experimental platform is presented. This is part of the development of a 7 DOF nonlinear model and nonlinear control design for a VARIO Benzin-Trainer scale model helicopter. Different to this modeling method is the inclusion of the main and tail rotor dynamics in the Lagrangian equations. Additionally, the inputs are taken as the actual helicopter inputs. The aerodynamic forces and torques used in the Lagrangian equations are presented. Next, the dynamics of the helicopter mounted on the experimental platform are derived using Lagrangian dynamics. Details of the derivation of the dynamics are given in [10]. Next a linearizing control design is presented of the reduced order model. This reduced order model only considers the pilot inputs for collective pitch of the main and tail rotors. The design is split into two phases: i) start-up and take-off, and ii) vertical flight. Simulation results show the ability of the controller to track a desired trajectory. However, it is obvious that the trajectory design is crucial for control design and must be chosen so as not to saturate the inputs. Experimental results are also presented for stabilization of the helicopter dynamics for various values of altitude and yaw.

In [20], a theoretical stability analysis is presented for a proposed nonlinear UAV rotorcraft controller. The controller is a hierarchical controller for position and attitude control using partial state feedback with time-scale separation between the translational and orientation dynamics. The proposed controller is analyzed using single perturbation theory and is found to be stable.

In [101], output tracking control is investigated. The helicopter dynamic model is derived from Newton-Euler equations. The controller is based on input/output linearization and by neglecting coupling between roll/pitch and lateral/longitudinal forces. Positions and headings are chosen as outputs in order to ensure that the approximated system is dynamically linearizable without zero dynamics. Simulation results are shown for controllers based on exact input/output linearization and approximated input/output linearization. The results show that the approximate model is able to track the trajectories without exciting oscillations in the internal model.

In [102], a control design based on differential flatness is presented. This design involves neglecting the coupling between the rolling/pitching moment and the lateral/longitudinal forces. The details of the dynamics equations used are given in [101] and are based on Newton-Euler equations. An approximate model is presented for control design followed by a modification for the exact helicopter model under trim flight conditions. The control scheme features an inner attitude control loop and outer position control loop. The outer controller consists of a mapping function that utilizes the flatness of the outer loop to generate the inner trajectory. It is assumed that there is an inner controller to drive the error to zero. For the inner loop two controllers are used. One is for tracking the attitude, and the other for tracking main rotor thrust. Attitude control is based on feedback linearization. Simulations are performed in which the controllers are required to achieve hover from an initial position at a considerably large distance to the desired origin and turning the heading to the desired orientation. The results show the controller's ability to drive the trajectory error to zero with the exact model and with the condition that the trajectory is in trim flight conditions.

In [18], dynamic feedback linearization is used for tracking the longitudinal dynamics. Feedback linearization is implemented on a Bergen Industrial Twin with compensation of small body forces in [64] and also combined with nonlinear $\mathcal{H}_\infty$ in [75] for trajectory tracking. Incremental nonlinear dynamic inversion is used on an 8 DOF nonlinear model for velocity reference tracking and attitude control in [172]. Other examples include [67, 164, 170, 186, 190, 205].

7.9 Nested Saturation Loops

In [15], a nonlinear controller is designed with the goal of asymptotically tracking a vertical, lateral and longitudinal reference while maintaining a constant yaw angle. This is done by taking advantage of techniques from [84] and modifying the control structure. The helicopter model is based on [101]. The forces and torques acting on the helicopter are nonlinear functions of 5 control inputs, $u = [P_M\ P_T\ a\ b\ T_h]^T$, the main and tail rotor collective pitch, the lateral and longitudinal cyclic angles, and engine throttle control, respectively. The helicopter dynamics are divided into 4 groups: the vertical, attitude, engine, and lateral/longitudinal dynamics. Quaternions are used to describe the rotation between the body and inertial reference frames and the helicopter attitude. The controller is designed to handle large uncertainties in parameters, including vehicle mass, inertia, aerodynamic coefficients, and the engine model. The inner loop is a high-gain feedback and controls the attitude dynamics. The outer loop is designed with a nested saturation structure and controls the lateral/longitudinal dynamics. The attitude dynamics for pitch and roll are used as virtual inputs to the lateral/longitudinal dynamics and for a virtual control law which is "step-back" to the actual control inputs $v = [a\ b\ T_h]^T$. The control law developed is inspired by [83]. Simulations are performed using parameters with assumed uncertainties of 30 %. The chosen trajectory is created using the 3$^{\text{rd}}$ order spline interpolation method and must satisfy bounds on the higher order time derivatives. The trajectory has three main movements: forward/lateral movement with ascent, lateral movement with descent, and reverse movement to start position. The simulations show the ability of the controller to maintain a relatively constant yaw angle while tracking a vertical/lateral/longitudinal reference trajectory.

In [125], a nonlinear controller is presented with the objective of controlling vertical, lateral, longitudinal and yaw attitude of a helicopter along a trajectory. The control design includes a combination of feedforward control actions, high gain feedback laws, and nested saturation feedback laws. The control structure consists of an inner loop to govern attitude dynamics, and an outer loop to govern the lateral-longitudinal dynamics. It is proposed that this control structure can achieve very aggressive maneuvers characterized by large attitude angles. In addition, it is proposed the controller is able to cope with the possibility of large uncertainties in the physical parameters. The helicopter dynamic model is derived from Newton-Euler equations of motion of a rigid body. This model includes 5 inputs, the main and tail rotor collective pitches, the lateral/longitudinal cyclic angles, and the motor throttle. The desired trajectories are defined as known time profiles with restrictions on the time derivatives dictated by functional controllability and physical constraints on the inputs. Experimental results are presented using a miniature commercial 60 series helicopter. Nominal values of controller gains are refined by trial and error. An aggressive maneuver is used to test the controller, which consists of fast forward speed with a constant desired yaw such that the maneuver required both pitch and roll aggressive attitudes. Altitude is fixed. A polynomial describing the maneuver is provided. The controller presented a small tracking error and slight fluctuations. These have been attributed to measurement precision and model uncertainty.

7.10 Nonlinear Model Predictive Controllers

Model Predictive Control (MPC) is a technique that utilizes a dynamic model of the system in order to anticipate and predict future behavior of the plant while considering constraints on states and inputs [6, 135]. This ability to predict future behavior allows for on-line solving of an optimization problem that minimizes the error over a future horizon. MPC is also known as moving horizon or receding horizon control (RHC) [96]. The general structure of an MPC controller is shown in Fig. 26.

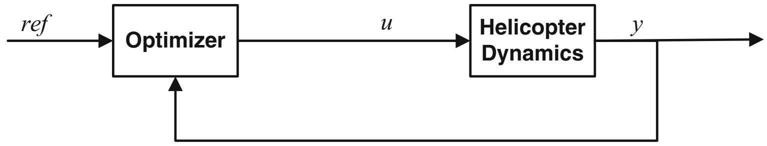

Fig. 26 Model predictive control block diagram

In [95, 96], a nonlinear model predictive tracking controller (NMPTC) is designed for the Berkeley Yamaha R-MAX. The helicopter model is a 12 parameter nonlinear model of the Yamaha R-Max. The MPC uses a cost minimization function with gradient descent for trajectory and tracking control. Simulations in both show the NMPTC is superior over the MLPID for a spiral ascent in the presence of heavy nonlinearities and coupling along with being robust to parameter uncertainty. This paper also presents an application to collision avoidance and vision guided landing. Experimental results are presented in [95].

In [41, 42], a nonlinear MPC is used for autorotation landing using a nonlinear model of the autorotation dynamics of a helicopter which includes the drop rate, altitude, engine RPM and inflow dynamics.

In [45], a predictive controller with a disturbance observer is designed for a Hirobo Shuttle Plus30 helicopter. The model used is a 10 parameter attitude model. A PID controller is used for comparison of the controller performance and experimental results are presented for attitude control using a test bench.

In [117], a piecewise MPC is used on a 14 parameter nonlinear model of a Hummingbird helicopter. Simulated and experimental results are presented for a square trajectory. In [115, 119], explicit nonlinear MPC (ENMPC) is used for trajectory tracking using a Trex 250 nonlinear model for square, pirouette and figure-8 trajectories. Both simulated and experimental results are presented. Lastly, nonlinear MPC is presented in [116] for path planning.

Other examples of MPC control include [9, 162, 175, 176, 199].

7.11 Other Nonlinear Methods

In addition to the nonlinear control methods discussed, there has been a fair amount of research introducing new or novel nonlinear techniques to helicopter navigation and stability control. One such method is sliding mode control, a robust method that forces the system behavior toward a particular trajectory, known as a sliding surface or manifold, in a finite amount of time and then maintain that behavior. Sliding mode control has been shown to be robust against uncertainties, [94]. Examples of sliding mode control include [25, 48, 173, 188].

Another approach involves using Linear Matrix Inequalities (LMI) in the design process, such as with $\mathcal{H}_\infty$ and $\mathcal{H}_2$ or optimal control techniques. This can be seen in [68, 128].

For completeness purposes, a brief summary of model-free techniques follows.

7.12 Model Free Techniques

Unlike model-based techniques, model-free control utilizes learning-based methods to control the helicopter. These techniques require several flight tests in order train the system using real flight data. Typically, a pilot will perform specified maneuvers while the FCS collects both navigational measurements and pilot commands. This input-output data is used by the learning-based controller to train the helicopter to mimic the maneuver. The most commonly used methods of model-free control include fuzzy logic, neural networks, and human-based learning. Though the prospect of controller development without the added task of identifying a sufficiently accurate model is appealing, it is difficult to determine the stability and robustness of these methods [93].

Fuzzy logic control is a method that seek to mimic the way humans think and make decisions by creating a set of rules that are used by the controller to analyze the input to determine the appropriate output. Examples of fuzzy controllers in helicopters include [51, 52, 90, 134, 137, 148, 178, 179].

Neural networks is a type of learning method that seeks to mimic the way human or animal brains work. That is, it seeks to mimic the human central nervous system. This structure utilizes input-output data to program the neurons in the network. Examples of neural network control in helicopters include [24, 29, 42, 54, 91, 139, 145].

Examples of human-based learning techniques include [1, 2, 55, 56, 110, 111]. Lastly, the use of model-free or learning-based methods, such as Neural Networks and Fuzzy Control, have been used to augment model-based methods or tune gains. These approaches include [37, 41, 42, 139, 193].

8 Comparison of Approaches

This section provides a detailed review of conducted research in the area of unmanned helicopters. Table 6 lists the helicopter platforms used in the reviewed methods. Tables 7 to 12 provide related abbreviations that facilitate better understanding of the reviewed control techniques. For example: Table 7 lists the types of results obtained in the reviewed control techniques. Table 8 provides a listing of model types and system identification. Table 9 lists the various maneuvers performed in the reviewed control techniques, while Table 10 lists the autonomy modes. Table 11 lists the state vectors used, and, Table 12 lists the control techniques reviewed.

8.1 Linear Controllers

A detailed review of linear control techniques used in unmanned helicopter navigation and control is presented in Table 13. These include classical, SISO, and MIMO linear model-based methods.

8.2 Nonlinear Controllers

A detailed review of nonlinear control techniques used in unmanned helicopter navigation and control is presented in Table 14. The reviewed techniques include backstepping control, feedback linearization, nested saturation, adaptive control, and sliding mode control, among other nonlinear techniques.

9 Proposed Comprehensive and Modular Navigation Control Architecture

In a typical rotorcraft FCS architecture the navigational sensors measure key controller parameters. The controller, then, determines the optimal inputs to the helicopter servos. These signals must pass through a switch that interfaces with the human operator following either the ‘human-on-the-loop’ or the ‘human-in-the-loop’ concept, depending on the human’s level of interaction.

Previous designs of the flight controller have largely been limited by processing capabilities, portability, accuracy and reliability of on-board flight control hardware and software. A major challenge of autonomous UAVs has been the level of on-board intelligence and the level of autonomy to be achieved in order to facilitate mission planning, decision making, control execution, data logging, real-time communication with a GCS, and online mission modification. Such functionalities are also tightly coupled with a timing architecture required to guarantee proper performance. Thus, a FCS must include the following components:

- Complete navigation sensor-suite
- Higher level mission planning and trajectory generation
- Sensor-based real-time control
- Failure detection and accommodation
- Vision capabilities
- Detect, See/Sense-and-avoid (DSAA)
- Pilot take-over or assisted flight
- Communication capabilities

The proposed FCS, developed by the DU^{2}SRI team and depicted in Fig. 27, includes modules to address various requirements during flight, as well as redundancy and safe operation. A suite/bank of navigational controllers provides real-time flight data used in the flight controller and for data transmission to the GCS. The on-board sensors include GPS, an Inertial Measurement Unit (IMU) and Inertial Navigation System (INS) that provide inertial measurements, also used for location estimation and sensor fusion; a magnetometer for heading information and an altimeter and/or laser range finder for altitude measurements and precision landing capabilities. A detect-sense-and-avoid (DSAA) module is used to detect and identify potential threats or opposing manned/unmanned aircraft, for midair collision avoidance, and for calculating/updating collision probabilities and possible evasive trajectories to avoid collisions. A see-and-avoid system (the on-board vision system component) with its own dedicated computer complements the

Table 6 Helicopter Platforms

P01	60 Series	P18	ServoHeli-40
P02	AF25B	P19	SF-40
P03	Align T-Rex 600	P20	THeli 260
P04	Bell 205	P21	Thundertiger Raptor 30v2
P05	Bell 412	P22	Tiny CP3 Heli
P06	Bergen Industrial Observer	P23	T-Rex 205
P07	Bergen Industrial Twin	P24	Vario 23cc
P08	EC Concept Electric RC	P25	Vario Benzine Trainer
P09	Graupner Avant Garde RC	P26	Vario XLC
P10	Hirobo Eagle	P27	Vario X-treme
P11	Hirobo Shuttle Plus	P28	X-Cell 50
P12	Humming Bird	P29	X-Cell 60
P13	Kyosho Concept 60 Graphite	P30	X-Cell Tempest
P14	Lynx Heli	P31	Yamaha R-50
P15	PUMA SA330	P32	Yamaha R-MAX
P16	Raptor 90-SE	P33	T-tail
P17	ServoHeli-20	P34	Unknown/Other

Table 7 Results

EXP	Experimental Flight Results	SIM	Simulation
GIM	Gimbaled Stand	THE	Theoretical Analysis
HIL	Hardware-In-the-Loop	XPL	X-Plane

Table 8 Helicopter modelling and identification

ALT	Altitude	MIMO	Multi-Input/Multi-Output
ATT	Attitude	NLN	Nonlinear Model
DCP	Decoupled	OUT	Outer Loop
DIR	Directional	POS	Position
HEA	Heave	SISO	Single-Input/Single-Output
INN	Inner Loop	TF	Transfer Function
LAT	Lateral	TRS	Translational
LIN	Linear Model	VEL	Velocity
LON	Longitudinal	VER	Vertical
ACT	Actuator Dynamics	LTI	Linear Time-Invariant
CNT	Continuous Time	LTV	Linear Time-Varying
DST	Discrete Time	NWTE	Newton-Euler
EWR	External Wrench Model	PEM	Prediction-Error Minimization
FLP	Flapping Dynamics	QUA	Quaternions
FRID	Frequency Response ID	TGYR	Tail Feedback Gyro
FSL	Fuselage dynamics	TVAL	Time Domain Validation
LGR	Lagrangian	CIFER	Comprehensive Identification from FrEquency Responses

Table 9 Flight maneuvers

ACC	Acceleration	INV	Inverted Flight
ASC	Ascent	LND	Landing
ATR	Auto-rotation	LOW	Low Velocity
BNK	Banked Turn	PIR	Pirouette
CIR	Circular	RLL	Roll
CRU	Cruise	SDW	Sideways
F-8	Figure-∞	SPR	Spiral Ascent/Descent
FWD	Forward	SQU	Square
HLX	Helix	TAN	Heading tangent to path
HOV	Hover	TKO	Take-off
HXT	Helical Turn	UPW	Flying Up

Table 10 Autonomy mode

3LP	3 Loop Pos/Vel/Att Control	PPL	Path Planning
ACAH	Altitude Command Attitude Hold	PTH	Trajectory Tracking/Path Following
ALT	Altitude	RC	Rate Command
ATT	Attitude Control	RCAH	Rate Command Attitude Hold
HS	Hover Stabilization	STB	Stabilization
HYW	Heave/Yaw	TRG	Target Tracking
LTLN	Lateral/Longitudinal	TRJ	Trajectory Generation
PIL	Pilot Commanded	VEL	Velocity Control
POS	Position Control	YAW	Yaw/Heading Control
TRK	Reference Tracking	SPD	Speed Tracking

Table 11 State vectors

6 ST:	$[\omega\ \Theta]$	8 ST:	$[u\ \ v\ \ p\ \ q\ \ \phi\ \ \theta\ \ a\ \ b]$
9 ST:	$[V\ \ \omega\ \ \Theta]$	10 ST ATT:	$[\omega\ \ \Theta\ \ a\ \ b\ \ c\ \ d]$
10 ST:	$[V\ \ \omega\ \ \phi\ \ \theta\ \ a\ \ b]$	11 ST:	$\left[V\ \ \omega\ \ \phi\ \ \theta\ \ a\ \ b\ \ r_{fb}\right]$
12 ST:	$[P\ \ V\ \ \omega\ \ \Theta]$	13 ST:	$\left[V\ \ \omega\ \ \phi\ \ \theta\ \ a\ \ b\ \ c\ \ d\ \ r_{fb}\right]$
13 ST THR:	$[P\ \ V\ \ \omega\ \ \Theta\ \ \Omega]$	14 ST:	$[P\ \ V\ \ \omega\ \ \Theta\ \ a\ \ b]$
LAT/LON1:	$[v\ \ p\ \ \phi\ \ b]\,/\,[u\ \ q\ \ \theta\ \ a]$	INN/OUT:	$\left[\omega\ \ \Theta\ \ a\ \ b\ \ r_{fb}\right]/\,[P\ \ V]$
LAT/LON2:	$[u\ \ v\ \ \phi\ \ \theta\ \ p\ \ q\ \ a\ \ b]\,/\left[w\ \ r\ \ r_{fb}\ \ \psi\right]$		
LON-VER/LAT-DIR:	$[u\ \ a\ \ w\ \ q\ \ z\ \ \theta]/[v\ \ b\ \ p\ \ r\ \ \phi]$		
30 ST:	$\left[u\ v\ w\ p\ q\ r\ \phi\ \theta\ \psi\ a_0\ a_1\ b_1\ \dot{a}_1\ \dot{a}_1\ \dot{b}_1\ c_1\ d_1\ \dot{c}_1\ \dot{d}_1\ \lambda_1\ \lambda_2\ \lambda_3\ \delta_{lat}\ \delta_{lon}\ \delta_{col}\ \delta_{ped}\right]$		
41 States:	9 fuselage (V, ω, Θ), and 32 main rotor states.		

Table 12 Control Techniques

1ST	1st (2nd) Order Compensator	LSF	Liouvillian System Feedback
AAP	Angular Acceleration Prediction	LTR	Loop Transfer Recovery
AC	Adaptive Control	MC	Modal Controllers
AI	Approximate Inversion	MLPID	Multi-Loop PID
BS	Backstepping	MPC	Model Predictive Control
CMP	Compensators	MS	Mixed Sensitivity
CNF	Composite Nonlinear Feedback	MTFC	Mamdani-Type Fuzzy Control
DF	Differential Flatness	μ	μ-Synthesis
DFL	Dynamic Feedback Linearization	NF	Notch Filter
EA	Eigenvalue Assignment	NMPTC	Nonlinear Model Predictive Tracking Control
FF	Feed Forward	NN	Neural Networks
FZ	Fuzzy Logic	NS	Nested Saturation
GS	Gain Scheduling	OBS	Observer
HFG	High feedback Gain	OPFB	Output Feedback Control
$\mathcal{H}_\infty$	$\mathcal{H}_\infty$ Control	OVC	Output Variance Constrained Control
$\mathcal{H}_2$	$\mathcal{H}_2$ Control	PD	Proportional-Derivative
I/O	Input-Output Linearization	PI	Proportional-Integral
IBS	Integral Backstepping	PID	Proportional-Integral-Derivative
KF	Kalman Filter	PP	Pole Placement
$\mathcal{L}_1$	$\mathcal{L}_1$ Adaptive Control	PPF	Positive Position Feedback
LYA	Lyapunov	RBF	Radial Basis Function
LFC	Linear Feedback Control	RC	Robust Compensation
LMI	Linear Matrix Inequalities	RL	Reinforcement Learning
LQFB	Linear Quadratic Feedback	RPT	Robust & Perfect Tracking
LQG	Linear Quadratic Gaussian	SBF	Small Body Force
LQI	LQR with Integral Action	SM	Sliding Mode
LQIFF	LQI with Feed Forward control	SOF	Static OPFB
LQR	Linear Quadratic Regulator	SPT	Set-Point Tracking
LS	Loop Shaping	UKF	Unscented Kalman Filter
BVP	Boundary Value Problem	LQ	Linear Quadratic
DI	Dynamic Inversion	MIV	Model Inversion
FBFN	Fuzzy Basis Fuzzy Networks	NLDI	Nonlinear DI
FBL	Feedback Linearization	OPT	Optimization
HBW	High Bandwidth	PCH	Pseudo Control Heading
INDI	Incremental Nonlinear DI	RHSOF	Robust $\mathcal{H}_\infty$ SOF
INV	Inversion	SW	Switched

DSAA component, implementing vision algorithms for a wide spectrum of tasks, also providing visual references to the GCS operator.

The flight controller software consists of three components: The Trajectory Tracking and Maneuvering component processes information from the navigational sensor suite, DSAA, vision system and GCS. Within this component, first a path planning/avoidance function receives waypoint and mission commands from the GCS along with potential threat information and visual references from the DSAA and vision system in order to determine a collision-free trajectory(ies). Next, a control mode selector/flight scheduling function selects the

Table 13 This table provides a detailed review of linear model-based control methods for unmanned helicopter navigation and control

REF	PL	MODEL	TECHNIQUE	MANEUVER	RESULTS
[3], 2010	P01	2nd order	PPF (INN), PI(OUT)	ATT	SIM
[8], 2006	P34	9 ST LIN	Eigenvalue assignment PI	ATT for roll pitch	SIM
[43], 2009	P06	13 ST LIN GIM	1st order CMP	ATT	SIM
[65, 66], 2012	P07	-	PID w/ FF gravity CMP	Translational	EXP
[63, 64], 2013	P07	-	PID	ATT	SIM
[88], 2002	P32	13 ST LIN w/ QUA	NN AC, PD CMP, PCH, AI	TRK, ATT	SIM, EXP
[89], 2005	P32	13 ST LIN HOV	PID, DI, NN	TRK, ATT	SIM, EXP
[95], 2003	P34	12 ST LTI	3LP MLPID, NLMPTC	SPA	SIM, EXP
[132], 2000	P31	13 ST, CIFER FREQ	PID ATT	HOV, FWD	SIM
[130], 2002	P28	LAT-DIR	NF, PID, LQ	RLL BNK	EXP
[145], 2011	P34	2nd Order YAW TF	RBF based PID	Yaw	SIM
[163], 2007	P28	14 ST	PID, MTFC, LQR	HOV, LOW	SIM
[166], 1998	P34	8 ST	PID, μ, FZ, I/O	-	SIM
[167], 2000	P13	11 ST	SISO MLPID	HOV, LOW	EXP
[197, 198], 2013	P20	SISO LIN FREQ	PD w/ Robust CMP for ATT, TRK	HOV, SQU	EXP
[202], 1994	P09	18 ST	Channelwise PD, LQG/TR, Modal	HOV, LOW	-
[19], 2007	P32	13 ST LIN	LQG(INN), FL(MID), PD(OUT)	F-∞ TAN	HIL, EXP
[23], 2007	P31	13 ST LIN (HOV, CRU)	LQR w/ bounded control	PTH: SQU, CIR	SIM
[57], 2002	P29	LON-VER/LAT-DIR	LQR, NF	PIL RLL, Vert ACAH	EXP
[58], 2003	P29	LON-VER/LAT-DIR	LQR, FF, NF	PIL RLL	EXP
[86], 2006	P34	12 ST LIN	LQR w/ UKF	HOV	SIM
[110, 111], 2011	P34	Model Free	LQR w/ RL	TRK	SIM
[112], 1993	P34	8 ST LIN	LQR/LTR Feedback	HOV	SIM, GIM
[114], 2012	P03	LAT/LON2	LQR SPT	INN	-
[120], 2012	P34	10 ST LIN	LQR	LIN VEL TRK	SIM
[126], 2012	P31	11 ST	LQI, KAL	HOV	SIM
[136], 1994	P08	6 ST	LQG SPT	HOV, LOW	GIM
[141], 2013	P15	25 ST	LQG OVC	CRU, BNK, HLX	SIM
[149], 2005	P04	LIN	LQ Optimal model following	HOV	SIM
[169], 2005	P19	8 ST	MIMO ATT/TRK, KAL LQI	HOV, TRK	SIM
[189], 2011	P26	LAT/LON1	LQI, LQIFF	TRK, CIR	SIM
[203], 2010	P34	12 ST	LQR w/ 1.25pt BVP	TRK, LND	SIM
[12], 2010	P34	8 ST LIN	$\mathcal{H}_\infty$ LS	HOV, LOW	SIM, EXP
[17], 1995	P08	6 ST DIS LTI	$\mathcal{H}_\infty$, LQG	HOV, PIL ATT	SIM, EXP
[28], 2013	P16	INN/OUT	3LP RPT: $\mathcal{H}_\infty$	TKO, HOV, LTLN, BNK, SLALOM, PIR	SIM, HIL, EXP
[34], 2013	P34	8 ST LIN PEM ID	$\mathcal{H}_\infty$ LS ATT	PIL RLL & Pitch	SIM
[49], 2008	P16	11 ST LIN	$\mathcal{H}_\infty/L_2$ ATT (INN), PTH (OUT)	HOV, POS, YAW	SIM
[50], 2008	P16	11 ST LIN	$\mathcal{H}_\infty$ LS ATT	HOV, BNK, PTH	SIM
[74], 2011	P34	LAT LIN	RHSOF	VEL(OUT), ACAH(INN)	SIM
[108, 109], 2003-2003	P31	30 ST	GS, $\mathcal{H}_\infty$ LS	-	SIM, EXP
[107], 2006	P31	30 ST	3LP $\mathcal{H}_\infty$	-	-

Table 13 (continued)

REF	PL	MODEL	TECHNIQUE	MANEUVER	RESULTS
[123, 124], 2013	P34	INN/OUT	Robust $\mathcal{H}_\infty/H_2$ ATT	Multi-section PTH	SIM
[128], 2011	P34	5 LIN Models	Switched LMI/H_2	HOV, ACC, ASC	SIM
[150], 2005	P04	13 ST	$\mathcal{H}_\infty$ FREQ Optimization	-	SIM, EXP
[152], 2011	P34	11 ST	Robust $\mathcal{H}_\infty$, IBS, PID	HOV	SIM
[161], 2013	P03	SISO TF	Robust $\mathcal{H}_\infty/H_2$, MS	TRK	PIL EXP
[180], 1994	P34	10 ST	Hybrid $\mu/\mathcal{H}_\infty$	-	SIM
[185], 2012	P02	10 ST HOV	$\mathcal{H}_\infty$ LS OPFB (OUT) ACAH (INN)	HOV	SIM
[196], 2012	P34	INN/OUT2	Robust $\mathcal{H}_\infty$ OPFB	POS TRK, SPA	SIM
[201], 1994	P09	18 ST	$H_2/\mathcal{H}_\infty$	POS	-
[142], 2013	P34	LIN HOV, CRU	MPC	PTH	SIM
[146], 2006	P34	FREQ Yaw Dynamics	LFC, OBS	Yaw	SIM
[156], 2011	P16	LAT-LON/ HEA-YAW	VEL/YAW Tracking	TRK	XPL SIM
[162], 2012	P26	LAT/LON1	MPC Cyclic control	CMD x-y POS	SIM
[174], 2000	P14	9 ST LTV	LSF	TRK	SIM
[181], 2006	P31	13 ST	Switched	HOV, CRU	SIM

The columns represent the referenced work and year published (REF), the platform used (PL), model structure (MODEL), control technique (TECHNIQUE), maneuver used for control testing and design (MANEUVER) and any results obtained (RESULTS)

appropriate flight mode (i.e. hover, cruise, take-off, etc.), control algorithm and gains in order to track the chosen trajectory(ies). This function also addresses any switching necessary to guarantee smooth transitions and stability between flight modes without saturating the inputs. Switching can be as simple as changing PID gains optimized at various cruise speeds, or changing to a completely different control approach, such as switching from a simple linear PID controller, for hover or cruise, to a nonlinear model predictive controller (MPC) to perform a more complex turn maneuver.

A separate module includes the fault detection function that assesses any potential faults or failures in the overall system (rotorcraft system). This includes monitoring functionality of each sensor, engine operation and structural integrity of the main and tail rotors, among other things. Model-based fault detection is employed to monitor system functionality as well as determining the severity and type of faults or failures. This information is provided to the GCS where a ground based pilot evaluates the situation choosing to initiate the pilot-in-the-loop take-over or send a new mission command via the GCS. If necessary, in the case of an engine or main/tail rotor failure, the fault function can initiate an emergency maneuver, such as the autorotation landing maneuver presented in [41, 42].

The third component consists of the desired navigational controller, which is the specific controller chosen to execute/track the derived trajectories, etc. Rotorcraft inputs are generated and transmitted through a servo controller and failsafe safety switch, which is connected to a ground based pilot with the ability to initiate a pilot-in-the-loop takeover via a RC transmitter.

The proposed FCS architecture is easily implemented on any rotorcraft with few modifications to the software. The same bank of linear and nonlinear control algorithms can be used by providing new gains optimized for the specific helicopter under consideration. Additionally, by keeping each component as a separate module, components can be easily excluded or modified without changing the overall FCS. For example, in much smaller vehicles, the navigational sensors can be changed for smaller, lighter models without changing the architecture or affecting the ability of the control loop to accomplish the mission. Alternatively, a single navigational sensor, such as an Attitude-Heading-Reference-System (AHRS), which provides all the necessary navigational sensor readings, may be used in place of individual sensors. If a

Table 14 This table provides a detailed review of nonlinear model-based control methods for unmanned helicopter navigation and control

REF	PL	MODEL	TECHNIQUE	MANEUVER	RESULTS
[5], 2009	P10	NLN	BS	LND	SIM
[11], 2003	P25	3DOF	FBL	ALT/YAW TRK	SIM, EXP
[15], 2005	P34	LAT-LON / HEA-YAW	HFBG (INN), NS (OUT)	ASC, LTLN, YAW	SIM
[18], 2013	P34	LON	DFL, DF	TRK	SIM
[20], 2008	P34	NLN	NLFB	POS/ATT	THE
[25], 2012	P34	HEA-YAW	LYA, SM: ALT	HOV	SIM
[36], 2013	P34	INN/OUT	BS	TKO, HOV	SIM, EXP
[37], 1998	P31	AI	AC, NN, AI	RCAH	HIL, PIL
[40], 2003	P27	NLN	GS, D-Methodology	PTH, SPA, ASC, CRU	SIM
[41, 42], 2009, 2011	P21	ATR	MPC, NN	ATR	SIM, HIL
[45], 2011	P11	9 ST ATT	MPC, PID	ATT	GIM
[47], 2000	P34	NLN	BS, PD	TRK, HOV, INV, SPA	SIM
[48], 2011	P23	NLN	SM, 3LP PID,	POS, TKO, LND	EXP
[62], 2013	P07	NLN	FBL SBP CMP	PTH, F-∞	SIM
[68], 2007	P27	NLN	H_2, LMI	PTH, HLX	SIM
[69], 2009	P27	NLN	$\mathcal{L}_1$ AC (INN)	SDW, HLX, HOV	SIM
[75], 2010	P34	NLN	FBL, $\mathcal{H}_\infty$	TRK	SIM
[84], 2003	P27	NLN	$\mathcal{L}_1$ AC, HBW (INN)	SDW,HLX, HOV	SIM
[96], 2002	P34	NLN	NMPTC	PTH, YAW, SPA	SIM
[101], 1998	P34	NLN NWTE	I/O	PO/YAW TRK	SIM
[102], 1999	P34	NLN	DF, FBL	POS/ATT TRK	SIM
[113], 2012	P22	7DOF LGR	Robust FBL	HOV, HLX	SIM, GIM
[117], 2011	P12	14 ST	Piecewise MPC	SQU	SIM, EXP
[115, 118], 2011, 2012	P23	NLN	Explicit NMPC	PTH, SQU, F-∞, PIR	SIM, EXP
[116], 2013	P34	LAT-LON/ HEA-YAW	MPC	PTH, PP	EXP
[122], 1999	P23	-	LYA, BS	TRK	THE
[121], 2004	P23	-	LYA, BS	PTH, SPA, POS	SIM
[125], 2007	P01	NLN NWTE	FF, HFG, NS	-	EXP
[139], 2013	P34	6DOF NLN	NN, BS, LYA	PTH, TRK, CIR	SIM
[147], 2007	P16	12ST Full Envelope	DI, PP, CNF	TKO, LND, HOV, PIR	EXP
[151], 2006	P32	NLN NWTE	BS	VEL	SIM
[4], 2007	P10	NLN	BS POS/VEL	HS	SIM
[164], 2013	P34	NLN/THR	MIV, PID, FF	HOV (THR)	SIM
[165], 2011	P34	DIS NLN	BS	TRJ/ TRG	SIM
[170], 2010	P33	NLN	INDI, AAP	TRJ/ TRG	SIM
[172], 2013	P34	8DOF NLN	INDI, PCH, AH	VEL TRK, PIR	SIM
[173], 1994	P28	NLN GIM	SM	ATT	SIM
[176], 2010	P17	NLN	Active MPC, GPC, AMSIPC	HOV $\rightarrow$ CRU	EXP
[175], 2013	P18	DCP LLHY	Active MPC	TRK	EXP
[182], 2011	P34	NLN, QUA	BS, SISO LQR	ATT	SIM, EXP
[183], 2012	P34	13 ST (THR)	Direct Optimal Control	ATR	SIM

Table 14 (continued)

REF	PL	MODEL	TECHNIQUE	MANEUVER	RESULTS
[186], 2013	P02	NLN	Adaptive FBL, BS	ALT/ATT	SIM
[190], 2012	P26	NLN	INV OPT, BS	PTH	SIM
[188], 2012	P34	NLN, QUA	OPT SM	ATT, HOV	SIM
[193], 2011	P34	NLN	AC BS, FBFN	HLX, PTH	SIM
[204], 2003	P34	3DOF TRA, 3DOF ATT	NLN $\mathcal{H}_\infty$	HOV, VEL/ATT	THE
[206], 2013	P34	INN/OUT	AC BS	TRK	SIM
[207], 2011	P34	NLN	AC BS	3D PTH	SIM

The columns represent the referenced work and year published (REF), the platform used (PL), model structure (MODEL), control technique (TECHNIQUE), maneuver used for control testing and design (MANEUVER) and any results obtained (RESULTS)

smaller, less powerful flight computer is chosen, control laws that are less computationally complex can be chosen from the bank of available controllers.

In order to guarantee real-time performance, it is necessary to design on-board software with the ability to meet the strict timing constraints and requirements

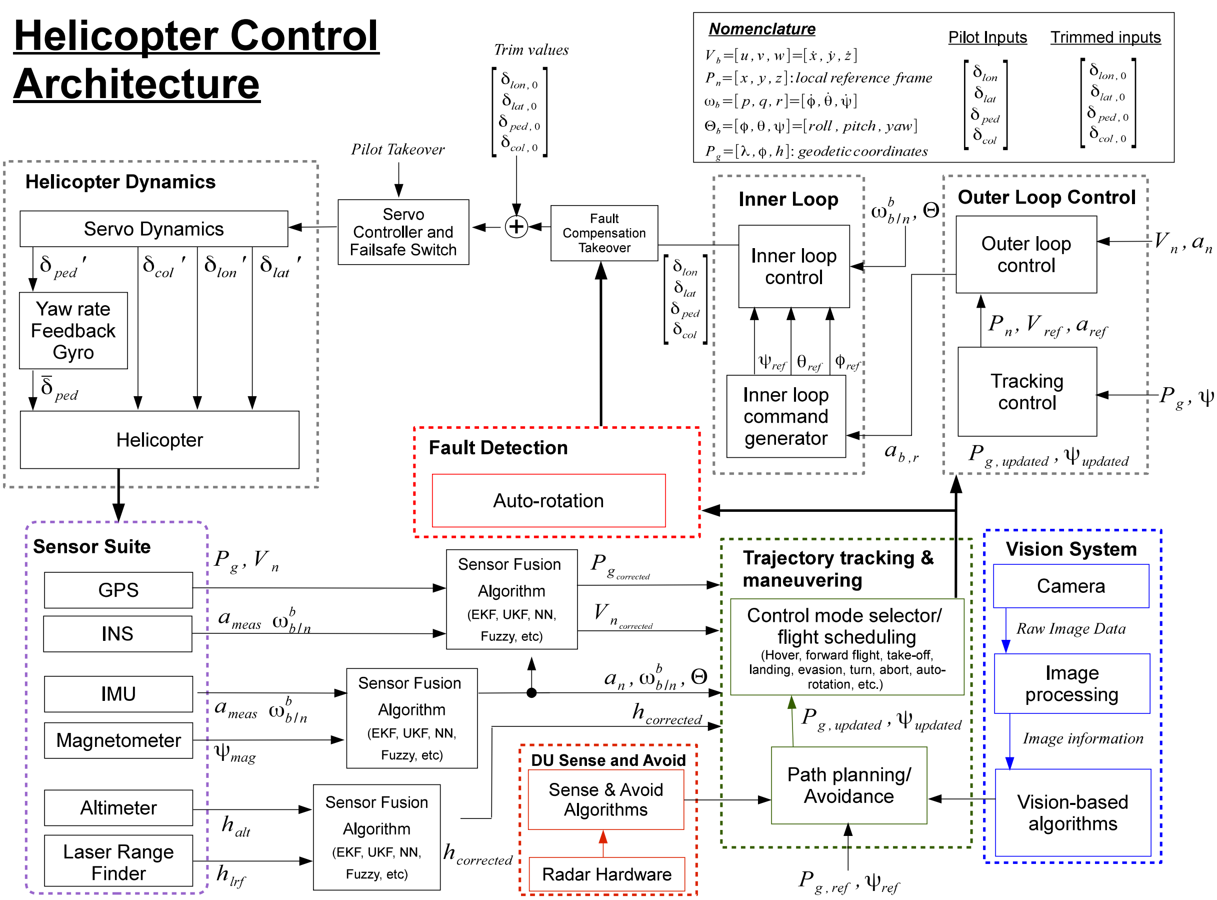

Fig. 27 The proposed comprehensive FCS architecture for unmanned rotorcraft

for proper performance of hard real-time systems. Identification of appropriate timing requirements requires the consideration of various factors, including control law execution, task management, scheduling, sensor feedback, hardware interaction, communication and data logging.

Design of control task timing requirements typically uses timing limitations based on sampling periods and hardware/software delays. Discretization of continuous control laws requires knowledge of sampling periods and actuation delays. Sampling periods are dictated by the sensor sampling rates, while delays include delays in sampling, control execution, actuation, computation and communication. Actuation delays depend on the speed of the hardware and control law calculation time. In order to determine a set of timing requirements, the data rates for all hardware components are considered. Because execution of control iterations is dependent on sensor feedback, it is common practice to choose timing requirements that coincide with sensor update rates. However, estimation algorithms may be used to provide estimated state measurements between sensor updates. These estimations are, then, corrected once the next sensor update becomes available.

For the proposed FCS architecture of Fig. 27, the set of tasks that must be executed for control implementation include: reading navigational and peripheral sensor measurements, engaging the control loop, transmitting commands to servos, communicating to the GCS and the DU^{2}SRI landing platform, obtaining readings from the vision and DSAA radar systems, fault detection, and data logging. In order to ensure timing requirements are met, management and scheduling of these tasks will be handled by the main FCS loop.

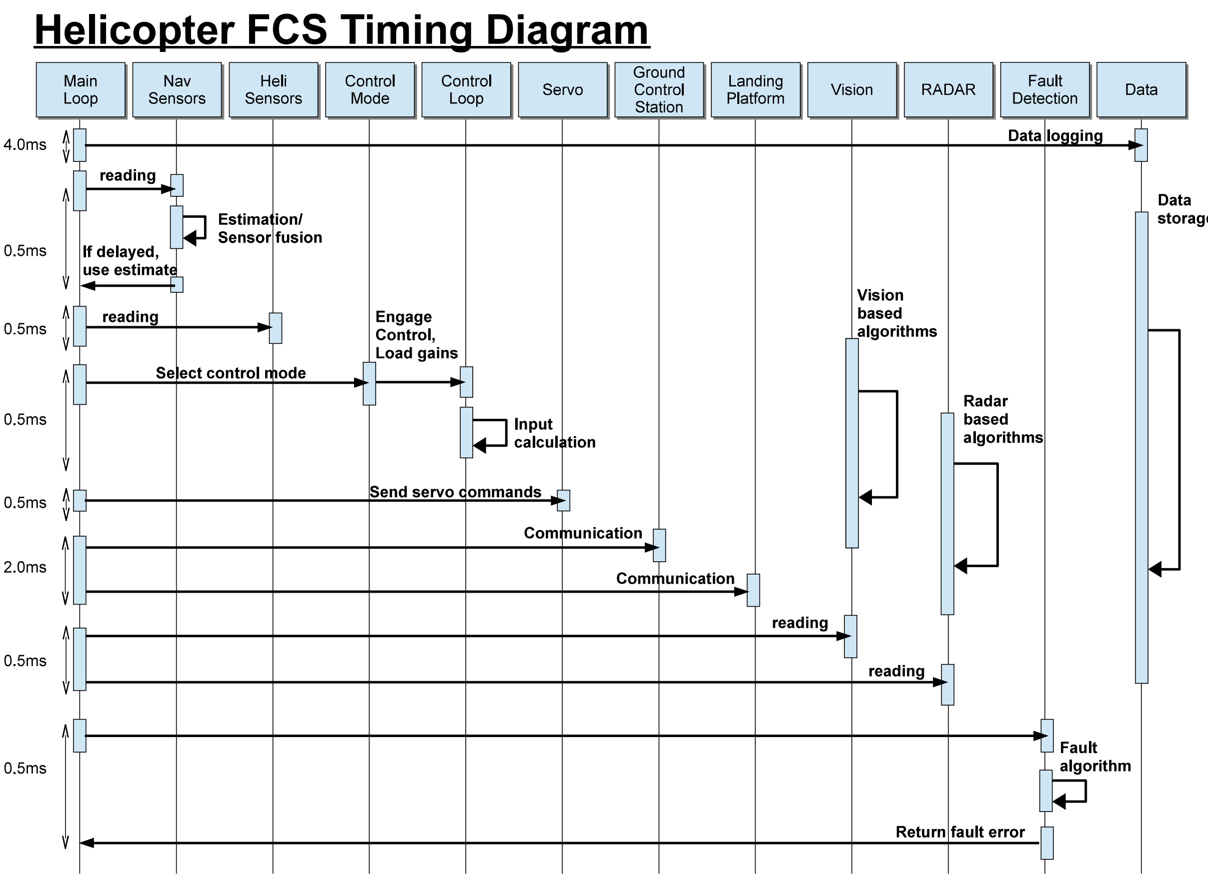

Fig. 28 The proposed comprehensive Timing Diagram for unmanned rotorcraft

Figure 28 shows the timing diagram for the FCS including proposed time allocations for each process and sequence of events following the methodology in [26] using the DU^{2}SRI Bergen fleet hardware specifications. This hardware includes a flight computer of 500 MHz processing speed, and a cycle period of 20ms based on a sensor update rate of 50Hz. While most tasks are estimated to take less than 3 % of the total cycle time, data logging can take upwards of 10–15 % of the total cycle time. Additionally, actuation delays can account for up to 50 % of the total cycle time from initiating an actuation command to execution and reading servo position. To work around such large time delays, many tasks are allowed to run in parallel. In the case of the actuation delay, the subsequent servo position reading may be used in the subsequent cycle. This approach may also be used for any tasks that cause a large time consumption. In order to protect against failure to meet timing requirements, that can lead to degraded performance, instability, and potential catastrophic failures, the FCS will include an additional state estimation algorithm, such as an EKF, to provide approximated navigational measurements in case of sensor failures or delays. A second safeguard requires the use of multiple controller gains corresponding to different sampling periods that can be switched according to delays in sensor readings.

The main FCS loop begins with reading of navigational sensor values. An estimator will run parallel to the main FCS loop. In the case the sensor reading request takes longer than the allocated time, the estimate is used for the controller. Next, the helicopter peripheral sensor values are requested. Once the sensor readings are obtained, the main loop engages the control mode function. This function will load the appropriate controller and gains for the control loop, where an optimal input is calculated. Next, the main loop transmits the input commands to the servo safety switch. Communication between the vehicle and the GCS and DU^{2}SRI landing platform is given 1 ms each. Since the vision system and radar-based DSAA modules have dedicated computers, processing is performed in parallel with the flight control software. The FCS must only spend time receiving data from these systems. The fault detection function will return an error in the event of a system fault or failure. Lastly, logging of flight data is initiated. While this task has the tendency to require the longest time, much of the process can be parallelized with the remaining FCS functions.

10 Conclusion

This survey has provided a comprehensive review of research in the area of flight navigation and control of rotorcraft, specifically the traditional main/tail rotor configuration helicopter, with the goal of providing a basis for comparison of model-based control techniques, implementations, and development of a flight control and timing architecture applicable to any RUAS platform. The following are observations that have resulted from this lengthy study. First, it is noted that linear control techniques dominate the field, despite the ability of nonlinear controllers to operate in a wider flight-envelope. This is largely due to their ease of implementation, especially when it comes to PID controllers that have shown adequate performance even without the need of an identified model. Second, there is still a large lack in presentation of significant experimental results when compared to simulation. Third, there exist no benchmarks to compare performance of control techniques. Each technique was designed specifically to a particular helicopter platform and model structure. Since no two helicopters perform alike, and it is impossible to recreate environmental conditions between two flights, it is a difficult task to compare the performance of one algorithm to another based solely on the limited results presented in past works. In this survey, a 'reference template' was proposed which presented a guideline for reviewing control approaches. This included the helicopter platform and model, control technique, loop structure, flight maneuvers, and results obtained. In order to understand the helicopter model and structure, the nonlinear helicopter dynamics and comprehensive base-line linearized model were presented. Next, the reviewed loop structures were generalized and discussed. Control techniques were categorized as linear, nonlinear or model-free methods. The advantages of each were outlined, and key examples were discussed for each. Next, a comprehensive table of existing research was presented, listing the key elements outlined in the proposed 'reference template'. Lastly, a comprehensive flight navigation control and timing architecture designed for use in any rotorcraft platform was discussed.

References

1. Abbeel, P., Coates, A., Ng, A.: Autonomous helicopter aerobatics through apprenticeship learning. Int. J. Robot. **29**(13), 1608–1639 (2010)
2. Abbeel, P., Coates, A., Quigley, M., Ng, A.Y.: An application of reinforcement learning to aerobatic helicopter flight. In: Advances in Neural Information Processing Systems 19, vol. 1, pp. 1–8. MIT Press (2007)
3. Ahmed, B., Pota, H.R.: Dynamic compensation for control of a rotary wing UAV using positive position feedback. J. Intell. Robot. Syst. **61**(1–4), 43–56 (2010)
4. Ahmed, B., Pota, H.R., Garratt, M.: Rotary wing UAV position control using backstepping. In: 46th IEEE Conference on Decision and Control, pp. 1957–1962 (2007)
5. Ahmed, B., Pota, H.R., Garratt, M.: Flight control of a rotary wing UAV using backstepping. Int. J. Robust Nonlinear Control (2009)
6. Allgower, F., Findeisen, R., Nagy, Z.K.: Nonlinear model predictive control: From theory to application. J. Chin. Inst. of Chem. Eng. **35**(3), 299–315 (2004)
7. Alvarenga, J., Vitzilaios, N.I., Valavanis, K.P., Rutherford, M.J.: Survey of rotorcraft navigation and control. Technical Report DU2SRI-2014-04-001. University of Denver (2014)
8. Antequera, N., Santos, M., de la Cruz, J.: A Helicopter Control based on Eigenstructure Assignment. In: 11th IEEE International Conference on Emerging Technologies and Factory Automation, pp. 719–724 (2006)
9. Avanzini, G., Thomson, D., Torasso, A.: Model predictive control architecture for rotorcraft inverse simulation. J. Guid. Control, and Dyn. **36**(1), 207–217 (2013)
10. Avila Vilchis, J.: Modélisation et commande d'hélicoptère. Ph.D. thesis. INGP (2001)
11. Avila Vilchis, J.C., Brogliato, B., Dzul, A., Lozano, R.: Nonlinear modelling and control of helicopters. Autom. **39**(9), 1583–1596 (2003)
12. Bai, Z., Liu, P., Wang, J., Hu, X., Zhao, X.: Control system design of a small-scale unmanned helicopter. In: 8th IEEE International Conference on Control and Automation, pp. 1414–1417 (2010)
13. Barczyk, M.: Nonlinear State Estimation and Modeling of a Helicopter UAV. Ph.D. thesis, University of Alberta (2012)
14. Barczyk, M., Lynch, A.: Control-oriented modeling of a helicopter UAV with a Bell-Hiller stabilizer mechanism. In: 2013 American Control Conference, pp. 313–320 (2013)
15. Bejar, M., Isidori, A., Marconi, L., Naldi, R.: Robust Vertical/Lateral/Longitudinal Control of a Helicopter with Constant Yaw-Attitude. In: 44th IEEE Conference on Decision and Control, pp. 6192–6197 (2005)
16. Béjar, M., Ollero, A., Cuesta, F.: Modeling and control of autonomous helicopters. Adv. Control Theory Appl. **353/2007**, 1–29 (2007)
17. Bendotti, P., Morris, J.: Robust hover control for a model helicopter. In: 1995 American Control Conference, vol. 1, pp. 682–687 (1995)
18. Benitez-Morales, J.G., Rodriguez-Cortes, H., Castro-Linares, R.: A static feedback stabilizer for the longitudinal dynamics of a small scale helicopter including the rotor dynamics with stabilizer bar. In: 2013 International Conference on Unmanned Aircraft Systems, pp. 634–641 (2013)
19. Bergerman, M., Amidi, O., Miller, J.R., Vallidis, N., Dudek, T.: Cascaded position and heading control of a robotic helicopter. In: 2007 IEEE/RSJ International Conference on Intelligent Robots and Systems, pp. 135–140 (2007)
20. Bertrand, S., Hamel, T., Piet-Lahanier, H.: Stability analysis of an UAV controller using singular perturbation theory. In: 17th World Congress of the International Federation of Automatic Control, pp. 5706–5711. Seoul, Korea (2008)
21. Bisgaard, M.: Modeling, Estimation, and Control of Helicopter Slung Load System. Ph.D. thesis, Aalborg University (2007)
22. Bramwell, A.R.S., Balmford, D., Done, G. Bramwell's helicopter dynamics, 2nd edn. Butterworth-Heinemann (2001)
23. Budiyono, A., Wibowo, S.S.: Optimal tracking controller design for a small scale helicopter. J. of Bionic Eng. **4**(4), 271–280 (2007)
24. Buskey, G., Wyeth, G., Roberts, J.: Autonomous helicopter hover using an artificial neural network. In: 2001 IEEE International Conference on Robotics and Automation, pp. 1635–1640, Seoul, South Korea (2001)
25. Butt, Y.A., Bhatti, A.I.: Robust altitude tracking of a helicopter using sliding mode control structure. In: 2012 IEEE International Conference on Emerging Technologies, pp. 1–7 (2012)
26. Cai, G., Chen, B.M., Lee, T.H.: Unmanned Rotorcraft Systems. Springer, London (2011)
27. Cai, G., Dias, J., Seneviratne, L.: A survey of small-scale unmanned aerial vehicles: Recent advances and future development trends. Unmanned Syst. **2**(2), 175–199 (2014)
28. Cai, G., Wang, B., Chen, B.M., Lee, T.H.: Design and Implementation of a Flight Control System for an Unmanned Rotorcraft using, R P T Control Approach. Asian J. Control **15**(1), 95–119 (2013)
29. Calise, A., Rysdyk, R.: Nonlinear adaptive flight control using neural networks. IEEE Control Syst. Magazine **18**(6), 14–25 (1998)
30. Castillo, P., Lozano, R., Dzul, A.: Modelling and Control of Mini-Flying Machines. Springer (2005)
31. Chao, H., Cao, Y., Chen, Y.: Autopilots for small unmanned aerial vehicles: A survey. Int. J. Control, Autom. Syst. **8**(1), 36–44 (2010)
32. Chen, R.T.N.: A simplified rotor system mathematical model for piloted flight dynamics simulation. Tech. Rep. A-7538;NASA-TM-78575, NASA (1979)
33. Chen, R.T.N.: Effects of primary rotor parameters on flapping dynamics. Tech. Rep. A-7777; NASA-TP-1431, NASA (1980)

34. Chen, X., Liu, Y., Hu, X.: Modeling and attitude control of the miniature unmanned helicopter. In: 32nd Chinese Control Conference, pp. 2723–2726 (2013)
35. Cheng, R., Tischler, M., Schulein, G.: RMAX Helicopter state-space model identification for hover and forward-flight. J. of the Am. Helicopter Soc., 202–210 (2006)
36. Chingozha, T., Nyandoro, O., Malani, A.: Low cost controller for small scale helicopter. In: 8th IEEE Conference on Industrial Electronics and Applications, pp. 439–444 (2013)
37. Corban, J., Calise, A., Prasad, J.: Implementation of adaptive nonlinear control for flight test on an unmanned helicopter. In: 37th IEEE Conference on Decision and Control, vol. 4, pp. 3641–3646 (1998)
38. Craig, J.C. Introduction to Robotics: Mechanics and Control, 3rd edn. Prentice Hall (2004)
39. Cunha, R.: Designing an Autonomous Helicopter Testbed: From Conception Through Implementation. Master's thesis. Instituto Superior Técnico, Lisbon, Portugal (2002)
40. Cunha, R., Silvestre, C., Pascoal, A.: A path following controller for model-scale helicopters. In: 7th European Control Conference (2003)
41. Dalamagkidis, K., Valavanis, K.P., Piegl, L.: Autonomous autorotation of unmanned Rotorcraft using nonlinear model predictive control. J. Intell. Robot Syst. **57**(1-4), 351–369 (2009)
42. Dalamagkidis, K., Valavanis, K.P., Piegl, L.A.: Nonlinear Model Predictive Control With Neural Network Optimization for Autonomous Autorotation of Small Unmanned Helicopters . IEEE Trans. on Control Syst. Technol. **19**, 818–831 (2011)
43. Datta, S., Patkar, U., Majumder, S.: Digital controller for attitude control of a rotary-winged flying robot in hover. 2009 IEEE Int. Symposium on Industrial Electronics pp. 390–395 (2009)
44. Etkin, B., Reid, L. Dynamics of Flight: Stability and Control, 3rd edn. John Wiley & Sons, Inc. (1996)
45. Fan, C., Guo, S., Li, D., Liu, Y.: Nonlinear predictive attitude control with a disturbance observer of an unmanned helicopter on the test bench. In: 5th IEEE International Conference on Robotics, Automation and Mechatronics, pp. 304–309 (2011)
46. Farrell, J.A.: Aided Navigation: GPS with High Rate Sensors. McGraw-Hill (2008)
47. Frazzoli, E., Dahleh, M., Feron, E.: Trajectory tracking control design for autonomous helicopters using a backstepping algorithm. In: 2000 American Control Conference, vol. 6, pp. 4102–4107 (2000)
48. Fu, J., Chen, W., Wu, Q.X.: Sliding mode control for a miniature helicopter. In: 17th International Conference on Automation and Computing, pp. 98–103 (2011)
49. Gadewadikar, J., Lewis, F., Subbarao, K., Chen, B.M.: Structured $\mathcal{H}_\infty$ command and control-loop design for unmanned helicopters. J. Guid. Control Dyn. **31**(4), 1093–1102 (2008)
50. Gadewadikar, J., Lewis, F.L., Subbarao, K., Peng, K., Chen, B.M.: $\mathcal{H}_\infty$ static output-feedback control for rotorcraft . J. Intell. Robot Syst. **54**(4), 629–646 (2008)
51. Garcia, R.D.: Designing an Autonomous Helicopter Testbed: From Conception Through Implementation. Ph.D. thesis. University of South Florida (2008)
52. Garcia, R.D., Valavanis, K.P., Kandel, A.: Autonomous helicopter navigation during a tail rotor failure utilizing fuzzy logic. In: 15th IEEE Mediterranean Conference on Control & Automation, pp. 1–6 (2007)
53. Garratt, M., Ahmed, B., Pota, H.R.: Platform enhancements and system identification for control of an unmanned helicopter. In: 9th IEEE International Conference on Control Automation Robotics and Vision. IEEE (2006)
54. Garratt, M., Anavatti, S.: Non-linear control of heave for an unmanned helicopter using a neural network. J. Intell. Robot Syst. **66**(4), 495–504 (2011)
55. Gavrilets, V.: Autonomous aerobatic maneuvering of miniature helicopters. Ph.D. thesis. Massachusetts Institute of Technology (2003)
56. Gavrilets, V., Frazzoli, E., Mettler, B., Piedmonte, M., Feron, E.: Aggressive maneuvering of small autonomous helicopters: A human centered approach. Int. J. of Robot. Research **20**(10), 795–807 (2001)
57. Gavrilets, V., Martinos, I., Mettler, B., Feron, E.: Control logic for automated aerobatic flight of miniature helicopter. In: 2002 AIAA Guidance, Navigation, and Control Conference and Exhibit, pp. 1–8, Monterey, California (2002)
58. Gavrilets, V., Martinos, I., Mettler, B., Feron, E.: Aggressive maneuvering flight tests of a miniature robotic helicopter. In: Siciliano, B., Dario, P. (eds.): Experimental Robotics VIII, Springer Tracts in Advanced Robotics, vol. 5, pp. 456–465. Springer Berlin Heidelberg (2003)
59. Gavrilets, V., Mettler, B., Feron, E.: Nonlinear model for a small-size acrobatic helicopter. In: 2001 AIAA Guidance Navigation, and Control Conference (2001)
60. Gavrilets, V., Mettler, B., Feron, E.: Dynamic model for a miniature aerobatic helicopter. Tech. rep. Massachusetts Institute of Technology (2003)
61. Glad, S., Harkegard, O.: Backstepping control of a rigid body. In: 41st IEEE Conference on Decision and Control, vol. 4, pp. 3944–3945 (2002)
62. Godbolt, B., Lynch, A.: A novel cascade controller for a helicopter UAV with small body force compensation. In: 2013 American Control Conference, pp. 800–805 (2013)
63. Godbolt, B., Lynch, A.F.: Model-based helicopter UAV control: experimental results. J. Intell. Robot. Syst. **73**(1–4), 19–31 (2013)
64. Godbolt, B., Lynch, A.F.: Control-oriented physical input modelling for a helicopter UAV. J. Intell. Robot. Syst. **73**(1–4), 209–217 (2014)
65. Godbolt, B., Vitzilaios, N., Bergen, C., Lynch, A.F.: Experimental validation of a helicopter autopilot: Time-varying trajectory tracking. In: 2013 International Conference on Unmanned Aircraft Systems, pp. 392–397 (2013)
66. Godbolt, B., Vitzilaios, N.I., Lynch, A.F.: Experimental Validation of a Helicopter Autopilot Design using Model-Based P I D Control. J. Intell. Robot. Syst. **70**(10–4), 385–399 (2013)

67. Grünhagen, W., Bouwer, G., Pausder, H., Henschel, F., Kaletka, J.: A high bandwidth control system for a helicopter in-flight simulator. Int. J. Control **59**(1), 239–261 (1994)
68. Guerreiro, B.: Trajectory tracking $\mathcal{H}_2$ controller for autonomous helicopters: An application to industrial chimney inspection. Autom. Control Aerosp **17**(1), 431–436 (2007)
69. Guerreiro, B., Silvestre, C., Cunha, R., Cao, C., Hovakimyan, N.: $\mathcal{L}_1$ adaptive control for autonomous rotorcraft. In: 2009 American Control Conference, pp. 3250–3255 (2009)
70. Hald, U.B., Hesselbæk, M.V.: Autonomous Helicopter Modelling and Control. Tech. rep. Aalborg University (2005)
71. Ham, J.A., Gardner, C.K., Tischler, M.B.: Flight-testing and frequency-domain analysis for rotorcraft handling qualities. J. Am. Helicopter Soc. **40**(2), 28 (1995)
72. Hamel, P.G., Kaletka, J.: Advances in rotorcraft system identification. Prog. in Aerosp. Sci. **33**(3–4), 259–284 (1997)
73. Hansen, R.S.: Toward a better understanding of helicopter stability derivatives. J. Am. Helicopter Soc. **29**(1), 15 (1984)
74. He, Y., Pei, H., Sun, T., Zhou, H.: Modeling, identification and robust $\mathcal{H}_\infty$ static output feedback control of lateral dynamics of a miniature helicopter. In: 5th IEEE International Conference on Robotics, Automation and Mechatronics, pp. 310–315 (2011)
75. He, Y.Q., Han, J.D.: Acceleration-Feedback-enhanced robust control of an unmanned helicopter. J. Guid. Control Dyn. **33**(4), 1236–1250 (2010)
76. Heffley, R., Mnich, M.: Minimum-complexity helicopter simulation math model. Tech. rep. NASA (1988)
77. Heffley, R.K.: A Compilation and Analysis of Helicopter Handling Qualities Data: Volume 2, Data Analysis. Tech. Rep. NASA-CR-3145;TR-1087-2, NASA (1979)
78. Heffley, R.K., Bourne, S.M., Curtiss, Jr., H.C., Hindson, W.S., Hess, R.A.: Study of Helicopter Roll Control Effectiveness Criteria. Tech. rep. NASA (1986)
79. Heffley, R.K., Jewell, W.F., Lehman, J.M., Van Winkle, R.A.: A Compilation and Analysis of Helicopter Handling Qualities Data, Volume 1, Data compilation. Tech. Rep. NASA-CR-3144; TR-1087-1, NASA (1979)
80. Hohenemser, K.: Hingeless Rotorcraft Flight Dynamics. Tech. rep., North Atlantic Treaty Organization (1974)
81. Ioannou, P., Fidan, B.: Adaptive Control Tutorial (Advances in Design and Control). SIAM Soc. Ind. Appl. Math. (2006)
82. Ioannou, P., Sun, J.: Robust adaptive control. Prentice Hall (1996)
83. Isidori, A., Marconi, L., Serrani, A.: Robust Autonomous Guidance. Springer, Boston (2003)
84. Isidori, A., Marconi, L., Serrani, A.: Robust nonlinear motion control of a helicopter. IEEE Trans. on Autom. Control **48**(3), 413–426 (2003)
85. Ji, S., Wu, A.: Study on dual-loop controller of helicopter based on the robust $\mathcal{H}_\infty$ loop shaping and mixed sensitivity. In: 2011 International Conference on Electrical and Control Engineering, 2, pp. 1291–1294 (2011)
86. Jiang, Z., Han, J., Wang, Y., Song, Q.: Enhanced LQR Control for Unmanned Helicopter in Hover. In: 1st International Symposium on Systems and Control in Aerospace and Astronautics, pp. 1438–1443 (2006)
87. Joelianto, E., Sumarjono, E.M., Budiyono, A., Penggalih, D.R.: Model predictive control for autonomous unmanned helicopters. Aircr. Eng. Aerosp. Technol. **83**(6), 375–387 (2011)
88. Johnson, E.N., Kannan, S.: Adaptive flight control for an autonomous unmanned helicopter. In: 2002 AIAA Guidance Navigation, and Control Conference and Exhibit (2002)
89. Johnson, E.N., Kannan, S.: Adaptive trajectory control for autonomous helicopters. J. Guid. Control Dyn. **28**(3), 524–538 (2005)
90. Kadmiry, B., Driankov, D.: A fuzzy flight controller combining linguistic and model-based fuzzy control. Fuzzy Sets and Syst. **146**(3), 313–347 (2004)
91. Kannan, S., Johnson, E.: Adaptive trajectory based control for autonomous helicopters. In: 21st Digital Avionics Systems Conference, vol. 2, pp. 8D1–1–8D1–12. IEEE (2002)
92. Kayton, M., Fried, W. Avionics Navigation Systems, 2nd edn. (1997)
93. Kendoul, F.: Survey of advances in guidance, navigation, and control of unmanned rotorcraft systems. J. Field Robot. **29**(2), 315–378 (2012)
94. Khalil, H.: Nonlinear Systems, 3rd edn. Prentice Hall (2001)
95. Kim, H., Shim, D.: A flight control system for aerial robots: algorithms and experiments. Control Eng. Pract. **11**(12), 1389–1400 (2003)
96. Kim, H., Shim, D., Sastry, S.: Nonlinear model predictive tracking control for rotorcraft-based unmanned aerial vehicles. In: 2002 American Control Conference, pp. 3576–3581 (2002)
97. Kim, S.: Modeling, identification, and trajectory planning for a model-scale helicopter. Ph.D. thesis. The University of Michigan (2001)
98. Kim, S., Tilbury, D.: Mathematical Modeling and Experimental Identification of a Model Helicopter. In: 1998 AIAA Guidance, Navigation and Control Conference (1998)
99. Kim, S., Tilbury, D.: Mathematical Modeling and Experimental Identification of an Unmanned Helicopter Robot with Flybar Dynamics. J. of Robot. Syst **21**(3), 95–116 (2004)
100. Koo, T., Ma, Y., Sastry, S.: Nonlinear control of a helicopter based unmanned aerial vehicle model (2001)
101. Koo, T., Sastry, S.: Output tracking control design of a helicopter model based on approximate linearization. In: 37th IEEE Conference on Decision and Control, vol. 4, pp. 3635–3640 (1998)
102. Koo, T., Sastry, S.: Differential flatness based full authority helicopter control design. In: 38th IEEE Conference on Decision and Control, vol. 2, pp. 1982–1987. IEEE (1999)
103. Koslowski, M., Kandil, A.A., Badreddin, E.: Modeling and identification of a small-scale unmanned autonomous helicopter. In: 2012 IEEE/RSJ International Conference on Intelligent Robots and Systems, pp. 2160–2165 (2012)

104. Krstć, M., Ioannis, K., Kokotovic, P.: Nonlinear and Adaptive Control Design. John Wiley & Sons (1995)
105. Kureeemun, R., Walker, D., Manimala, B., Voskuijl, M.: Helicopter Flight Control Law Design Using $\mathcal{H}_\infty$ Techniques. In: 44th IEEE Conference on Decision and Control, pp. 1307–1312 (2005)
106. La Civita, M.: Integrated modeling and robust control for full-envelope flight of robotic helicopters. Ph.D. thesis. Carnegie Mellon University (2002)
107. La Civita, M.: Design and Flight Testing of an $\mathcal{H}_\infty$ Controller for a Robotic Helicopter. J. of Guid. Control Dyn. **29**(2), 485–494 (2006)
108. La Civita, M., Papageorgiou, G., Messner, W., Kanade, T.: Design and Flight Testing of a High-Bandwidth $\mathcal{H}_\infty$ Loop Shaping Controller for a Robotic Helicopter. In: 2002 AIAA Guidance, Navigation and Control Conference (2002)
109. La Civita, M., Papageorgiou, G., Messner, W., Kanade, T.: Design and flight testing of a gain-scheduled $\mathcal{H}_\infty$ loop shaping controller for wide-envelope flight of a robotic helicopter. In: 2003 American Control Conference, vol. 5, pp. 4195–4200 (2003)
110. Lee, D., Choi, M., Bang, H.: Model-free linear quadratic tracking control for unmanned helicopters using reinforcement learning. In: 5th International Conference on Automation, Robotics and Applications, 3, pp. 19–22 (2011)
111. Lee, D.J., Bang, H.: Model-free LQ control for unmanned helicopters using reinforcement learning. In: 11th International Conference on Control. Autom. Syst. **6**, 117–120 (2011)
112. Lee, E., Shim, H., Park, H., Lee, K.: Design of hovering attitude controller for a model helicopter. Proc. of Soc. of Instrument and Control Eng. pp. 1385–1389 (1993)
113. Leonard, F., Martini, A., Abba, G.: Robust Nonlinear Controls of Model-Scale Helicopters Under Lateral and Vertical Wind Gusts. IEEE Trans. Control Syst. Technol. **20**(1), 154–163 (2012)
114. Liang, J., Wang, T., Wang, C., Zhang, Y., Chen, Y.: Combined of vector field and linear quadratic Gaussian for the path following of a small unmanned helicopter. IET Control Theory Appl. **6**(17), 2696–2703 (2012)
115. Liu, C., Chen, W., Andrews, J.: Explicit non-linear model predictive control for autonomous helicopters. Proc. of the Institution of Mechanical Eng., Part G. J. of Aerosp. Eng. **226**(9), 1171–1182 (2011)
116. Liu, C., Chen, W.H.: Hierarchical path planning and flight control of small autonomous helicopters using MPC techniques. In: 2013 IEEE Intelligent Vehicles Symposium, pp. 417–422 (2013)
117. Liu, C., Chen, W.H., Andrews, J.: Piecewise constant model predictive control for autonomous helicopters. Robot. Auton. Syst. **59**(7-8), 571–579 (2011)
118. Liu, C., Chen, W.H., Andrews, J.: Tracking control of small-scale helicopters using explicit nonlinear MPC augmented with disturbance observers. Control Eng. Pract. **20**(3), 258–268 (2012)
119. Liu, L., Shen, Y., Dowell, E.H.: Integrated adaptive fault-tolerant $\mathcal{H}_\infty$ output feedback control with adaptive fault identification. J. Guid. Control Dyn. **35**(3), 881–889 (2012)
120. Lungu, R., Ispas, S., Iancu, M., Lungu, M.: Optimal control of helicopter motion. In: 2012 International Conference on Applied and Theoretical Electricity, 4, pp. 1–5 (2012)
121. Mahony, R., Hamel, T.: Robust trajectory tracking for a scale model autonomous helicopter. Int. J. Robust Nonlinear Control **14**(12), 1035–1059 (2004)
122. Mahony, R., Hamel, T., Dzul, A.: Hover control via Lyapunov control for an autonomous model helicopter, In: 38th IEEE Conference on Decision and Control, vol. 4, pp. 3490–3495. IEEE (1999)
123. Marantos, P., Dritsas, L., Kyriakopoulos, K.: Robust attitude control for an unmanned helicopter in near-hover flights. In: 2013 European Control Conference, pp. 347–352 (2013)
124. Marantos, P., Dritsas, L., Kyriakopoulos, K.J.: Robust $\mathcal{H}_2$ / $\mathcal{H}_\infty$ Position Tracking control of an Unmanned Helicopter for near-hover flights. In: 21st Mediterranean Conference on Control and Automation, pp. 161–166 (2013)
125. Marconi, L., Naldi, R.: Robust full degree-of-freedom tracking control of a helicopter. Autom. **43**(11), 1909–1920 (2007)
126. Masajedi, P., Ghanbarzadeh, A., Shishesaz, M.: Optimal Control Designing for a Discrete Model of Helicopter in Hover. In: 2012 International Conference on Control Engineering and Communication Technology, pp. 407–412 (2012)
127. Mcewen, M.D., Duren, R., Wood, E.R., Author, S., Matthew, D.: Dynamic System Identification and Modeling of a Rotary Wing U A V for Stability. Master's thesis. Naval Postgraduate School (1998)
128. Megawati, N.Y., Solikhatun, S., Joelianto, E., Budiyono, A.: Robust switched linear controller for multimode helicopter models. In: 2nd International Conference on Instrumentation Control and Automation, pp. 152–156 (2011)
129. Mettler, B.: Identification Modeling and Characteristics of Miniature Rotorcraft. Springer, Boston (2003)
130. Mettler, B., Gavrilets, V., Feron, E., Kanade, T.: Dynamic compensation for high-bandwidth control of small-scale helicopter. In: American Helicopter Society Specialist Meeting (2002)
131. Mettler, B., Kanade, T., Tischler, M.: System identification modeling of a model-scale helicopter. J. Am. Helicopter Soc., 1–25 (2000)
132. Mettler, B., Tischler, M.: Attitude control optimization for a small-scale unmanned helicopter. In: 2000 AIAA Guidance Navigation, and Control Conference and Exhibit (2000)
133. Mettler, B., Tischler, M.B., Kanade, T.: System identification of small-size unmanned helicopter dynamics. In: American Helicopter Society 55th Forum (1999)
134. Montgomery, J., Bekey, G.: Learning helicopter control through "teaching by showing". In: 37th IEEE Conference on Decision and Control, vol. 4, pp. 3647–3652 (1998)
135. Morari, M.: Model predictive control: Multivariable control technique of choice in the 1990s?. In: Clarke, D. (ed.): Advances in Model-Based Predictive Control, pp. 22–37. Oxford Science Publications (1994)

136. Morris, J., van Nieuwstadt, M., Bendotti, P.: Identification and control of a model helicopter in hover. In: 1994 American Control Conference, vol. 2, pp. 1238–1242 (1994)
137. Nighat Khizer, A., Yaping, D., Ali, S.A., Yang, X.X.: Takagi-Sugeno fuzzy model identification for small scale unmanned helicopter. TELKOMNIKA Indones. J. Electr. **12**(1) (2014)
138. Nikravesh, P.: Computer-Aided Analysis of Mechanical Systems. Prentice Hall (1988)
139. Nodland, D., Zargarzadeh, H., Jagannathan, S.: Neural Network-Based Optimal Adaptive Output Feedback Control of a Helicopter UAV. IEEE Trans. Neural Netw. Learn. Syst. **24**(7), 1061–1073 (2013)
140. Oktay, T.: Constrained control of complex helicopter models. Ph.D. thesis. Virginia Polytechnic Institute and State University (2012)
141. Oktay, T., Sultan, C.: Constrained predictive control of helicopters. Aircr. Eng. and Aerosp. Technol. **85**(1), 32–47 (2013)
142. Oktay, T., Sultan, C.: Simultaneous Helicopter and Control-System Design. J. of Aircr. **50**(3), 911–925 (2013)
143. Ollero, A., Merino, L.: Control and perception techniques for aerial robotics. Annu. Rev. in Control **28**(2), 167–178 (2004)
144. Padfield, G.D.: Helicopter Flight Dynamics. Blackwell Publishing Ltd, Oxford (2007)
145. Pan, Y., Song, P., Li, K.: PID Control of Miniature Unmanned Helicopter Yaw System based on RBF Neural Network. Intelligent Computing and Information Science pp. 308–313 (2011)
146. Peng, K., Cai, G., Chen, B., Dong, M., Lee, T.: Comprehensive Modeling and Control of the Yaw Dynamics of a UAV Helicopter. In: 2006 Chinese Control Conference, pp. 2087–2092 (2006)
147. Peng, K., Miaobo, D., Chen, B., Cai, G., Kai-Yew, L., Lee, T.: Design and Implementation of a Fully Autonomous Flight Control System for a UAV Helicopter. In: 2007 Chinese Control Conference, pp. 662–667 (2007)
148. Phillips, C., Karr, C., Walker, G.: Helicopter flight control with fuzzy logic and genetic algorithms. Eng. Appl. Artif. Intell. **9**(2), 175–184 (1996)
149. Pieper, J., Baillie, S., Goheen, K.: Linear-quadratic optimal model-following control of a helicopter in hover. In: 1994 American Control Conference, vol. 3, pp. 3470–3474 (1994)
150. Postlethwaite, I., Prempain, E., Turkoglu, E., Turner, M.C., Ellis, K., Gubbels, A.: Design and flight testing of various controllers for the Bell 205 helicopter. Control Eng. Pract. **13**(3), 383–398 (2005)
151. Pota, H.R., Ahmed, B., Garratt, M.: Velocity Control of a UAV using Backstepping Control. In: 45th IEEE Conference on Decision and Control, pp. 5894–5899 (2006)
152. Pradana, W.A., Joelianto, E., Budiyono, A., Adiprawita, W.: Robust MIMO Integral-Backstepping PID Controller for Hovering Control of Unmanned Model Helicopter. J. Aerosp. Eng. **24**(4), 454–462 (2011)
153. Prasad, J., Calise, A., Pei, Y., Corban, J.: Adaptive nonlinear controller synthesis and flight test evaluation on an unmanned helicopter. In: 1999 IEEE International Conference on Control Applications, pp. 137–142 (1999)
154. Prouty, R.: Helicopter Performance, Stability and Control. Krieger Publishing Company (1995)
155. Raptis, I., Valavanis, K.: Linear and nonlinear control of small-scale unmanned helicopters. Intelligent Systems, Control and Automation: Science and Engineering. Springer, Netherlands (2011)
156. Raptis, I.A., Valavanis, K.P.: Velocity and heading tracking control for small-scale unmanned helicopters. In: 2011 American Control Conference, pp. 1579–1586 (2011)
157. Raptis, I.A., Valavanis, K.P., Moreno Wilfrido, A.: A Novel Nonlinear Backstepping Controller Design for Helicopters Using the Rotation Matrix. IEEE Trans. Control Syst. Technol. **19**(2), 465–473 (2011)
158. Raptis, I.A., Valavanis, K.P., Moreno, W.A.: System Identification and Discrete Nonlinear Control of Miniature Helicopters Using Backstepping. J. Intell. Robot. Syst. **55**(2–3), 223–243 (2008)
159. Raptis, I.A., Valavanis, K.P., Vachtsevanos, G.J.: Linear Tracking Control for Small-Scale Unmanned Helicopters. IEEE Trans. on Control Syst. Technol. **20**(4), 995–1010 (2012)
160. Ren, B., Ge, S.S., Chen, C., Fua, C.H., Lee, T.H.: Modeling, Control and Coordination of Helicopter Systems. Springer, New York (2012)
161. Safaee, A., Taghirad, H.D.: System identification and robust controller design for the autopilot of an unmanned helicopter. In: 9th Asian Control Conference, pp. 1–6 (2013)
162. Samal, M.K., Garratt, M., Pota, H., Teimoori, H.: Model predictive flight controller for longitudinal and lateral cyclic control of an unmanned helicopter. In: 2nd Asutralian Control Conference, November, pp. 386–391 (2012)
163. Sanchez, E.N., Becerra, H.M., Velez, C.M.: Combining fuzzy, PID and regulation control for an autonomous mini-helicopter. Inf. Sci **177**(10), 1999–2022 (2007)
164. Sandino, L.A., Bejar, M., Kondak, K., Ollero, A.: Improving hovering performance of tethered unmanned helicopters with nonlinear control strategies. In: 2013 International Conference on Unmanned Aircraft Systems, pp. 443–452 (2013)
165. Sconyers, C., Raptis, I.A., Vachtsevanos, G.J.: Rotorcraft control and trajectory generation for target tracking. In: 19th Mediterranean Conference on Control & Automation, pp. 1235–1240 (2011)
166. Shim, H., Koo, T., Hoffmann, F., Sastry, S.: A comprehensive study of control design for an autonomous helicopter. In: 37th IEEE Conference on Decision and Control, vol. 4, pp. 3653–3658 (1998)
167. Shim, H., Sastry, S.: Control system design for rotorcraft-based unmanned aerial vehicles using time-domain system identification. In: 2000 IEEE International Conference on Control Applications, pp. 808–813 (2000)
168. Shim, H.D.: Hierarchical Flight Control System Synthesis for Rotorcraft-based Unmanned Aerial Vehicles. Ph.D. thesis. University of California, Berkeley (2000)
169. Shin, J., Nonami, K., Fujiwara, D., Hazawa, K.: Model-based optimal attitude and positioning control of small-scale unmanned helicopter. Robot **23**(1), 51–63 (2005)

170. Sieberling, S., Chu, Q.P., Mulder, J.A.: Robust Flight Control Using Incremental Nonlinear Dynamic Inversion and Angular Acceleration Prediction. J. Guid. Control Dyn. **33**(6), 1732–1742 (2010)
171. Simone, D.: In-flight identification of the augmented flight dynamics of the RMAX unmanned helicopter. In: Houria, S. (ed.): 17th IFAC Symposium on Automatic Control in Aerospace, pp. 217–222 (2007)
172. Simplício, P., Pavel, M., van Kampen, E., Chu, Q.: An acceleration measurements-based approach for helicopter nonlinear flight control using Incremental Nonlinear Dynamic Inversion. Control Eng. Pract. **21**(8), 1065–1077 (2013)
173. Sira-Ramirez, H.: Dynamical sliding mode control approach for vertical flight regulation in helicopters. In: IEE Proceedings - Control Theory and Applications, vol. 141, p. 19 (1994)
174. Sira-Ramirez, H., Castro-Linares, R., Liceaga-Castro, E.: A Liouvillian systems approach for the trajectory planning-based control of helicopter models. Int. J. Robust Nonlinear Control **10**(4), 301–320 (2000)
175. Song, D., Han, J., Liu, G.: Active Model-Based Predictive Control and Experimental Investigation on Unmanned Helicopters in Full Flight Envelope. IEEE Trans. Control Syst. Technol. **21**(4), 1502–1509 (2013)
176. Song, D., Qi, J., Han, J., Liu, G.: Active model based predictive control for unmanned helicopter in full flight envelope. In: 2010 IEEE/RSJ International Conference on Intelligent Robots and Systems, pp. 616–621 (2010)
177. Spong, M., Hutchinson, S., Vidyasagar, M.: Robot Modeling and Control. Wiley (2005)
178. Sugeno, M., Griffin, M., Bastian, A.: Fuzzy hierarchical control of an unmanned helicopter. In: International Fuzzy Systems and Applications Conference, pp. 179–182, Seoul, South Korea (1993)
179. Sugeno, M., Howard, W., Isao, H., Satoru, K.: Intelligent control of an unmanned helicopter based on fuzzy logic. In: 51st American Helicopter Society Annual Forum, pp. 791–803, Fort Worth, Texas (1995)
180. Sun, X.D., Clarke, T.: Application of μ / $\mathcal{H}_\infty$ Control to Modern Helicopters. In: International Conference on Control '94, pp. 1532–1537 (1994)
181. Sutarto, H., Budiyono, A., Joelianto, E., Hiong, G.T.: Switched Linear Control of a Model Helicopter. In: 9th International Conference on Control, Automation, Robotics and Vision, pp. 1–8 (2006)
182. Suzuki, S., Nakazawa, D., Nonami, K., Tawara, M.: Attitude Control of Small Electric Helicopter by Using Quaternion Feedback. J. Syst. Des. Dyn. **5**(2), 231–247 (2011)
183. Taamallah, S., Bombois, X., Hof, P.V.D.: Optimal Control For Power-Off Landing Of A Small-Scale Helicopter A Pseudospectral Approach. In: 2012 American Control Conference, pp. 914–919 (2012)
184. Talbot, P., Tinling, B., Decker, W., Chen, R.: A mathematical model of a single main rotor helicopter for piloted simulation. Tech. rep., NASA (1982)
185. Tang, J., Wei, C., Yang, F.: Static $\mathcal{H}_\infty$ Loop-Shaping Control for Unmanned Helicopter. In: 10th World Congress on Intelligent Control and Automation, pp. 2882–2886 (2012)
186. Tang, S., Zhang, L., Zheng, Z.: Adaptive height and attitude control of small-scale unmanned helicopter. In: 25th Chinese Control and Decision Conference, pp. 1–6 (2013)
187. Tao, G.: Adaptive Control Design and Analysis. Wiley-IEEE Press (2003)
188. Teimoori, H., Pota, H.: Attitude control of a miniature helicopter using optimal sliding mode control. In: 2nd Australian Control Conference, pp. 295–300 (2012)
189. Teimoori, H., Pota, H.R., Garratt, M., Samal, M.K.: Planar trajectory tracking controller for a small-sized helicopter considering servos and delay constraints. In: 37th Annual Conference of the IEEE Industrial Electronics Society, pp. 681–686 (2011)
190. Teimoori, H., Pota, H.R., Garratt, M., Samal, M.K.: Helicopter flight control using inverse optimal control and backstepping. In: 12th International Conference on Control Automation Robotics & Vision, vol. 2012, pp. 978–983 (2012)
191. Tischler, M.: System identification methods for aircraft flight control development and validation. Adv. in Aircr. Flight Control (1996)
192. Tischler, M., Cauffman, M.: Frequency-response method for rotorcraft system identification: Flight applications to BO coupled rotor/fuselage dynamics. J. Am. Helicopter Soc. **37**(3), 3–17 (1992)
193. Tsai, C.C., Lee, C.T., Hwang, K.S.: Intelligent adaptive trajectory tracking control using fuzzy basis function networks for an autonomous small-scale helicopter. In: 2011 IEEE International Conference on Systems Man, and Cybernetics, pp. 2255–2260 (2011)
194. Verdult, V., Lovera, M., Verhaegen, M.: Identification of linear parameter-varying state-space models with application to helicopter rotor dynamics. Int. J. Control **77**(13), 1149–1159 (2004)
195. Wang, G., Zhu, J., Yang, C., Xia, H.: System identification for helicopter yaw dynamic modelling. In: 3rd International Conference on Computer Research and Development, pp. 54–57 (2011)
196. Wang, J., Pei, H., Su, W., He, Y.: A gust-attenuation robust $\mathcal{H}_\infty$ output-feedback control design for unmanned autonomous helicopters. In: 2012 American Control Conference, pp. 3260–3265 (2012)
197. Wang, X., Chen, Y., Lu, G., Zhong, Y.: Robust attitude tracking control of small-scale unmanned helicopter. Int. J. Syst. Sci., 1–14 (2013)
198. Wang, X., Chen, Y., Lu, G., Zhong, Y.: Robust flight control of small-scale unmanned helicopter. In: 32nd Chinese Control Conference, pp. 2700–2705 (2013)
199. Wang, X., Wang, X., Yao, C.: Design of hovering altitude holding control system for helicopter. In: 2012 IEEE International Conference on Information and Automation June, pp. 180–183 (2012)
200. Wang, X., Zhao, X.: A practical survey on the flight control system of small-scale unmanned helicopter. In: 7th World Congress on Intelligent Control and Automation, pp. 364–369 (2008)
201. Weilenmann, M., Christen, U., Geering, H.: Robust helicopter position control at hover. In: 1994 American Control Conference, vol. 3, pp. 2491–2495 (1994)

202. Weilenmann, M.F., Geering, H.P.: Test bench for rotorcraft hover control. J. Guid.Control Dyn. **17**(4), 729–736 (1994)
203. Xia, X., Ge, Y.: Finite-horizon optimal linear control for autonomous soft landing of small-scale helicopter. In: 2010 IEEE International Conference on Information and Automation, pp. 1160–1164 (2010)
204. Yang, C.D., Liu, W.h.: Nonlinear $\mathcal{H}_\infty$ Decoupling Hover Control Of Helicopter With Parameter Uncertainties. In: 2003 American Control Conference, pp. 3454–3459 (2003)
205. Yang, X., Garratt, M., Pota, H.: Flight validation of a feedforward gust-attenuation controller for an autonomous helicopter. Robot. Auton. Syst. **59**(12), 1070–1079 (2011)
206. Zhang, L., Ding, Z.: Nonlinear control design and stability analysis of a small-scale unmanned helicopter. In: 10th IEEE International Conference on Control and Automation, pp. 1662–1667 (2013)
207. Zhu, B., Huo, W.: Adaptive backstepping control for a miniature autonomous helicopter. In: 50th IEEE Conference on Decision and Control and European Control Conference, 1, pp. 5413–5418 (2011)